TÉCNICO LISBOA

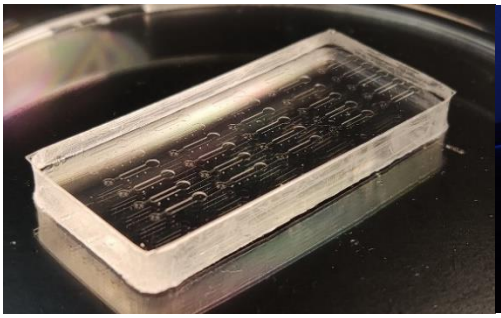
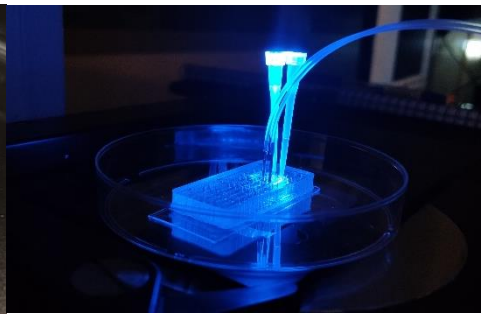

Detection of Cancer Biomarkers from an Ionic-Liquid System using a Microfluidic Device

Ana Filipa Do Carmo Flora Teixeira Ribeiro

Thesis to obtain the Master of Science Degree in

Biomedical Engineering

Supervisor(s): Prof. Dr. João Pedro Estrela Rodrigues Conde
Prof. Dr. Mara Guadalupe Freire Martins

Examination Committee

Chairperson: Prof. Dr. João Miguel Raposo Sanches
Supervisor: Prof. Dr. João Pedro Estrela Rodrigues Conde
Members of the Committee: Prof. Dr. Ana Margarida Nunes da Mata Pires de Azevedo

November 2021

Preface

The work presented in this thesis was performed at INESC MN (Lisbon, Portugal), during the period March-November 2021, under the supervision of Professor Doctor João Pedro Estrela Rodrigues Conde and within the frame of PTDC/EMD-TLM/3253/2020 (ILSurvive) project, funded by national funds (OE), through FCT/MCTES. The thesis was co-supervised at Universidade de Aveiro/CICECO by Professor Doctor Mara Guadalupe Freire Martins.

Declaration

I declare that this document is an original work of my own authorship and that it fulfils all the requirements of the Code of Conduct and Good Practices of the Universidade de Lisboa.

Acknowledgements

In first place, I would like to thank Prof. Dr. João Pedro Conde for giving me the opportunity to work at INESC-MN in such an enthusiastic and supporting environment. I am extremely grateful for being able to work in such a challenging and interesting project under his involved and motivational supervision. I also want to thank my co-supervisor Prof. Dr. Mara Guadalupe Freire Martins for her encouragement, motivation and advice and Dr. Francisca Silva for all the support and guidance given during this project, which were crucial in the development of my thesis. I would like to thank Dr. Virginia Chu for all support and advice throughout the entire semester.

At INESC-MN, I would like to thank Cristiana Domingues and Pedro Monteiro for their amazing and dedicated mentorship and invaluable support throughout the entire project, Catarina Caneira for her help and good advice during troubleshooting times and the remaining group members for the encouragement. It was a pleasure to work alongside such knowledgeable and dedicated group of people. I would like to thank my colleagues Rafaela Rosa, Rui Meirinho, Sofia Relvas e Rodolfo Rodrigues for their help and encouragement and for all the good moments in the lab.

I would like to thank my friends from Biomedical Engineering integrated master for all the support and shared moments throughout our academic journey, helping me achieve my goals, even during the most difficult times.

I would like to thank my family, in particularly to my mom, grandmother Celsa and grandfather Eduardo who have always believed in my capabilities and celebrate my achievements and for being the fundamental pillars in my life for my personal growth and success. Finally, a special thanks to my partner Tiago Lopes, for the love, friendship, understanding and support.

Abstract

In recent years, cancer biomarkers have received remarkable attention in the biomedical field, since they are considered valuable indicators for the presence or absence of tumours, improving rapid and early cancer detection, efficacy of treatment, and allowing monitorization of disease progression. The development of a bead-based microfluidic system for the detection of prostate specific antigen (PSA) promises great potential for the development of a portable, low-cost, rapid, and sensitive platform for prostate cancer diagnosis and prognosis. In the present work, detection of PSA was performed not only in PBS but also in human serum and several ionic liquids. Ionic liquids are promising molten salts in extraction and concentration of analytes present in complex biological fluids and highly used in Aqueous Biphasic Systems.

For this work, a sandwich-type immunoassay was selected, in which a capture antibody was immobilized on Protein G beads and fluorescence intensity was measured after the binding event between target analyte PSA and labelled detector antibody. Different optimization protocols regarding microbeads choice, blocking method and capture antibody concentrations were performed. Calibration curves for different concentrations of PSA for both PBS and human serum were obtained. The detection of target concentration in ng/mL range was reached and detection limits of 10.8 ng/mL and 12.2 ng/mL were obtained for each methodology studied, both close to clinically relevant range of 4-10 ng/mL.

KEYWORDS: microfluidic system, beads, PSA, cancer biomarkers, aqueous biphasic systems, ionic liquids

Resumo

Nos últimos anos, diversos biomarcadores têm ganho destaque na área da biomédica, sendo considerados bons indicadores da presença ou ausência de tumores, facilitando uma deteção mais rápida e atempada, melhorado a eficácia do tratamento e permitindo a monitorização da doença. O desenvolvimento de um sistema microfluídico, baseado em beads para a deteção do antigénio específico da próstata apresenta grande potencial para o desenvolvimento de uma plataforma portátil, de baixo custo, rápida e de elevada sensibilidade para o diagnóstico e prognóstico do cancro da próstata. No presente trabalho, a deteção de PSA foi realizada em solução tampão PBS, em soro humano e em vários líquidos iónicos. Líquidos iónicos são sais promissores na extração e concentração de moléculas-alvo presentes em fluidos biológicos complexos e são comumente utilizados em Sistemas Aquosos Bifásicos.

Para este trabalho, foi selecionado um imunoensaio do tipo sandwich, no qual um anticorpo de captura foi imobilizado em beads de proteína G e o sinal de fluorescência foi medido depois da ligação entre a molécula-alvo e o anticorpo de deteção marcado com um fluoróforo. Foram realizados diferentes protocolos de otimização relativos ao método de bloqueio, escolha do tipo de beads e concentração do anticorpo de captura. Foram obtidas curvas de calibração para diferentes concentrações de PSA em solução tampão PBS e em soro humano. Foi possível obter valores de deteção na ordem dos ng/mL e os limites de deteção obtidos variam entre os 10.8 e 12.2 ng/mL, ambos próximos da gama de valores considerada clinicamente relevante (4-10 ng/mL).

Palavras-chave: Sistema microfluídico, beads, PSA, biomarcadores, sistemas aquosos bifásicos, líquidos Iónicos

Index

List of Tables

List of Figures

List of Abbreviations

ABS	Aqueous Biphasic Systems
AFB1	Aflatoxin B1
BPH	Benign Prostatic Hyperplasia
BPSA	Benign Prostate Specific Antigen
BSA	Bovine Serum Albumin
CA	CaptoAdhere
CA125	Cancer-Antigen 125
CAD	Computer-Aided Design
CEA	Carcinoembryonic Antigen
DI	Deionized
DON	Deoxynivalenol
DRE	Digital Rectal Examination
DWL	Direct Write Laser
EDRN	Early Detection Research Network
ELISA	Enzyme-Linked Immuosorbent Assay
FDA	Food and Drug Administration
FITC	Fluorescein Isothiocyanate
HC	Heavy Chains
hK2	Kallikrein 2
HS	Human Serum
IgY	Immunoglobulin Y
IL	Ionic Liquid
IL-ABS	Ionic Liquid-based Aqueous Biphasic System
inPSA	Inactive Prostate Specific Antigen
IPA	Isopropanol
LC	Light Chains
LoB	Limit of Blank
LoC	Lab-on-Chip
LoD	Limit of Detection
LoQ	Limit of Quantification
OTA	Ochratoxin A
PBS	Phosphate Buffer Saline
PC	Prostate Cancer
PCR	Polymerase Chain Reaction
PDMS	Polydimethylsiloxane
PEG	Polyethylene Glycol
PGMEA	Propylene Glycol Methyl Ether Acetate

PIN	Prostatic Intraepithelial Neoplasia
PMMA	Polymethyl Methacrylate
POC	Point-of-Care
proPSA	Prostate Specific Antigen precursor
PS	Polystyrene
PSA	Prostate Specific Antigen
QS	Q-Sepharose
TZ	Transitional Zone
UV	Ultraviolet

1. Introduction

1.1. Motivation

Cancer is a major public health problem worldwide[1] and survival rates of this disease tend to be low, as it is commonly diagnosed at a later stage, when it is already metastasized to other sites of the body[2,3]. Therefore, early-stage cancer diagnosis is extremely important in timely and effective treatment and for monitoring disease progression[3]. In this context, cancer biomarkers have been receiving remarkable attention from biomedical researchers due to their high clinical significance[4], since they are specific indicators of tumour development, response to treatment, and disease recurrence.

Despite the recent efforts in developing powerful and reliable techniques for early diagnosis, most of the conventional methods applied for the detection of cancer biomarkers, including enzyme-linked immunosorbent assay (ELISA), polymerase chain reaction (PCR), and macroscale colorimetric, fluorescence and electrochemical assays present some limitations, namely the consumption of large amounts of reagents, slowness in detection and the fact that skilled personnel and bulky equipment is a mandatory requirement [4,5]. Therefore, it is crucial to invest in fully integrated and automated strategies capable of performing specific molecular recognition of multiple target cancer biomarkers in a simultaneous, simple, and cost-effective manner for an accurate diagnosis.

Within this framework, biomarker detection in microfluidic devices has been studied as a promising alternative to traditional methods. In fact, microfluidic systems allow for low-cost and fast *in situ* diagnosis, with increased sensitivity and efficiency and smaller reagents volume[6]. Therefore, these are potentially good candidates for on-chip point-of-care (POC) testing near patient site in environments with low-resource settings, including undeveloped countries and in situations of emergency. Due to these remarkable characteristics, several microfluidic devices have been created in recent years for the detection of several diseases, including not only cancer, but also infectious diseases, cardiac diseases, Alzheimer, among others[6]. Despite recent advances, microfluidic systems are not routinely applied in clinical settings yet, since there are still some limitations regarding analysis of complex samples[7] and, in some cases, lack of integration of several important components (valves, pumps, sensors, heater, etc.), automation and low reproducibility. Therefore, before their implementation in the medical field, these challenges must be overcome so that microfluidic devices can improve early-cancer diagnosis and cause a positive impact in global health care.

1.2. Cancer Biomarkers

Cancer is a disease defined by an uncontrollable growth of cells beyond their regular boundaries, which invade adjacent tissues or even migrate to different organs (metastasis). Despite the efforts to reduce the incidence of this disease, cancer is considered a major public health problem worldwide[1], with breast and prostate cancer being the most common types of cancer diagnosed in women and men, respectively. However, if the cancer is detected at an early stage, treatment strategies will be more effective and there is a good chance of curing the disease or at least turning it into a chronic disease. Therefore, there has been an increasing interest in the development of new methods to detect early-stage cancers, particularly in the discovery of biomarkers, which are valuable tools in the prevention, diagnosis and treatment of this disease.

Biomarkers are indicators of the physiological state of a cell at a given time, providing information on cellular processes and alterations and disruptions to cellular pathways. According to the National Cancer Institute, a biomarker is described as a "biological molecule found in blood, other body fluids or tissues that is a sign of normal or abnormal process, or of a condition or disease". Biomarkers can either be directly produced by a tumor itself or secreted by other tissues as a response to the presence of a malignancy[2,8]. There is a wide variety of cancer biomarkers, which include proteins or fragments of proteins (e.g., enzymes, membrane receptors, growth factors), nucleic acid-based biomarkers, tumor suppressor genes, oncogenes, and tumor-specific antigens and they can be found in the whole blood, plasma, or serum or in secretions like urine, stool or sputum[8].

The measurement of biomarker levels in cancer can be useful to assess the risk of an individual to develop cancer, non-invasive screening of apparently healthy individuals for malignancy and detection of occult tumours, diagnose patients with symptoms of cancer, provide a prognosis for individuals who have already been diagnosed with the disease, differentiate from malignant and benign forms of tumours and also distinguish different types of malignancies and monitor the status of the disease, by predicting the likelihood of tumour recurrence or therapy response[8] (**Figure 1**).

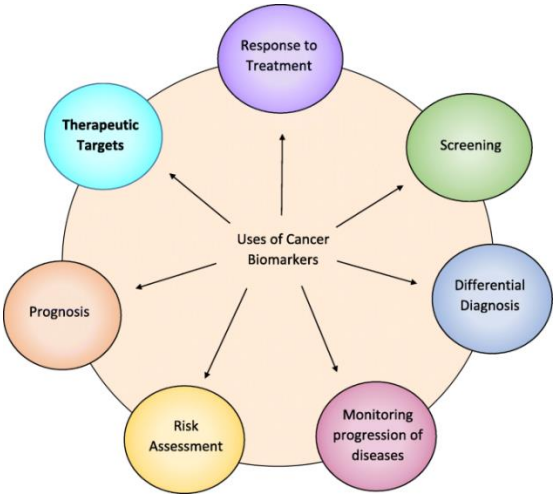

Figure 1 *- Clinical uses of Cancer Biomarkers. Adapted from M. Townsend, G. Shrestha, et al. (2018)*[9]

Based on their utility, cancer biomarkers can be classified[10] as (1) Early detection biomarker – which is used to identify early stages of cancer; (2) Diagnostic biomarkers - used to detect the presence or absence of a tumour in an individual. Cancer-antigen 125 (CA125) and prostate specific antigen (PSA) are examples of diagnostic biomarkers used in the clinical field; (3) Prognostic biomarker – used to predict tumour behaviour including recurrence of the disease and identify the aggressive phenotype. It also provides information regarding patient survival probabilities, allowing for more personalised therapies. Examples of this type of biomarkers are PSA in prostate cancer and hormone receptors in breast cancer; (4) Predictive biomarker – used to assess the effectiveness of a specific drug, helping in the identification of the best treatment options; (5) Target biomarker – used in the identification of molecular targets of new therapies to help select patients that will benefit from those particular treatments. (6) Surrogate end point biomarker – used to substitute a clinical end point, which is a "characteristic or variable that reflects how a patient feels, functions, or survives" [11] or to determine the clinical benefit or lack of benefit based on scientific evidence [11,12].

Regardless of the type of biomarkers, an ideal tumor marker[1] should (i) only be produced by tumour cells, (ii) be present at high concentrations in an individual with cancer, but be undetectable in a person without the disease or with benign disease, (iii) be present at measurable quantities at an early stage of the disease, (iv) demonstrate predictive, diagnostic and prognostic value simultaneously and (v) be measured, even when present in small concentrations, through a relatively inexpensive and reliable assay, with high analytical specificity (percentage of normal individuals that test negative for the biomarker, i.e., ability to exclude false positives) and high analytical sensitivity (likelihood of an individual with the disease testing positive for the biomarker, i.e., ability to detect true positives).

Both sensitivity and specificity are essential criteria to evaluate the usefulness of a biomarker. Indeed, there are serious challenges that must be addressed when screening for cancer. Firstly, false-positive screening tests are frequent, since several tumour markers tend to have high sensitivity and low specificity, which ultimately may result in unnecessary and invasive diagnostic procedures, increasing the suffering and anxiety of patients. In order to prevent false-positive tests, multiple biomarkers must be assessed simultaneously to increase the specificity and sensitivity of cancer diagnosis screening tests. Secondly, biomarker screening can also lead to false negative test results, entailing serious complications as delayed diagnosis and treatment. Thirdly, overdiagnosis, which translates in the detection of a condition that would not have led to clinically significant symptoms during an individual's lifetime[13,14]. Moreover, several factors can directly affect the sensitivity and specificity of tumour detection tests, including how efficient is the recognition and attachment of the target analyte to the antibody molecule, the amount of measurable signal arising from the binding event, the signal interference caused by non-specific interactions, the influence of non-target proteins present in the sample under analysis, among others. Therefore, it is important to establish detection methods capable of enhancing the performance of biomarker screening, by minimizing background signal, impeding non-specific interaction between molecules in the sample and amplifying the signal obtained.

Indeed, there are no perfect biomarkers, i.e., a biomarker which is detected in every individual with cancer (100% sensitivity) and absent in every individual without cancer (100% specificity) and it is precisely the lack of sensitivity and specificity that prevents many potential biomarkers from progressing from discovery to clinical applications[1,2,14]. The discovery of new cancer biomarkers is an extremely important step in cancer diagnosis however, it is a highly regulated and time-consuming process. In fact, before being approved as clinical screening tools, biomarkers must go through a rigorous evaluation and validation process proposed in 2001 by the National Cancer Institute's Early Detection Research Network (EDRN). This process consists of a five-phase approach, which includes: Phase 1 – Preclinical Exploratory Studies; Phase 2 – Clinical Assay Development and Validation; Phase 3 – Retrospective Longitudinal Studies; Phase 4 – Prospective Screening Studies; Phase 5 – Cancer Control Studies[15]. To be accepted as a screening tool, biomarkers must go through all these steps and reach the last phase successfully. However, this process is expensive and can take several years to be concluded, and so far, only few biomarkers were able to be successfully approved. Therefore, more effective and reliable strategies are required to determine which potential tumor marker justifies the major investment of money and time needed for biomarker validation. Attempts are being made to discover new biomarkers, ensuring a good analytical sensitivity and specificity, thereby maximizing the probability that these markers will be useful screening tests for early detection and treatment follow-up [2]. Considering this prerequisite, investigators have been using a variety of technologies for biomarker discovery and measurement, including DNA sequencing, mass spectrometry and electrophoresis, flow cytometry, immunohistochemistry, protein microarrays and antibody microarrays[16]. Although these technologies have the potential to identify novel tumour markers, it is crucial for an assay to have a great level of precision, robustness, sensitivity, and specificity. Finally, it is imperative to determine how these new biomarkers will be assessed and integrated in the clinical arena, since this assay must be cost-effective, robust and the samples obtained in a non-invasive manner[2].

1.3. Antibodies and Immunoassays

1.3.1. Antibody Structure

Currently, the most used method for biomolecules detection and quantitative measurement are antibody-based detection systems[16]. Antibody molecules are Y-shaped proteins produced by the immune system of animals and humans as an immunological response to the presence of antigens. Antibodies consist of four peptide chains: two identical light chains (LC) and two identical heavy chains (HC). Each of the light and heavy chains is linked through dissulfide bonds, thereby forming a heterodimer. In turn, each heavy chain is connected to the other through dissulfide bridges, linking the two heterodimers together and forming a 4-chain immunoglobulin[17]. Each chain consists of a series of about 110 amino acid sequence, in which the light chain has two of such domains, whereas the heavy chains are made up of four [18].

The antibody structure has two different regions, a variable region (V) located at the end of the amino-terminal region of heavy and light chains (limited to the first 110 amino acids approximately), which presents a great variability among different antibodies of different specificity and is involved in antigen binding reactions and a constant domain (C), which is the remaining part of the antibody molecule, presenting less sequence variability between different antibodies. The C domain is responsible for interactions with effector cells and molecules[17,18].

Light chains can have two amino acid sequences in the C domain, thereby existing two distinct types of light chains: λ and κ. Each antibody molecule can only have one single type of light chain, never both. Regarding the heavy chains, five different amino acid sequences can be identified in the C domain, which determine the functional activity of the antibody: $\mu, \gamma, \delta, \epsilon$ and α (**Figure 2**). According to these different types of heavy chains, antibodies can be classified as IgM, IgG, IgD, IgE or IgA[17]. The most abundant isotype of antibody molecule is IgG, consisting of 80% of total serum immunoglobulin.

Depending on the antibody class, heavy chains can contain three or four constant domains, named C_H1, C_H2, C_H3 and C_H4 and one variable domain, termed V_H, whereas light chains contain one constant domain and one variable domain, named C_L and V_L, respectively. These protein regions associate to form larger domains, therefore identical domains are linked to each other through non-covalent interactions (C_H2/ C_H2, C_H3/ C_H3 and/or C_H4/ C_H4), whereas V_L and C_L domains are paired with V_H and C_H1 domains, respectively, through dissulfide bonds, forming the antigen binding site of the antibody molecule[19]. The set of complete light chains linked to heavy chain domains V_H and C_H1 form Fab fragment of the antibody molecule, which stands for **F**ragment **a**ntigen **b**inding. Fab fragment is, in turn, linked to Fc fragment (**F**ragment **c**rystallize) of the antibody, through a hinge region, corresponding to the association of C_H2, C_H3, or C_H4 domains from both heavy chains[18,19].

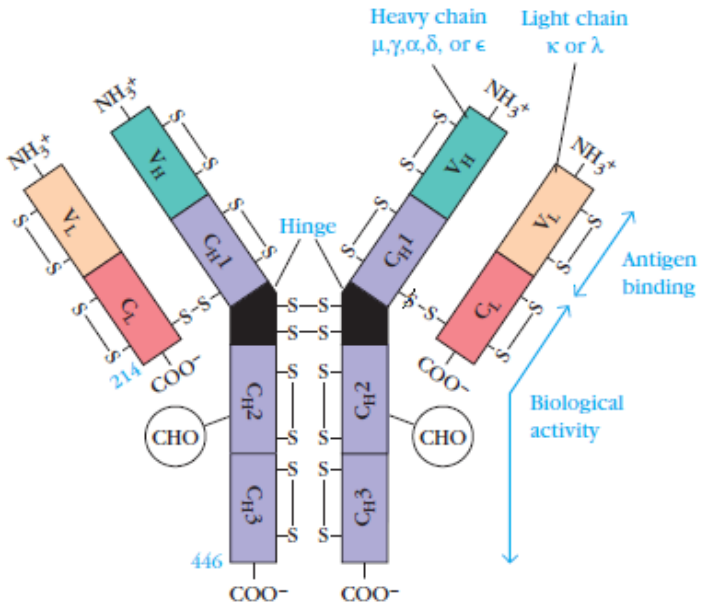

Figure 2 *- Schematic representation of antibody molecule structure. Adapted from Goldsby, R. et al. (2002)* [17]

Antigen-antibody binding involves several non-covalent interactions, including hydrophobic interaction, electrostatic interactions, hydrogen bonds and Van der Walls forces between the epitope of the antigen and the variable complex domain (V_L – V_H) of the antibody[20]. These interactions are weak in comparison with covalent interaction, therefore several bonds are required so that a strong antigen-antibody interaction is formed. The strength of these non-covalent bonds between the antigen epitope and the binding site on the antibody determines the affinity of the antibody to that specific epitope. Antibodies that are bound tightly to the antigen are high-affinity antibodies, thereby remaining linked to the antigen longer, whereas antibodies that are weakly bound to the antigen, called low-affinity antibodies, are likely to dissociate easily from the antigen[17]. The high specificity and affinity that describes antigen-antibody interactions have paved the way for the use of immunoassays as an important tool in the biomedical field for disease diagnosis, monitoring and treatment.

1.3.2. Immunoassays

Over the past few decades, several types of immunoassays have been developed for the detection and quantification of biological analytes. Immunoassays are biochemical methods that depend on the recognition and binding of an antibody to a specific site of the target antigen (epitope). In response to the antigen-antibody binding reaction, a signal is generated, and its detection relies on several labels, which are attached either to the antigen or antibody, depending on the type of immunoassay. Common immunoassay labels include enzymes, radioisotopes, fluorophores, and chemiluminescent tags and according to these labels, different detection methods can be applied (chemiluminescence, fluorescence, radioactivity)[21]. Due to the labelling agents, immunoassays are usually the method of choice mainly because of their high sensitivity, specificity, and ability to achieve low detection limits[22].

1.3.2.1. Types of immunoassays

Immunoassays can be classified into two types: competitive or non-competitive. In competitive immunoassays, the analyte of interest competes with a similar amount of labelled analyte for a limited number of antibody binding sites. Therefore, when the reaction reaches equilibrium, the signal obtained is inversely proportional to the concentration of the analyte to be quantified. These type of assays presents a high ability to detect smaller analytes, such as hormones or drugs. Immunoassay can also be non-competitive, which are also known as immunometric immunoassays, in which an excess of labelled antibodies captures the analyte of interest. One of the most used types of non-competitive assays is two-site or sandwich immunoassays, first demonstrated in 1971 by Wide[23]. In this sandwich method, the analyte reacts with an excess of unlabelled antibody immobilized on a solid-phase and is subsequently detected by an excess of labelled antibody, which binds the analyte at a different epitope. Thus, in non-competitive immunoassays, the antigen concentration is directly proportional to the amount of labelled antibody[24,25].

In sandwich assays the target antigen is captured between two recognition molecules: a capture antibody or recognition probe and a second antibody, called detector antibody. Upon the formation of an immune complex composed of the analyte and the two recognition molecules, the label attached to the detector antibody outputs a detectable signal, revealing the presence and concentration of the target analyte. Due to the usage of two molecules for the recognition of the target analyte, the sandwich immunoassays are more robust and usually give higher sensitivity and better signal-to-noise ratio, thereby being currently the prevailing method in research and clinical diagnosis, including the quantification of cancer biomarkers[24,25].

After antigen-antibody reaction, the unbound analytes need to be removed and separated from the bound analytes. According to this separation, two other types of immunoassays can be distinguished: heterogeneous and homogeneous immunoassays. In heterogeneous immunoassays, after the immobilization of the antibody on a solid-phase and subsequent binding of the antigen, the unbound antigen is washed and separated from the surface, whereas in homogeneous immunoassays, the antigen-antibody binding occurs in solution, and the separation of unbound and bound antigens is done through chemical or physical changes resulting from the binding reaction[25]. The latter type of immunoassays is less common and since no wash is required, some substrates in solution can interfere with the immunoassay, decreasing its efficiency. The choice between these different types of immunoassays relies on antibody and antigen nature, labelling agent available, and the desired analytical criterion, such as specificity, sensitivity, precision, detection limit.

1.4. Prostate Cancer

1.4.1. General Concepts

Prostate Cancer (PC) is the second most frequent cancer affecting men worldwide, after lung cancer, with approximately 1.4 million new cases reported in 2020 [26]. At an early stage, prostate cancer can be asymptomatic, thus making the early diagnosis difficult. PC is described as an abnormal growth of cells, which causes an enlargement of prostate gland[27]. This marks the beginning of prostate malignant evolution which consists of a multistep process, starting as prostatic intraepithelial neoplasia (PIN), followed by localized prostate cancer[28]. If the cells continue to grow in an uncontrollable manner, it progresses to an advanced prostate adenocarcinoma with invasive characteristics, ultimately spreading to other tissues and organs, in a process known as metastasis (**Figure 3**).

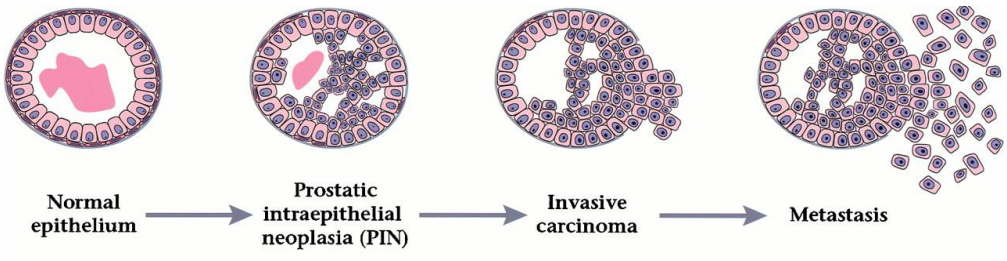

Figure 3 *- Stages of progression of human prostate cancer. Adapted from Elo et al. (2001)* [29]

Advanced and metastatic prostate cancer increases rates of mortality; however, most men are diagnosed with prostate cancer when the disease is still at a localized stage, which increases rates for successful disease management and cure, consequently improving patients' overall survival rates[30]. Therefore, early detection of prostatic malignancies is highly beneficial in terms of treatment options and control of the disease progression. The most routinely used test for early detection of PC is Prostate-Specific Antigen (PSA) blood test, which revolutionized the world of diagnosis, prognosis, and monitoring of this disease[31].

1.4.2. Prostate Specific Antigen (PSA)

PSA was the first cancer biomarker ever approved for patient screening and diagnosis in 1994 by the United States Food and Drug Administration (FDA)[32]. PSA is a glycoprotein that belongs to the family of kallikrein proteases, also called kallikrein 3 (hK3), and is expressed by prostate epithelium and secreted into seminal plasma, in both cancerous and normal prostatic tissue. Its main function is to cleave proteins Semenogelin I and Semenogelin II that constitute seminal coagulum formed after ejaculation in order to dissolve it[32]. Despite PSA being considered a valuable tool in the detection of PC, there is no consensus among the scientific community regarding the reliability and utility of routinely PSA screening tests, with some specialists arguing the lack of sensitivity and specificity of PSA as a biomarker for the detection of PC. In fact, PSA can only be considered a prostate-specific biomarker instead of a PC-specific biomarker, since elevated serum levels of PSA are associated with several prostatic pathologies and not only cancer, including benign abnormalities, such as Bening Prostatic Hyperplasia (BPH) and physical trauma of the prostate. The most promising approach used to enhance the specificity of PSA and consequently improve PC diagnostic accuracy relies on the measurement of different molecular forms of PSA in serum.

PSA can be found both free or bound to other proteins, such as α_1-antichymotrypsin (PSA-ACT), which accounts for about 75% of PSA in serum, or in minor portions with α_2-macroglobulin (PSA-A2M) or α_1- protease inhibitor (PSA-API). Complex PSA, which comprises PSA-ACT and PSA-API, is not very used in clinical practice because in patients diagnosed with PC, PSA-API values tend to be reduced, while PSA-ACT levels are increased. Therefore, complex PSA does not seem to be associated with malignant disease. To quantify the levels of complex PSA, it is common to recur to immunoassays or, alternatively, quantify the totalPSA and then subtract to it the freePSA levels[33].

The remaining PSA is considered freePSA, which is unbounded to protease inhibitors and comprises at least three inactive forms: PSA precursor (proPSA), benign PSA (BPSA) and intact inactive PSA (inPSA). PSA is produced by prostate epithelium cells as proPSA, which is an inactive proenzyme with an amino-terminal pro-leader peptide, also referred to as [-7]pPSA in addition to the 237 amino acid sequencing that constitutes mature PSA. Upon migration of proPSA to prostatic ducts, this amino terminal is removed so that PSA becomes active. Kallikrein 2 (hK2) is the peptidase responsible for the

activation of the PSA. Moreover, Mikolajczyk *et al*.[34] proved that the truncated forms of proPSA, such as [-4]pPSA, [-5]pPSA and [-2]pPSA originated by proteolytic cleavage of pro-leader peptide [-7]pPSA, are highly expressed in serum of individuals with PC and diminished in the prostatic transitional zone (TZ). In the same study, they proved that these truncated forms, with special emphasis for the isoform with pro-leader peptide with only 2 amino-acids, are more cancer-specific than other PSA-isoforms, since they are prevailingly expressed in epithelium of carcinogenic prostatic tissue. BPSA is considered a degraded form of native PSA (with the same 237 amino-acids) since it is believed to result from proteolytical cleavage of amino-acid residues from intact free PSA at Lys182 and Lys145. Seems to be a good indicator of prostate enlargement, being significantly elevated when BPH symptoms are present, because several studies found a correlation between its secretion and a large-volume prostate TZ, thereby being considered a promising biomarker for BPH, especially if used in combination with proPSA immunoassays[33,35,36]. This isoform of PSA is not detectable in healthy individuals and is present at lower concentrations in patients with PC. BPSA can be found in the blood and seminal plasma[36]. Regarding inPSA, it is identical to native PSA but in an enzymatically inactive form, essentially due to conformational or structural alterations[36]. While proPSA and BPSA are associated with the presence of PC and BPH, respectively, there is no evidence suggesting a correlation between inPSA and cancer, some studies even attest a decrease in inPSA levels in PC, therefore it is more associated with benign disease[37,38]. The three different molecular isoforms of freePSA are depicted in **Figure 4**.

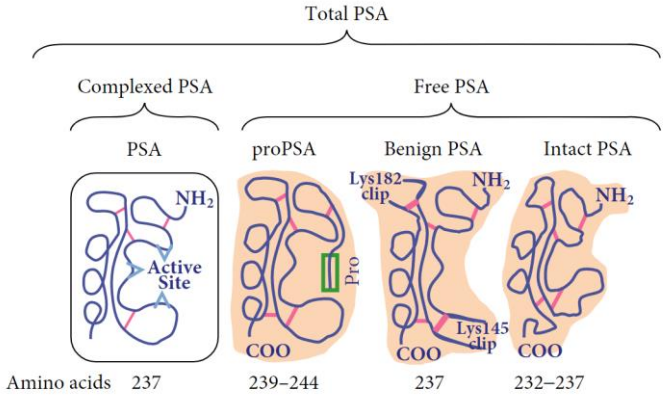

Figure 4 *- Isoforms of PSA. Majority of PSA in serum exists as a complexed form, i.e., PSA associated with several protease inhibitors. FreePSA consists of three molecular forms: PSA precursor (pPSA), benign PSA (BPSA) and intact inactive PSA (inPSA). Only pPSA is relevant in prostate cancer. BPSA is associated specifically with Benign Prostate Hyperplasia (BPH), whereas inPSA correlates with benign disease. Adapted from Hori et al. (2013)*[37].

PSA is produced in secretory epithelial cells present in prostate glands and is directly secreted into the lumen. Around these epithelial cells, there is a layer of basal cells and an adjacent basement membrane, which acts as a barrier impeding PSA from escaping. In normal conditions, the proPSA produced by epithelial cells is secreted into the lumen and subsequently activated by human glandular kallikrein 2 (hK2). Part of this active form of PSA can then travel into peripheral circulation where it is complexed with available protease inhibitors. Additionally, in the lumen, the other portion of active PSA can become inactive via proteolytic cleavage and can also migrate to the peripheral circulation, where it travels as free unbound PSA. However, in PC cases, both the basement membrane and layer of basal

cells is disrupted, and the architecture of normal lumen is lost, which causes an influx of proPSA and bound PSA directly to the bloodstream, since the activation of proPSA and further inactivation is decreased[35] (**Figure 5**). Therefore, in healthy individuals, secreted proPSA goes directly to seminal plasma and does not enter the blood circulation and freePSA in blood represents the native protein that was inactivated, whereas in prostate cancer, proPSA is release to the blood and the inactive fraction of freePSA is highly decreased, leading to a lower freePSA to totalPSA ratio.

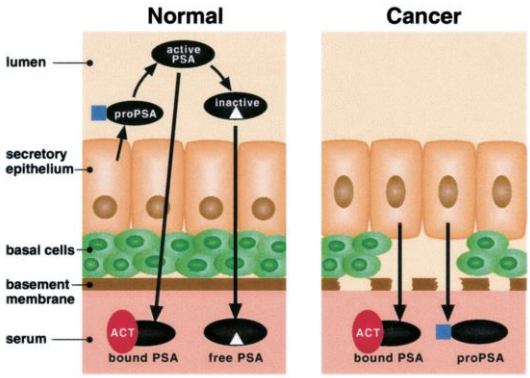

Figure 5 *- Biosynthesis of Prostate Specific Antigen Isoforms in normal versus carcinogenic prostatic tissue. Adapted from Balk et al. (2003)[35].*

The standard procedure to diagnose PC is to test the levels of total PSA (free plus complexed PSA). When these levels stand above 10 ng/mL, the patient is regarded as suspicious for cancer, thus indicating the need for further biopsy procedures and digital rectal examination (DRE). When the level of totalPSA is included in the diagnostic "gray zone", between 4 ng/mL and 10 ng/mL, then the freePSA to totalPSA ratio, also called the percentage of freePSA (%fPSA), can be advantageous in the discrimination of PC from benign prostatic disease, even though it is associated with many false positives. Catalona and co-workers[39] studied the relation between the freePSA to totalPSA for differentiation of benign prostate disease and prostate cancer in a cohort of 773 men, in which 379 had prostate malignancy and 394 benign prostate disease. The study concluded that man with PSA levels within the "gray zone" present a risk of PC of less than 8% when the %fPSA is greater than 25%, whereas a %fPSA of less than 10% is associated with a risk of PC greater than 56%. The measurement of %fPSA has proved to be valuable in the reduction of unnecessary biopsy procedures[40], improving the sensitivity of cancer detection for total PSA values between 4-10 ng/mL. Therefore, the risk of having prostate cancer increases as the %fPSA decreases. However, in patients with PC, increased prostate volume is associated with higher %fPSA, due to a dilution effect caused by prostate enlargement. Consequently, patients with BPH might receive false-negative results, increasing the risk of delayed diagnosis[41]. In fact, the assessment of totalPSA values is still regarded as the gold standard because it is capable of detecting clinically insignificant prostate disease, being able to minimize unnecessary biopsies[42]. Nevertheless, all isoforms of PSA can be further analysed to verify whether they promote a more accurate and reliable PC diagnosis, particularly if used in combination with several other biomarkers, to enhance system sensitivity.

1.5. Aqueous Biphasic Systems and Ionic Liquids

Generally, cancer biomarkers are primarily found in biological fluids, namely whole blood, plasma, serum, or urine, which poses some challenges, regarding their detection and quantification. Firstly, biological fluids are often composed by a miscellaneous of proteins present at high abundance, which can hinder the detection of a specific marker and lead to higher signal background, as a consequence of non-specific interactions. For instance, serum contains more than 10,000 proteins, with albumin being the most abundant component with a concentration varying between 35 to 50 mg/mL[43], which in most cases represents 10 orders of magnitude difference in comparison with the concentration of some target cancer biomarkers present in serum. Secondly, target tumour markers exist in low concentration in biological fluids and do not have the ability to replicate themselves to increase their concentration, as, for instance, nucleic acids. Therefore, in order to detect and reliably quantify low concentration of cancer biomarkers integrated into complexed biological matrices and prevent interferences from non-target proteins, an appropriate sample pre-treatment is necessary to ensure an accurate diagnosis. This sample pre-treatment may consist of amplification, pre-concentration, purification, or extraction of the target analyte from the complexed sample.

Even though conventional methods for purification and extraction of active biomolecules have well established protocols, are easily obtained and present good immiscibility properties, in recent years, there has been a greater tendency to search for more ecological and “greener” methods, while maintaining a high degree of efficiency. In that context, Aqueous Biphasic Systems (ABS), originally presented by Albertsson in 1958[44] can be seen as good alternatives for conventional methods, being widely employed in the separation and purification of active substances, like proteins, enzymes, cells, and nucleic acids.

ABS are considered a highly biocompatible method, essentially due to their aqueous composition in both phases. They are formed by two phases, which can be based on two polymers, a polymer, and a salt or two salts, dissolved in aqueous media. Specifically, each of the two aqueous phases becomes enriched in one of the two components and, above a certain concentration of the polymer and/or the salt, these solutions separate into two immiscible phases, which promotes partitioning of target bioactive substances between them[45]. This partitioning relies on specific properties of the molecule itself, namely its polarity, hydrophobicity, affinity for each water-rich phase and electrical charge, which will define which one of the two phases the molecule will migrate to[45]. Polymer-based ABS have received remarkable attention in the past few years, with several published studies attesting their suitability for extraction and concentration of different biomolecules, including extraction of extracellular vesicles from human serum, which can be used as biomarkers in tumor detection[46], separation of alkaline phosphatase from its corresponding isoforms[47], study of partitioning behaviour of PSA in the presence of non-target serum protein[48], partitioning of DNA genomic fragments and subsequent detection step for early cancer detection[49], among others. Despite being considered a promising technique, polymer-based systems have some limitations, such as the high viscosity of some polymers, which hampers mass transfer of the target biomolecule and delays the separation of the two phases. Furthermore,

polymers present a limited polarity range, which restricts their applicability in several extraction procedures and hinders their use in scaled-up processes. Therefore, ionic liquid-based systems have been gaining ground since Gutowsky *et al.* [50] induced aqueous solution of ionic liquids to form ABS by adding inorganic salts, specifically, kosmotropic salts. Ionic liquids (ILs) are salts liquid at a temperature below 100ºC, constituted by organic cations and organic/inorganic anions[51]. ILs are recognized by their good thermal and chemical stability, as well as for displaying negligible volatility and being non-flammable and easily recyclable components. Additionally, ILs present a high degree of tunability, due to the elevated number of possible combinations of their anions and cations and strong solvation ability for a large selection of compounds. Due to these excellent properties, ILs are being considered the best eco-friendly alternatives for replacing polymers in formation of ABS [52,53]. The chemical structures of commonly used cations and anions' acronyms that make up ILs are illustrated on **Figure 6**.

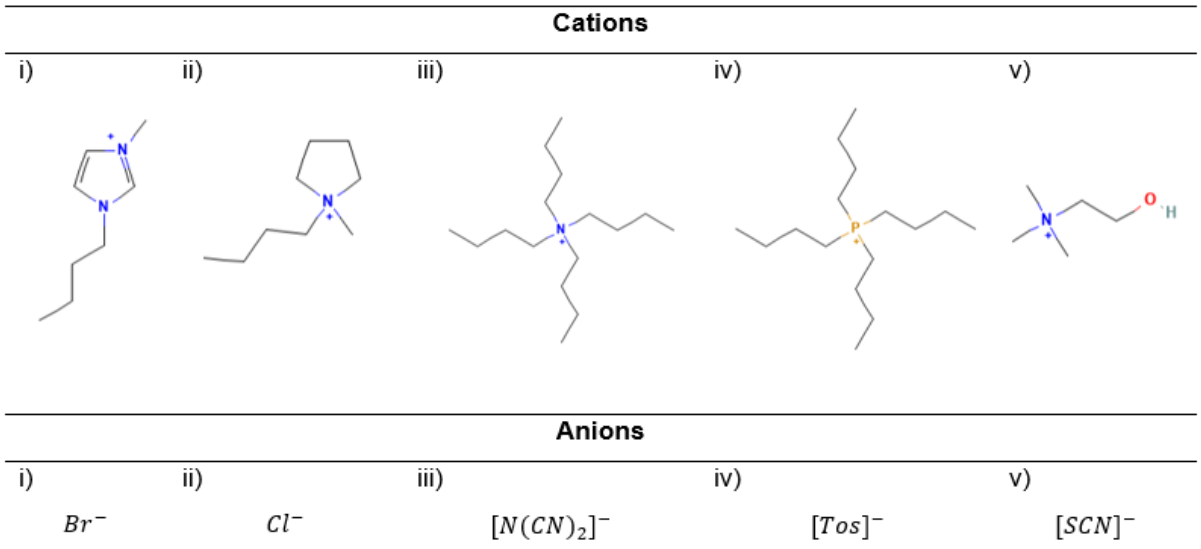

Figure 6 *- Chemical structure of cations and acronyms of anions for ionic liquids commonly studied. Cations: i) 1-butyl-3-methylimidazolium; ii) 1-butyl-1-methylpyrrolidinium; iii) Tetrabutylammonium; iv) Tetrabutylphosphonium; v) Choline. Anions: i) Bromide; ii) Chloride; iii) Dicyanamide; iv) Tosylate; v) Thiocyanate. A combination of all cations and anions i) and ii) was used in the present work.*

Several studies demonstrate the applicability of IL-based aqueous biphasic systems (IL-ABS) in the extraction of different biomolecules, including alkaloids[54], immunoglobulin Y[55], bovine serum albumin[56,57], trypsine[56,57], haemoglobin[57,58], antioxidants and carbohydrates[59], pepsin[58], among others. In 2010, Freire *et al*.[54] reported for the first time the usage of several imidazolium-based ionic liquids as constituents of aqueous biphasic systems for the extraction of alkaloids. The group work concluded that is possible to extract caffeine and nicotine from aqueous or urine-type solutions in a single step procedure, with the advantage of using green and recyclable solvents instead of volatile and toxic components. Furthermore, the study also proved that this IL-based ABS are promising in the obtention of concentrated samples of nicotine and caffeine for a posterior analysis. In 2015, Taha and co-workers[55] proposed a novel system for the extraction and purification of immunoglobulins Y (IgY) based on a new

class of ILs. The group work took advantage of the low toxicity and biodegradability of cholinium cations and paired them with Good's Buffer anions, which are highly beneficial in protein studies, due to their non-toxicity and minimum interaction with reaction components. These novel cholinium-based Good's buffer type ILs allowed the formation of biocompatible ABS in combination with poly(propylene) glycol with the ability to extract and purify IgY from egg yolk aqueous solutions. Extraction efficiencies ranging from 79% to 94% were reported, making these systems good candidates for extraction and purification of other proteins in future studies. Moreover, Li *et al*.[56] also documented the usage of cholinium-based ILs in combination with poly(propylene) glycol in the formation of green aqueous two phase systems for the extraction of several proteins, namely, bovine serum albumin, trypsin, papasin and lysozyme. The study proved that with a single step process it is possible to successfully extract 86.4% to 99.9 % of these proteins to the IL-rich phase and it was even possible to increase the activity of one of the proteins under analysis, trypsin, in most of the IL-rich phases tested. Additionally, Lin *et al*.[57] reported the usage of aqueous two-phase systems based on eight different hydrophobic ILs and inorganic salts and analysed the performance of these types of systems in the extraction of four proteins, bovine serum albumin, haemoglobin, trypsin and lysozyme. Remarkable recovery efficiencies were attained ranging from 90.5% to 94.5% for the referred proteins. Therefore, Lin and co-workers were able to prove ILs-ABS systems are a valuable technique for the extraction, purification, and concentration of several bioactive molecules.

Despite all scientific evidence regarding the powerfulness of IL-based ABS, to the best of our knowledge, there are no reports concerning the applicability of these systems in the efficient extraction of cancer biomarkers from body fluid samples and subsequent quantitative analysis through a microfluidic system. Therefore, the present work presents an initial evaluation on the effects and possible interferences of ionic liquids in the detection of cancer biomarkers in microfluidic systems, paving the way for further application of these greener and recyclable solvents in ABS for extraction/concentration of tumor biomarkers, potentially improving early cancer detection.

1.6. Microfluidics

1.6.1. General Concepts

In recent years, microfluidics has emerged as a novel fluid manipulation technique with several applications in the biomedical and biotechnology fields, namely the development of more affordable and easy handling devices for disease diagnosis, pharmaceutical drugs quality assessment and evaluation of water and food safety. As stated in the previous sections, immunoassays are biochemical tests employed for the identification and quantification of certain analytes based on antigen-antibody recognition, which usually relies on highly skilled personnel, bulky equipment and high-volume samples and reagents. Besides, conventional immunoassays can take several hours to be completed, since they include a series of incubation, mixing and washing steps. Therefore, microfluidics plays an important role in the miniaturization and automation of immunoassays, significantly reducing the consumption of

samples and reagents, reducing the assay time by simplifying procedures, allowing a faster analysis and detection, and reducing the costs of traditional immunoassays[60]. Furthermore, considering the wide range of materials and techniques available nowadays, investigators can create different microfluidic designs for the detection of several biological molecules. These attractive features have led, over the past few decades, to the transition of benchtop systems to lab-on-chip (LOC) devices (**Figure 7**).

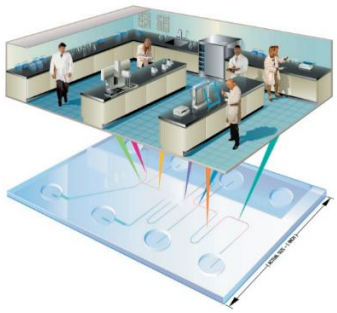

Figure 7 *- Transition of laboratory processes to microfluidic devices. Adapted from Chow, A. W. (2002)* [61].

1.6.2. Lab-on-chip devices for Point-of-Care diagnosis

The key benefits associated with LOC devices are portability, automation, and integration of multiple assay steps into one device. These devices have the ability to integrate several functions in only one chip, minimizing multiple assay steps, which are time-consuming and can cause experimental errors, thereby leading to faster analysis which would not be achieved otherwise. Automation enables results of higher quality, since operations performed in these systems become more reproducible and more precise, whereas portability paves the way for point-of-care (POC) diagnosis, thereby reducing the time interval between diagnosis and treatment. These three attractive features combined culminate in high-throughput screening and high-quality results, as well as simplification of complex processes. Therefore, LOC devices have gained major importance in the medical field, especially in disease diagnosis arena, since they are capable of providing rapid, accurate and on-site diagnostic results at relatively low cost. The vast majority of LOC devices derives from microfluidic technologies, taking advantage of small volume fluid handling in microscale channels. Furthermore, thanks to microfluidic technologies, LOC systems encompass all the abilities of a laboratory, since they can perform pre-treatment of samples and analytical separation, mixing solutions, signal amplification, and detection of specific targets by means of electrochemical or optical sensors integrated on a single device. Additionally, the higher surface area-to-volume ratio of microfluidic channels, enables a faster sample analysis, translating into faster diagnosis, which can dictate patient recovery or survival. Owning to these advantages, POC testing has gained special interest among researchers, who have been exploiting them in terms of usability and development[62–64]. Consequently, advances are being made in the development of reliable point-of-care tests for disease diagnosis, namely in cancer patients for tumour biomarkers detection [65,66].

An ideal POC test would consist of a user-friendly device in which a non-trained person could load an extracted body fluid sample, such as blood, saliva, or urine, and obtain informative, sensitive, and accurate results in a much faster and non-invasive manner, at the patient-site without the need to perform the test in a specialized laboratory. These small medical devices can be used for the detection of several biomarkers, such as nucleic acids, proteins, metabolites, and cells. Besides, the device should have a high sensitivity limit to be able to detect low analyte concentrations, a large dynamic range, and should be capable of performing multiplexed detection [62].

1.6.3. Polydimethylsiloxane (PDMS)

The fabrication of the first microfluidic devices was based on microelectronic processes, such as photolithography and etching, using glass or silicon. However, glass amorphous structure hinders etching process on vertical walls of the glass device and silicon is not indicated for use with optical detection systems, since is an opaque material[67]. Furthermore, both materials make the fabrication process time-consuming and often associated with costly equipment and consumables. Therefore, polymers have been exploited in the fabrication of cost-effective microfluidic devices. Polymethyl methacrylate (PMMA), polycarbonate, polystyrene (PS), and polydimethylsiloxane (PDMS) are some examples of polymers used in the fabrication of these devices. In general, polymers are cheaper than glass and silicon and enable the formation of microfluidic channels by means of embossing or molding, instead of etching. Nowadays, the most commonly used polymer is PDMS, which shows and excellent permeability to gas, is chemically inert and biocompatible, and presents a good thermal stability (below 150ºC), which are useful features for certain chemical applications, especially in microfluidics. Besides these characteristics, PDMS also presents a good flexibility, optical transparency down to 230 nm, enabling direct optical access into microchannels and real-time assessment of the process, low autofluorescence, and its low thermal conductivity allows PDMS to be used as good thermal isolator ($thermal\ conductivity\ \approx 0.15\ W\ m^{1}\ K^{-1}$). The chemical structure of PDMS is depicted in **Figure 8**.

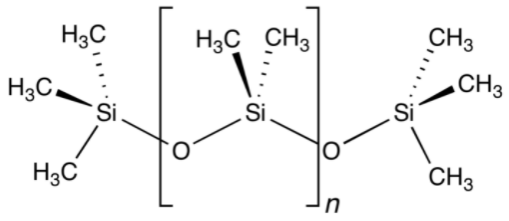

Figure 8 *- Polydimethylsiloxane chemical structure. Adapted from* [68].

Initially, the most used microfabrication technique for microfluidic devices was photolithography, however, this technique presents several limitations, for instance, it is very expensive, since the equipment used in this technology was specially created for the development of microelectronic devices; provides a limited surface chemistry control; it is less accessible because it requires a cleanroom

environment and does not allow the patterning of non-planar surfaces [69,70]. Therefore, in 1998, Whitesides and his research group created a novel technology, called soft lithography, which is define as "non-photolithography set of microfabricating methods (…) to generate micropatterns and microstructures" [69]. In comparison with photolithography, soft lithography is a much cheaper, accessible, and easy to learn technique, allowing pattern generation in nonplanar surfaces and usage of a wide range of materials. In soft lithography, an elastomer, typically PDMS, is poured on top of a mold with embedded patterned features on its surface and cured for a few hours at elevated temperatures and, in the end, it is peeled from the mold [69]. However, the master mold fabrication is still dependent on photolithography technique, in which a patterned, designed in computer-aided design (CAD) software is projected on a photomask with is then used to create relief structures onto a photoresist film [71,72]. Therefore, once the mold development is complete, the procedure can continue to take place outside the cleanroom, which facilitates the process.

The commercially available PDMS is supplied in a two-part kit, composed of a curing agent and a silicon agent that are mixed in a ratio of 1:10 and subsequently placed in a vacuum chamber to release all the air bubbles formed. After being cast against the mold and cured, the liquid mixture becomes solid, and its low surface energy allows PDMS structures to be easily removed from the master mold[73,74]. However, this property also makes the PDMS surface strongly hydrophobic, which poses challenges when used in immunoassays, due to nonspecific protein adsorption, formation of air bubbles, and poor surface wettability hindering liquid delivery. To address this problem, several techniques to activate/modify the surface of the PDMS can be applied, such as oxygen plasma treatment, ultraviolet (UV) radiation, and corona discharges. The oxidation of the PDMS surface using oxygen plasma is the most commonly used method, which converts the silane groups ($Si\text{-}CH_3$) on the surface into silanol groups (Si-OH), increasing the wettability of the surface and rendering it more hydrophilic. Besides the activation of PDMS surface, this treatment is also used to seal the structures against another PDMS or glass surface, forming an irreversible sealing and allowing the structure to withstand high pressures (30-50 psi). On the one hand, PDMS surfaces can quickly recover their hydrophobicity within minutes, when exposed to air. On the other hand, if the surfaces are exposed to oxygen plasma treatment for extended periods, undesirable cracks can appear on these surfaces, impairing the bonding of the structure. Therefore, the surface treatment of PDMS structures must be well controlled[75].

1.6.4. Microbead-based Immunoassays

The performance of microfluidic heterogeneous immunoassays can be enhanced using microbeads as a solid surface for the immobilization of biomolecules. Indeed, the exploitation of microbead-based immunoaffinity assays has been growing interest among the scientific community, with several publications describing the use of these platforms for biomolecules detection[73,76–78]. Even though naked microfluidic channels yield a large surface-to-volume ratio, microbeads provide a significantly higher surface for immobilization. For instance, if one considers 1 g of beads with a diameter of 0.1 µm, the surface area available for immobilization will account for 60 m^2 approximately[79].

Consequently, there is a better interaction between target and reagents, which translates into a higher sensitivity. Besides, other three aspects make the use of microbead-based immunoassays stand out in comparison with traditional configurations. Firstly, microbeads have a higher ability to bind a greater amount of molecules per volume of solution, thereby enhancing limits of detection. Secondly, the surface of microbeads can be functionalized, which improves their binding affinity[80]. The third aspect to consider is the transport of analytes. When, instead of a planar configuration beads are used, molecules can be easily transported by means of electric fields or pressure-driven systems, and packed beads also present an advantage in term of analyte transportation, since gaps between closed beads are smaller, thereby diffusion distances are minimized[79]. Therefore, microbeads provide a great improvement in the delivery and analysis of different types of biomolecules, making them suitable for the accurate detection of several biomarkers in microfluidic systems.

In the past two decades, several studies focused on developing and testing microbead-based assays for the detection of biomarkers for potential point of care diagnosis. In 2001, Sato *et al.* developed a successful microchip-based system for the detection of carcinoembryonic antigen (CEA), an important serological marker for colon cancer diagnosis, in which anti-CEA antibody coated polystyrene beads were used. In comparison with an assay in a microtiter plate, which took 30h to complete, this microchip system was able to perform the detection of CEA antigen in only 30 minutes and with better sensitivity than traditional methods[81]. Furthermore, in 2017 Qui *et al*. proved that a fully integrated single polycarbonate bead-based microchip can be used for the enumeration of CD4+T lymphocyte, through the detection of CD4 antigen from samples of lysed blood. The quantitative detection of CD4 was completely achieved within only 30 minutes after loading of blood samples on the microchip, with decent sensitivity and good detection limit, thereby proving to be efficient for POC testing[82]. Recently, in 2020, Lee *et al* developed a bead-bead multiplexed assay in which magnetic beads were used as solid support and conjugated with δ-catenin antibody to quantify δ-catenin levels, a potential cancer biomarker. The overexpression of this p120catenin subfamily member is associated with some types of cancer, such as prostate, ovarian, and lung cancer, among others. The group work managed to detect δ-catenin with increased analytical sensitivity in comparison with western blot method[83]. In the same year, Yuan *et al* studied a bead-based multiplexed system for the detection of two potential dengue virus biomarkers, DENV-NS1 protein and DENV-specific IgG antibodies, both present in blood samples of patients infected with the virus. In this experiment carboxyl-modified beads were separated into two different sets: bead set A was conjugated with anti-DENV-NS1 antibody to capture DENV-NS1 protein, whereas bead set B was conjugated with DENV-NS1 to capture anti-DENV-NS1 IgG antibodies. These beads were then introduced in microfluidic channels for multiplexed assay detection and calibration curves were obtained for different concentrations of the target analytes. In terms of detection limits and sensitivity, both assays were comparable with conventional ELISA methods, with lower limits of detection reaching 7.8 ng/mL for DENV-NSI and 15.6ng/mL for IgG, which are below the levels considered clinically relevant[84].

Beads can be classified into two types: magnetic and non-magnetic beads. Magnetic beads present advantageous characteristics in terms of microfluidic utility. Aside from its increased surface area-to-volume ratio, they are easily manipulated through the usage of magnetic fields, which eliminates the requirement of specific microstructures to trap beads in microfluidic systems to perform immunoaffinity experiments. Unlike magnetic beads, non-magnetic beads do need special structures to be retain in microfluidic channels[24,60]. However, these beads are extremely popular in the microfluidic assays, especially for DNA hybridization and proteins or toxins detection. Regarding DNA hybridization, Caneira and co-workers[76] developed a bead-based microfluidic model for detection of a specific DNA strand, which matches a sequence of miRNA commonly used as cancer and cardiovascular disease biomarker. The developed method relies on probe DNA immobilization on two different types of beads: electrostatic beads, namely Q Sepharose (QS) beads, and multi-mode beads, i.e., beads presenting hydrophobic and electrostatic interactions, namely CaptoAdhere (CA) beads. This single-step and cost-effective immobilization strategy was successfully achieved in 10 minutes. Overall, the reported system achieved a LoD of (9.5 ± 1.1) pM and (10.6 ± 0.6) pM for CA beads and QS beads, respectively, values comparable with similar studies, and a total analysis time of 10 minutes. Furthermore, food safety is another application of bead-based immunoassays. Indeed, in 2018 Soares *et al.*[85] reported a novel bead-based microfluidic competitive immunosensor for the simultaneous detection of three mycotoxins: aflatoxin B1 (AFB1), ochratoxin A (OTA), and deoxynivalenol (DON), commonly present in food and feed and often associated with carcinogenic and immunosuppression effects or hepatotoxicity on individuals. The main goal of the device was to detect the referred mycotoxins at relevant limits, minimizing the total time of analysis and the number of total steps required to perform the complete assay. Protein G agarose beads functionalized with anti-mycotoxin antibodies were used and packed in four microfluidic channels and integrated photodiodes were used for continuous fluorescent signal acquisition. The cost-effective and single step multiplexed microfluidic system proposed in this paper achieved a total analysis time of 60 seconds and low limits of detection, comparable to those established by the majority of EU regulations, fulfilling all the proposed objectives.

In the present work, agarose beads were used due to their extremely advantageous properties. These types of beads can be easily scalable, since they are produced in large batches and derive from low-cost and easily obtainable sources, like seaweed. Moreover, the agarose percentage can be controlled, which enables the management of analytes mass transport properties, since a lower agarose percentage allows for larger pore sizes, which increases the speed of mass transport of analytes in the bead matrix, thereby allowing faster binding rates. Other advantages include, good optical properties, important for separation purposes and for optical detection, allowing chemiluminescence, fluorescence and colorimetry, low non-specific binding properties, and the ability to be used in both competitive and sandwich assays[86].

1.6.5. Reynolds Number

Fluid dynamics classification into laminar or turbulent flow in microfluidics is predicted by a single dimensionless number, the Reynolds number. Considering that microfluidic channels present a small-scale dimension and stationary and incompressible flows are characterized by a single spatial scale, l, the Reynolds number can be defined as:

$$Re = \frac{Ul}{\nu}, \tag{1}$$

where U is the characteristic fluid velocity and ν is the fluid kinematic viscosity. Since microfluidic systems present microchannel dimensions on the order of tens of micrometres and usually fluid velocities do not surpass 1 cm/s, the Reynolds number is lower than 0.1. Moreover, it is considered that the scaling law for parameter U satisfies the relation $U \sim l$. From this, it is possible to obtain the scaling law followed by Reynolds number, which can be described as:

$$Re \sim l^2 \tag{2}$$

Therefore, systems miniaturization tends to benefit low Reynolds numbers, which consequently translates into a laminar flow regime. In this regime, diffusion is the most important phenomenon for mass transport[74].

1.7. Limit of Detection (LoD)

The implementation of any assay requires the assessment of analytical data, therefore method validation plays an important role in the production of accurate and reliable assay results. Hence, some parameters are commonly used for the characterization of analytical performance of any clinical assay, namely, the limit of blank (LoB), limit of detection (LoD) and limit of quantification (LoQ). These expressions are related, however, there is a lack of consensus among several regulatory agencies on the best way to describe them.

According to Armbruster and Pry[87], LoB is the highest concentration of target analyte that can be detected in replicates of a blank sample, i.e., in a sample with only buffer and no analyte present. It is obtained through the calculation of the mean value and standard deviation of blank sample, as described by the following equation:

$$LoB = mean_{Blank} + 1.645\ (SD_{Blank}) \tag{3}$$

LoD is considered as the lowest amount or concentration of target analyte in a sample that can be distinguished with certainty from LoB. A standard approach to determine LoD is to obtain the LoB and the standard deviation of replicas of a sample known to contain a low concentration of the target analyte. Therefore, the general formula used to calculate LoD is given by equation (4):

$$LoD = LoB + 1.645(SD_{low\ concentration\ sample}) \quad (4)$$

Another acknowledged method to calculate LoD is based on the mean value of the blank sample and the standard deviation of blank sample multiplied by a factor of three. Thus, this alternative can be written as:

$$LoD = mean_{Blank} + 3 \times SD_{Blank} \quad (5)$$

This definition of LoD indicates that if the non-specific signal between antibodies and antigen adsorption, responsible for excessive background signal, can be minimized, then it is possible to obtain better values for the LoD, thereby enhancing the sensitivity of the immunoassay.

Finally, LoQ is described as the smallest target analyte concentration which can be detected, with acceptable signal and trueness, operating as bias estimator parameter for low concentrations of analyte (difference between the measured value obtained from several repeated measurements and reference value). The LoQ can either be equal or bigger than LoD, but never smaller (6):

$$LoQ \geq LoD \quad (6)$$

Therefore, all these analytical parameters should be integrated in any method of evaluation of assays that focus on distinguishing the presence and absence of specific analytes, thus attesting the reliability and accuracy of the results obtained [87].

1.8. Objective

The goal of the present work is to develop a microfluidic platform capable of detecting a specific prostate cancer biomarker, PSA, with a limit of detection within clinically relevant range. For this, a sandwich-type immunoassay was implemented to increase the system sensitivity and the detection was performed via fluoresce microscopy. Several blocking agents were tested to reduce non-specific interactions and background noise. Calibration curves were obtained, not only in PBS, but also in human serum, to mimic physiological conditions. Furthermore, it was expected that the detection of PSA could be performed also in several ionic liquids, since they are considered promising in sample pre-treatment procedures using ABS, which tend to increase system analytical sensitivity and improve detection limits. Therefore, the developed strategy is expected to work as basis for a future development of a microfluidic device with fully integrated IL-based ABS and detection system capable of accurate diagnosis of prostate cancer from complex biological fluids.

2. Materials and Methods

2.1. Reagents and Materials

2.1.1. Solutions

For the experiments performed in the present work, Phosphate Buffer Saline (PBS) was prepared by diluting a PBS 10x stock solution (1.37 M NaCl, 0.027 M KCl and 0.119 M phosphate) in Milli-Q water to a final working solution of 1x (pH 7.4, 25°C). PBS was used as the main buffer and was necessary to prepare several other solutions. Furthermore, different blocking agents were tested, namely Bovine Serum Albumin (BSA), whose dry stock was weighted in an analytical scale and diluted in PBS to a final concentration of 4% (w/v) BSA, ready-to-use Blocker™ Casein in PBS 1% (w/v), and Human Normal Immunoglobulin (Gammanorm®), diluted in PBS to a working solution of 5 mg/mL. Furthermore, polyethylene glycol (PEG) 8000 was used as a suspension solution to help pack the beads in microchannels, since it promotes beads dispersion throughout the solution, and it was diluted to a final concentration of 30% (w/w). For the experiments regarding PSA detection, apart from PBS, a solution of Human Serum was also used. **Table 1** describes all the reagents and equipment necessary to prepare the referred solutions.

Table 1 *- Summary of equipment and reagents required for preparing the solutions necessary for the experiments.*

Equipment	Analytical Scale d=0.0001 g, Scientech (Bradford, MA/USA)
Reagents	Phosphate Buffer Saline (PBS) 10x, ThermoFisher Scientific (BP3991)
	Bovine Serum Albumin (BSA), Sigma Aldrich (A2153)
	Blocker™ Casein in PBS, ThermoFisher Scientific (37528)
	Human Normal Immunoglobulin 165 mg/mL (Gammanorm®), Octapharma (J06B A01)
	Polyethylene glycol (PEG) 8000, Sigma Aldrich (P4463)
	Human Serum from human male AB plasma, Sigma Aldrich (H4522)

Additionally, several salts (phosphate buffer and citrate buffer), polymers (PEG1000, PEG2000, PPG400, DEX500k, UCON, PL35, NaPA8000) and ionic liquids solutions ([C_4C_1im]Cl, [C_4C_1pyrr]Cl, [N_{4444}]Cl, [P_{4444}]Cl, [P_{4444}]Br, [Ch]Cl) were also used to attest the interference of these solution in the detection of target biomolecules. All these solutions are thoroughly described in **Table 2** and were kindly prepared and supplied by Universidade de Aveiro/CICECO.

Table 2 *- Summary of all salts, polymers and ionic liquids tested.*

Sample	Reagents	Mass (g)	Mass percentage %(w/w)	pH
		Salts		
Citrate buffer	Potassium citrate tribasic monohydrate, 99%, extra pure (Acros Organics) Citric acid 1-hydrate for analysis, ACS, ISO (99.5-102.0%) (Panreac)	$C_6H_5K_3O_7 \cdot H_2O$=2.5427 $C_6H_8O_7 \cdot H_2O$=0.1032 H_2O=2.3593	49.87	6.87
Phosphate buffer	di-potassium hydrogen phosphate trihydrate, extra pure (98-102%) (Sharlau) potassium dihydrogen orthophosphate, analytical reagent grade (99.95%) (Fisher Chemical)	$K_2HPO_4 \cdot 3H_2O$ = 1.6202 H_2O = 1.2224 KH_2PO_4 = 0.7378 H_2O =1.4482	39.27	7.13
		Polymers		
PPG400	Polypropylene glycol (P 400) (Sigma)	PPG400=3.0203 PBS=2.0344	59.75	6.25
PEG1000	Polyethylene glycol (1000) (Alfa Aesar)	PEG1000=3.0596 PBS=2.0145	60.30	8.48
Dex500k	Dextran from Leuconostoc spp. (Mr 450000-650000) (Sigma)	Dex500k=1.5093 PBS=3.5564	29.79	7.18
UCON	Poly(ethylene glycol-ran-propylene glycol) (Mn ≈2500)	UCON=3.0574 PBS=2.0176	60.24	7.45
PL35	Poly(ethylene glycol)-block-poly(propylene glycol)-block-poly(ethylene glycol) (Mn ≈1900) (Sigma)	PL35=3.0713 PBS=1.9984	60.58	4.30
NaPA8000	Poly(acrylic acid, sodium salt) solution (Mw ≈8000, 45 %(w/w) in H_2O) (Sigma)	NaPA8000 (45%(w/w) in H_2O) =3.4592 PBS=1.5986	30.78	7.52
PEG2000	Polyethylene glycol (2000) (Alfa Aesar)	PEG2000=3.0186 PBS=2.0418	59.65	8.15
		Ionic Liquids		
$[C_4C_1im]$ Cl	1-butyl-3-methylimidazolium chloride, 99% (Iolitec)	$[C_4C_1im]$ Cl=3.0242 PBS=1.9964	60.24	8.54
$[C_4C_1pyrr]$ Cl	1-butyl-1-methylpyrrolidinium chloride, 99% (Iolitec)	$[C_4C_1pyrr]$ Cl=3.0973 PBS=2.0200	60.53	8.62
$[N_{4444}]$ Cl	Tetrabutylammonium chloride, ≥97% (Sigma)	$[N_{4444}]$ Cl=3.0144 PBS=2.0061	60.04	7.99
$[P_{4444}]$ Cl	Tetrabutylphosphonium chloride, >95% (Iolitec)	$[P_{4444}]$ Cl=3.0484 PBS=2.0125	60.23	3.82
[Ch]Cl	Choline chloride, 99% (Acros Organics)	[Ch]Cl (5 %(w/w) of H_2O) =2.0891 PBS=3.0067	38.95	7.91
$[P_{4444}]$ Br	Tetrabutylphosphonium bromide, >95% (Iolitec)	$[P_{4444}]$ Br=3.0326 PBS=2.0305	59.90	0.53

2.1.2. Beads

In the present work, two different microbeads were used, MabSelect™ and Protein G Sepharose® 4 Fast Flow, both from Cytiva. Commercially MabSelect™ consists of highly cross-linked agarose beads with Protein A ligand, which favours an oriented binding, improving coupling capacity with IgG molecules. Moreover, it presents low non-specific binding capacity, essentially due to the hydrophilic nature of its resin matrix. These Protein A based beads were supplied in 20% (v/v) ethanol solution, presenting an average particle size of ~ 85 µm, and were used to immobilize anti-BSA antibodies. Protein G Sepharose® 4 Fast Flow consists of recombinant protein G coupled to 4% cross-linked agarose matrix, offering a large IgG binding spectrum, presenting complementary binding specificities to Protein A beads. These beads were also supplied in 20% (v/v) ethanol solution and presented an average diameter of ~ 90 µm. Protein G beads were utilised to immobilize anti-PSA probe antibody. Both protein A and protein G beads were first incubated with anti-BSA and anti-PSA solutions, respectively, prior to their packing. Incubation for both anti-BSA and anti-PSA solutions will be described in detail in section **2.3.2**. After the incubation step is complete, beads solutions are supplemented with PEG 30% (w/w) in PBS, in order to provide a more viscous media, thus facilitating beads packing. **Table 3** describes the microbeads used in the experiments of the present work.

Table 3 *- Summary of microbeads used in the present work.*

Reagents	Protein G Sepharose® 4 Fast Flow, Cytiva (17-0618-01)
	MabSelect™, Cytiva (17-5199-01)

2.1.3. Antibodies and Antigens

In order to test the interference of the several salts, polymers and ionic liquids in the detection of target analytes, a model system consisting of anti-BSA antibodies immobilized on the surface of Protein A for the capture of fluorescein isothiocyanate (FITC) conjugated BSA was used. FITC presents an excitation peak at 490 nm and an emission peak at 525 nm, allowing fluorescence intensity quantification. Anti-BSA antibody solutions presented an initial concentration of 1 mg/mL and were diluted in PBS to a final concentration of 50 µg/mL. Similarly, BSA-FITC with an initial concentration of 1.25 mg/mL was further diluted to a working concentration of 50 µg/mL.

Furthermore, for the experiments of PSA detection, a sandwich immunoassay was the method applied. For this purpose, a pair of anti-PSA antibodies was purchased to work as capture and detector antibody and commercially available target antigen PSA was also acquired. The capture anti-PSA antibody solution, with an initial concentration of 5.25 mg/mL, and the detector anti-PSA antibody solution, with an initial concentration of 5.4 mg/mL, were both diluted in PBS to working solutions of 100 µg/mL, whereas the target PSA analyte, with an initial concentration of 1.5 mg/mL was diluted in PBS and Human Serum, in concentrations ranging from 0 ng/mL to 25 ng/mL. The detector anti-PSA antibody was posteriorly conjugated to the amine reactive dye Alexa Fluor® (A430) NHS ester – with an excitation peak at 430 nm and emission peak at 545 nm –, enabling fluorescence detection. To do

the labelling procedure of anti-PSA antibody, 100 µL of the commercial antibody was diluted in 400 µL of 100mM sodium bicarbonate at pH 9.2 and then conjugated with 10 µL of the Alexa Fluor® (A430) dye, previously dissolved in DMSO at 10 mg/mL. The mixture was incubated in the dark for 1 hour at room temperature. The excess non-conjugated dye was then removed through a series of washing steps using a 10KDa Amicon Ultra-0.5 centrifugal filter unit, previously washed with 500 µL of PBS and centrifuged at 14,000 g for 10 minutes. For this, the incubated antibody-dye solution was added to the Amicon centrifugal unit and centrifuged at 14,000 g for 10 minutes. After centrifugation was complete, the permeate at the bottom of the tube was discarded, then 500 µL of PBS was added to initiate the washing process and the solution was centrifuged for 14,000 g for 10 min. This latter step was repeated a series of 6-7 times until the permeant becomes colourless, indicating that there was no more non-conjugated dye in the solution. Then, the labelled antibody solution was collected by reverse centrifugation at 2,000 g for 2 minutes and the remaining volume was measured and made up to the initial volume with PBS. The specific molecules and materials used in all experiments are described in **Table 4**.

Table 4 *- Summary of materials, antibodies, target analytes and dye used in the experiments.*

Materials	Amicon Ultra-0.5 Centrifugal Filters (MWCO of 10KDa), Merck Millipore (UFC501024)
Reagents	Bovine Serum Albumin (BSA) Antibody, ThermoFisher Scientific (MA5-15238), Mouse, Monoclonal
	BSA-FITC, ThermoFisher Scientific (A23015)
	anti-PSA antibody, Sigma Aldrich (MABX5523), Mouse, Monoclonal
	anti-PSA antibody, Sigma Aldrich (MABX5532), Mouse Monoclonal
	Prostate Specific Antigen (PSA), Sigma Aldrich (P3338)
	Alexa Fluor® 430 (A430) NHS ester, ThermoFisher Scientific (A10169)

2.2. Microfabrication

2.2.1. Hard mask fabrication

The fabrication of the hard mask started with the design of the microfluidic structure in AutoCAD software, where the structure was designed according to the dimensions desired. **Table 5** described the equipment, materials, and reagents necessary for the fabrication process.

Table 5 *- Summary of equipment, materials and reagents requires for the fabrication of hard mask.*

Equipment	AutoCAD software (Autodesk Inc., Mill Valley, CA/USA)
	Nordiko 7000 magnetron sputtering system, Nordiko Technical Services LTD (Havant, Hampshire, UK)
	SVG Resist coater and developer track, Silicon Valley Group Inc. (San Jose, CA/USA)
	DWL lithography, Heidelberg Instruments (Heidelberg, DE)
Material	Clean glass substrate, Corning Inc. (Corning, NY/USA)
	Silicon wafer (150 mm diameter), University Wafer (South Boston, MA/USA)

Reagents	Acetone (99,6%), LabChem Inc. (Zelienople, PA/USA)
	Isopropanol (IPA), (99,9%), LabChem Inc. (Zelienople, PA/USA)
	Deionized (DI) water
	Alconox solution, Alconox Inc. (White Plains, NY/USA)
	Aluminium etchant TechniEtch A180, Microchemicals (Ulm, DE)
	Photoresist PFR 7790G, JSR (Sunnyvale, CA/USA)

For the hard mask fabrication, a glass substrate was previously washed with acetone, IPA and DI water before being immersed in an Alconox™ solution at 65℃ for 30 minutes, followed by another washing step with DI water and finally a drying step. Subsequently, using a Nordiko 7000, a 200 µm layer of Aluminium was poured on the substrate by magnetron sputtering. Afterwards, a layer of 1.5 µm of positive photoresist was spin-coated on top of the Aluminium layer, using a SVG track/automatic coating track. The substrate was then baked for 60 seconds at 85℃. The mask design obtained in AutoCAD software was transferred to the photoresist through a Heidelberg DWL (direct write laser) lithography equipment, using a laser wavelength of 405 nm. After baking the photoresist for 60 seconds at 110℃ and letting it cool down, the photoresist was developed for 60 seconds, which exposes selected areas of the aluminium layer. The exposed areas were then etched with a proper aluminium etchant until they were completely dissolved. To conclude the hard mask fabrication process, a final washing step with acetone and isopropanol was performed to ensure that the remaining photoresists was completely removed. All these steps were performed under class 100 cleanroom conditions, except photolithography step which was performed in a class 10 cleanroom. The experimental procedure described is illustrated in **Figure 9**.

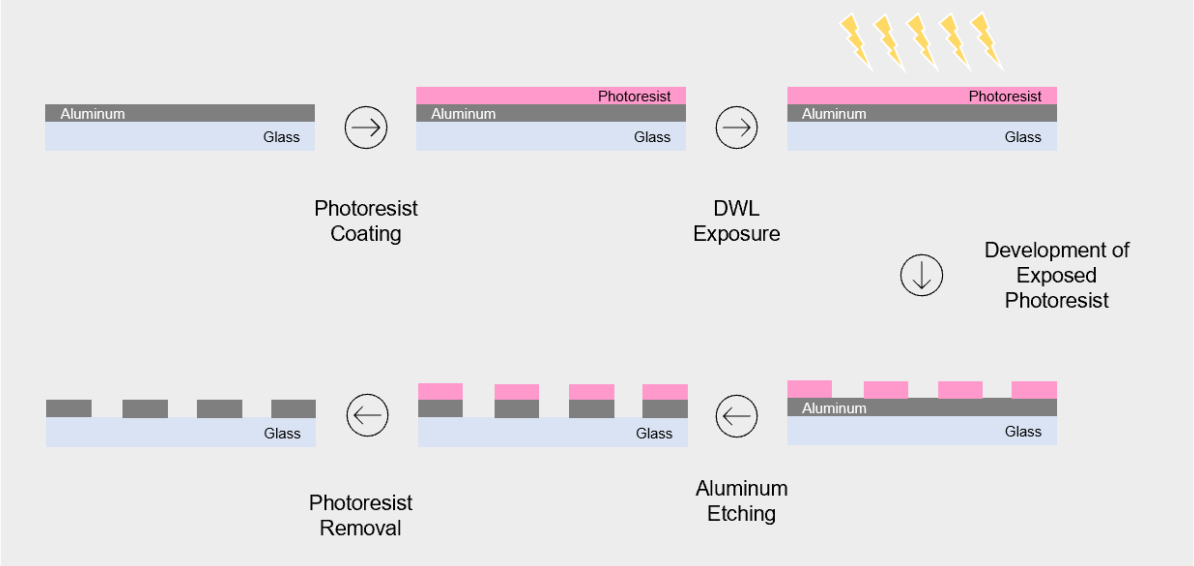

Figure 9 *- Schematics of hard mask fabrication (side view). Elements not to scale.*

In the present work, the structure was composed of columns with 2 different heights, a 100 µm height chamber, and another 20 µm height channel connected to the former. Therefore, two different hard masks (**Figure 10**) were designed in the AutoCAD software and fabricated, one for each required height.

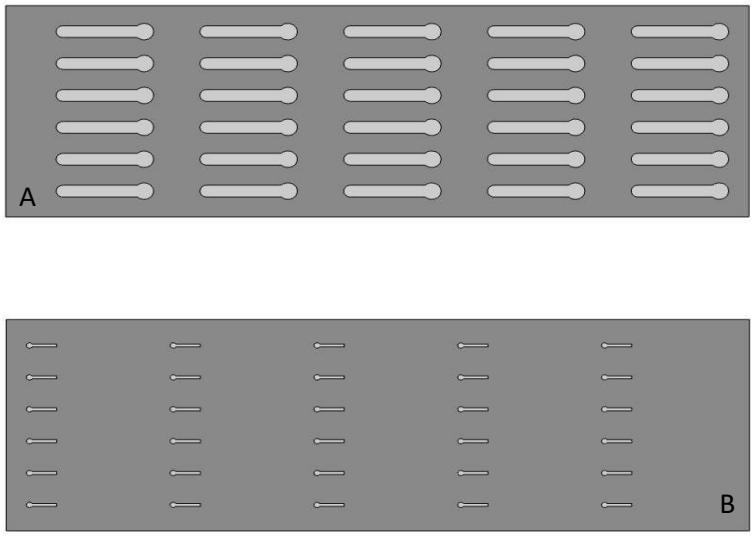

Figure 10 *- Schematic representation of the two hard masks fabricated and used in the present work. Mask for a height of 100 µm (**A**) and 20 µm (**B**).*

2.2.2. Master mold fabrication

The two hard masks obtained were then used to produce a SU-8 mold that allows the fabrication of the PDMS structures. **Table 6** presents the equipment, materials, and reagents necessary for the master mold fabrication.

Table 6 *- Summary of equipment, materials and reagents requires for the fabrication of master mold.*

Equipment	Kerry Ultrasonic Cleaning Bath, Guyson (Skipton, North Yorkshire, UK)
	UVO Cleaner 1444AX-220, Jelight Company, Inc. (Irvine, CA/USA)
	Spin coater, Laurell Technologies Corp. (North Wales, PA/USA)
	Vertical laminar airflow cabinet, FASTER-BSC-EN (Cornaredo, IT)
	Hotplate, Stuart (Staffordshire, UK)
	UV light (254 nm, 400 W), UV Light Technology Limited (Birmingham, UK)
	Stereo microscope, AmScope (Irvine, CA/USA)
Materials	Silicon wafer (150 mm diameter), University Wafer (South Boston, MA/USA)
Reagents	Acetone (99,6%), LabChem Inc. (Zelienople, PA/USA)
	Isopropanol (IPA), (99,9%), LabChem Inc. (Zelienople, PA/USA)
	Deionized (DI) water
	Alconox solution, Alconox Inc. (White Plains, NY/USA)

	Propylene glycol methyl ether acetate (PGMEA) (99,5%), Sigma-Aldrich (St. Louis, MO/USA)
	SU-8 2015 photoresist, Microchem Corp. (Newton, MA/USA)
	SU-8 50 photoresist, Microchem Corp. (Newton, MA/USA)

The first step of the mold fabrication consists of cleaning a silicon substrate with acetone, IPA and DI water, to remove any residues on the surface and then immerse it in an Alcanox™ solution in a hot water bath at 65℃ for 20 minutes. Afterwards, the substrate was cleaned with DI water, then dried with compressed air and placed for 15 minutes in a UVO cleaner to degrade any contaminants. After the cleaning process was complete, to prepare the 20 µm layer, a negative photoresist (SU-8 2015) was poured onto the substrate and spin coated in a two-step process: first the substrate was spin-coated at 500 rpm and 100 rpm/min for 10 seconds followed by 34 seconds at 1700 rpm and 300 rpm/min. The substrate was then placed in a hot plate at 95℃ for 4 minutes and cooled down for 1 minute (pre-exposure baking). Subsequently, the 20 µm height hard mask was placed on top of the SU-8 layer, with the aluminium surface facing down, and exposed to an UV light for 30 seconds. After the exposure, the substrate was baked in a hot plate at 95℃ for 5 minutes. After cooling down for 2 minutes, the stack was immersed in a PGMEA 99% solution for 2 minutes with manual agitation, which allows the non-exposed photoresist to develop. Then the substrate was cleaned with IPA and dried with compressed air.

For the development of the 100 µm layer, a similar process was required. A negative photoresist (SU-8 50) was deposited on top of the previously cleaned silicon substrate and spin coated first at 500 rpm and 100 rpm/min for 10 seconds, followed by a second step at 1000 rpm and 300 rpm/min for 30 seconds. Afterwards, the substrate was submitted to sequential pre-exposure bake process in a hot plate that initiated with 10 minutes at 65℃ and followed by 30 minutes at 95℃. After cooling down for 1 min, the 100 µm hard mask was placed over the SU-8 layer, ensuring the aluminium surface was facing down and it was aligned with a low power AmScope microscope. Subsequently, the hard mask together with the silicon substrate was exposed to an UV light for 70 seconds and then baked for 1 minute at 65℃ in a hotplate. The temperature of the hotplate was increased until 95℃ and the substrate was left there for further baking for 10 minutes, followed by a cooling down step for 2 minutes at room temperature. The substrate with the photoresist was then developed in a PGMEA 99% solution with manual agitation for 10 minutes, cleaned with IPA and dried with a compressed air gun.

A final baking step can be added to the master mold fabrication process to ensure that the SU-8 properties remain unchanged. Therefore, the substrate can be placed in the hotplate for 15 minutes at 150℃, with finalizes the fabrication of the master mold. The experimental procedure described is illustrated in **Figure 11**.

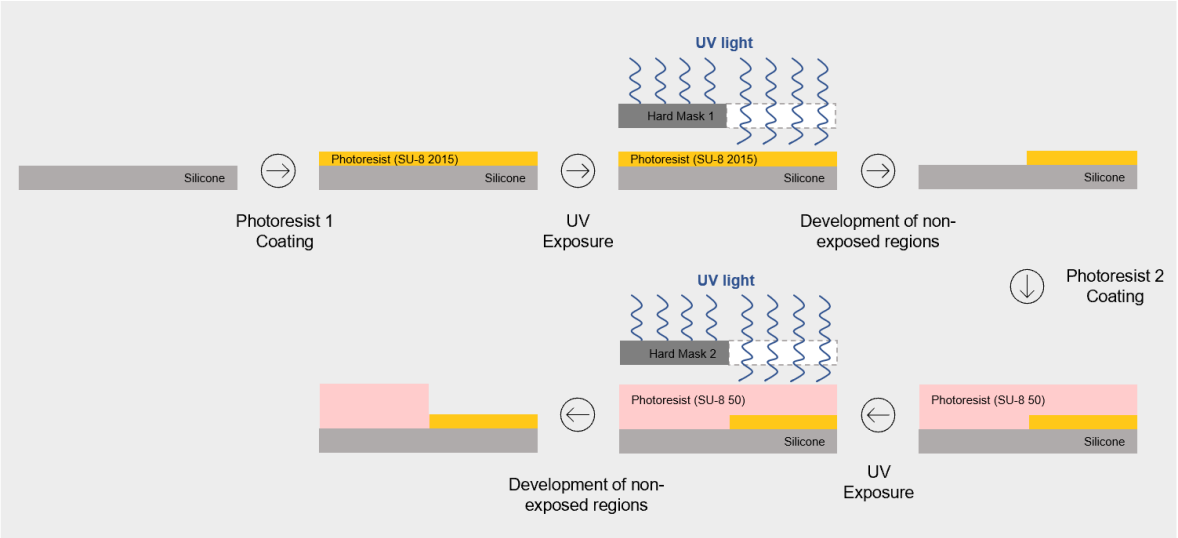

Figure 11 *- Schematics of master mold fabrication (side view). Elements not to scale.*

2.2.3. PDMS structures fabrication

The master mold obtained in the previous section was then used to cast the PDMS structures, using soft lithography technique. **Table 7** describes the equipment, materials, and reagents required for the fabrication of PDMS structures.

Table 7 *- Summary of equipment, materials and reagents used for the fabrication of PDMS structures.*

Equipment	Analytical Balance, Scientech (Bradford, MA/USA)
	Vacuum desiccator, Bel-Art Products (South Wayne, NJ/USA)
	Oven loading model 100-800 (70_C), Memmert (Schwabach, DE)
	Expanded oxygen plasma cleaner PDC-002-CE (200W), Harrick Plasma (Ithaca, NY/USA)
	Spin coater, Laurell Technologies Corp. (North Wales, PA/USA)
Materials	Luer Stub (Blunt Needles) 20 Gauge (LS20), Instech Laboratories, Inc. Plymouth Meeting, PA/USA)
	Luer Stub (Blunt Needles) 18 Gauge (LS18), Instech Laboratories, Inc. Plymouth Meeting, PA/USA)
	Silicon wafer (150 mm diameter), University Wafer (South Boston, MA/USA)
Reagents	Sylgard 184 PDMS and curing agent KIT, Dow Corning (Midland, MI/USA)

The process started with mixing a curing agent with polydimethylsiloxane (PDMS) base in a 1:10 weight ratio. After homogenisation, the mixture was placed in the desiccator for 45 minutes to degas. Subsequently, the SU-8 mold was glued to a PMMA frame with tape and the PDMS is poured on top of the SU-8 mold, until reaching the top of the frame. The PMMA frame with the PDMS structure was then secured with four binding clips and placed in the oven for 90 min at 70℃ to cure. The cured PDMS was then cut with a scalp and separated from the mold with the help of tweezers. In order to

open the inlets and outlets in the structure, needles of 20Ga and 18Ga, respectively, were used to punch the holes in the PDMS.

To seal the PDMS structure a 500 µm PDMS membrane was prepared. For this, the PDMS mixture was poured on top of a cleaned silicon wafer and spin coated at 250 rpm with an acceleration of 100 rpm/min for 25 seconds. Afterwards, the wafer was placed in the oven for 90 minutes at 70℃ and then cut in pieces slightly bigger than the PDMS structure containing the microchannels. To seal the PDMS structure against the membrane, both surfaces were oxidized with a plasma cleaner (Harrick Plasma) at high power for 60 seconds. This treatment oxidizes the exposed surfaces by generating hydroxyl groups, which allows the combination of both surfaces, forming a covalent bond between them. To ensure an irreversible and long-lasting sealing the structure must be used only after 12h of performing this procedure. The experimental procedure described is illustrated in **Figure 12**.

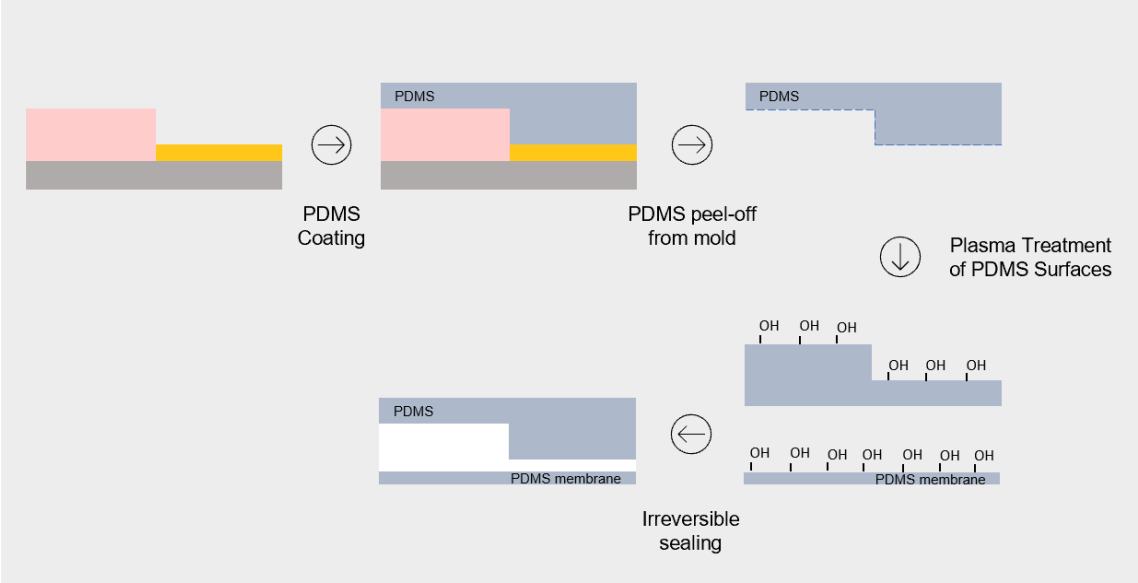

Figure 12 *- Schematics of PDMS structures fabrication and sealing process (side view). Elements not to scale.*

2.3. Microfluidic device handling

2.3.1. General concepts

During experimental assays, a double syringe pump was used for the fluid manipulation, assembled with two 1 mL syringes, filled with PBS. Each syringe was connected to a luer stub adapter and a polyethylene tube, with an open stainless-steel adapter at the other end. This metallic adapter is connected to the outlet of the microfluidic channel, where a negative pressure is applied, pulling the desired solutions dispensed in the inlet through a pipette tip, driving the fluid towards the outlet. **Table 8** summarizes the basic components and equipment necessary to perform the experimental assays.

Table 8 *- Summary of equipment and materials required for microfluidic handling.*

Equipment	Syringe pump NE-1002X, New Era Pump Systems, Inc. (Farmingdale, NY/USA)
Materials	Insulin syringe 1 mL U-100, Codan (Lensahn, DE)
	Polyethylene tubing (BTPE-90), 030x.048in, Instech Laboratories, Inc. (Plymouth Meeting, PA/USA)
	Luer Stub (Blunt Needles) 20ga (LS20), Instech Laboratories, Inc. Plymouth Meeting, PA/USA)
	Stainless Steel adapter, 20ga x 15mm (SC20/15), Instech Laboratories, Inc. Plymouth Meeting, PA/USA)

The methodology used to manipulate fluid inside the microchannels was pulling the required solutions from the inlet towards the outlet, by applying negative pressure at the stainless-steel adapter placed at nearly contact distance with PDMS membrane at the channel outlet. Apart from pulling, the syringe pump can also push the liquid from the inlet to the outlet. In this case the stainless-steel adapter would have to be placed at the inlet, instead of the outlet. However, pulling the liquid revealed to be a more reliable and easier technique than pushing it, mainly because it showed a reduction in the air bubbles recurrently formed and led to more reproducible results. The microchannels used in all experiments of the present work have a length of 1 cm and are composed of two sections, the first consists of a column with 100 µm height and 700 µm width, whereas the smaller portion presents 20 µm height and 200 µm width (**Figure 13**).

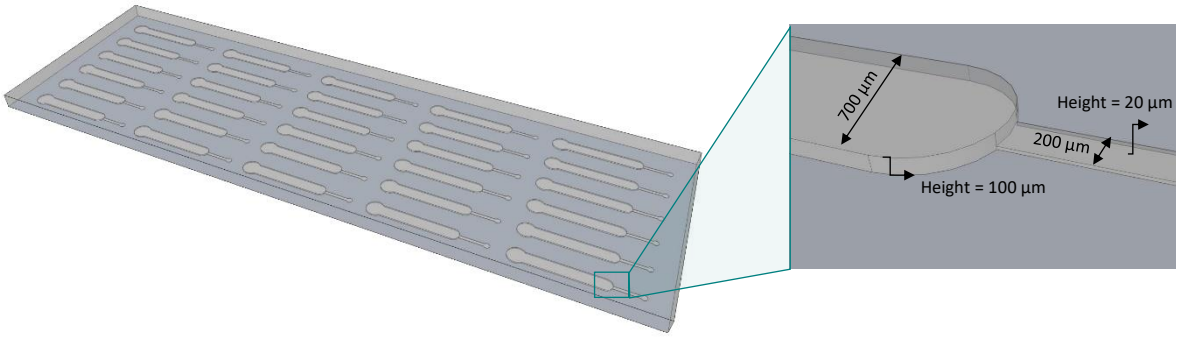

Figure 13 *– Microfluidic structure obtained after peeling the PDMS from master mold. The microfluidic structure is composed of 30 microchannels with two sections, in which the first consists of a column with 700 µm width and100 µm height, and the second has 200 µm width and 20 µm height.*

2.3.2. Bead preparation

In the present work, two types of beads were used, Protein A and Protein G beads, as previously described in section **2.1.2**. The protocol for the preparation of both beads starts with homogenisation of the bead suspension. For the Protein A beads, 3 µL of bead stock solution (~50% (v/v) bead resin) was added to 20 µL of anti-BSA IgG previously prepared in PBS to a final concentration of 50µg/mL. The mixture was then incubated for 15 min using a rotator mixer at 250 rpm. A similar procedure was followed for Protein G beads, by adding also 3 µL of bead stock solution to 20 µL of anti-PSA antibody solution prepared in PBS with a concentration of 100 µg/mL. The mixture was also incubated for 15 min with the

same agitation parameters. After incubation, in both cases, 110 µL of PEG 30% (w/w) in PBS was added to each solution, to ensure a homogeneous dispersion of beads, providing a more viscous media, thus facilitating beads packing. **Figure 14** depicts the protocol described for beads preparation.

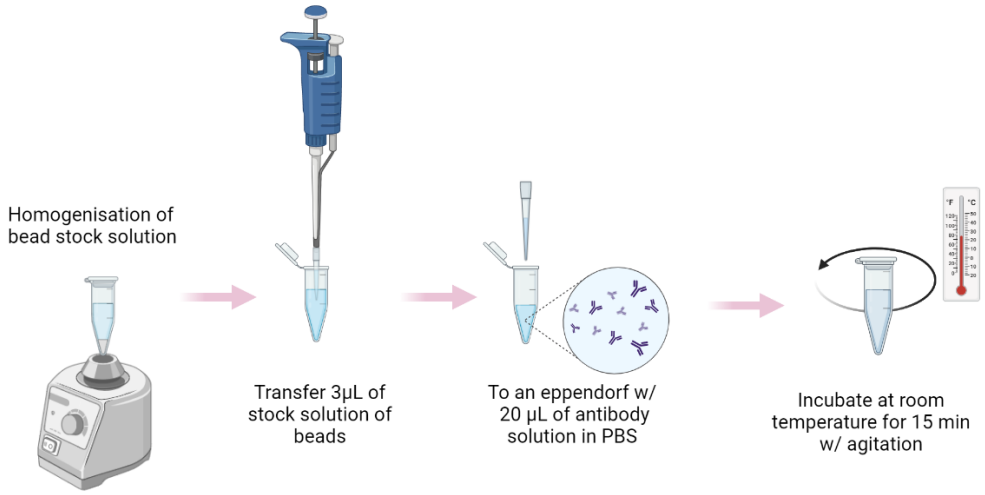

Figure 14 *- General protocol for preparing beads before packing them inside microfluidic channel. Elements not to scale.*

2.3.3. Packing Method

Regarding the packing method, a syringe pump was used to efficiently insert in the microchannel the beads solution prepared as described in section **2.3.2**. For this purpose, the microchannel was first washed with PBS and then a pipette tip with 10 µL of beads was inserted in the inlet in order to dispense the bead solution inside the microchannels. A negative pressure at a flow rate of 5 µL/min was applied at the outlet, where a stainless-steel adapter was placed, connected to a polyethylene tube and a syringe, controlled by the syringe pump. The negative pressure forces the bead solution to enter the microcolumn through the inlet, which reduces the formation of air bubbles in comparison with a pushing mechanism. The packing was always performed until the microchannel was ¾ full (**Figure 15**). The size of the beads allows them to be trapped in the highest microfluidic column since, the smaller channel has a heigh of only 20 µm and Protein A and Protein G beads present an average size diameter of 85 µm and 90 µm, respectively.

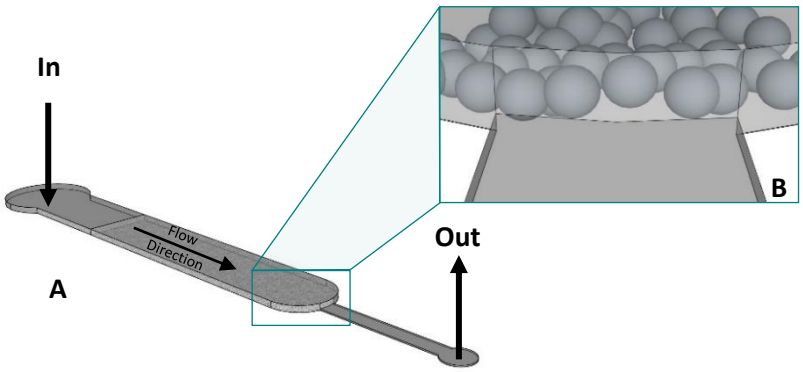

Figure 15 *– Schematic representation of microchannel used for all experiments. (A) The beads are inserted in the inlet through a pipette tip and a negative pressure is applied at the outlet forcing the bead solution to enter the microchannel. (B) Beads packed in the microchannel.*

2.4. Fluorescence Immunoassays Experiments

2.4.1. Fluorescence Measurement

For all the immunoassays experiments described below, a fluorescence microscope (Olympus Microscope, CHX41) with a 50W mercury lamp as a light source was used to measure fluorescence intensity in the microchannels. One of the light filters this microscope is equipped with is a blue light filter, with an excitation band between 450 nm and 490 nm, which was the one used throughout the experiments with antibodies labelled either with FITC or Alexa430 dyes. The Olympus microscope is connected to a XC30 camera which in turn is linked to a local computer, therefore images could be captured and stored to be posteriorly analysed as described in detail in section **2.4.2**. All images were acquired with a 4x objective and with an exposure time of 2 seconds and a gain of 0dB, since higher gain proved to increase background noise, impairing signal-to-noise ratio. Considering all the experiments required fluorescence measurement, it was crucial to ensure all measurements were performed at a minimum light environment, to minimize noise. Moreover, all antibody molecules labelled with fluorophores were stored in the dark, in eppendorfs protected with aluminium foil, when necessary, since they are extremely light sensitive. Temperature was also controlled, ensuring a constant temperature throughout all the experiments. **Table 9** describes the equipment and their specificities required for fluorescent measurements.

Table 9 *- Summary of equipment necessary for fluorescence measurements.*

Materials	Inverted Fluorescent Microscope CKX41, Olympus (Shinjuku, Tokyo, JP)
	CCD color camera XC30, Olympus (Shinjuku, Tokyo, JP)
	Mercury short arc, HBO 50W AC L2, OSRAM (69214) (Wilmington, MA/USA)

2.4.2. Image Analysis

In the present work, the images acquired using the XC30 camera coupled to the Olympus Microscope were analysed using ImageJ software (National Institutes of Health, USA). The images are loaded on the software and split in channels (blue, green and red). In this case in particular, the green channel was the only one considered in the analysis of the results. The measurements obtained correspond to the mean values from independent experiments, always considering a certain area the exterior of the microchannels (background signal) and subtracting that value from the one obtained by selecting the same area in the interior of the microchannel. An example of image analysis performed with ImageJ is depicted in **Figure 16**.

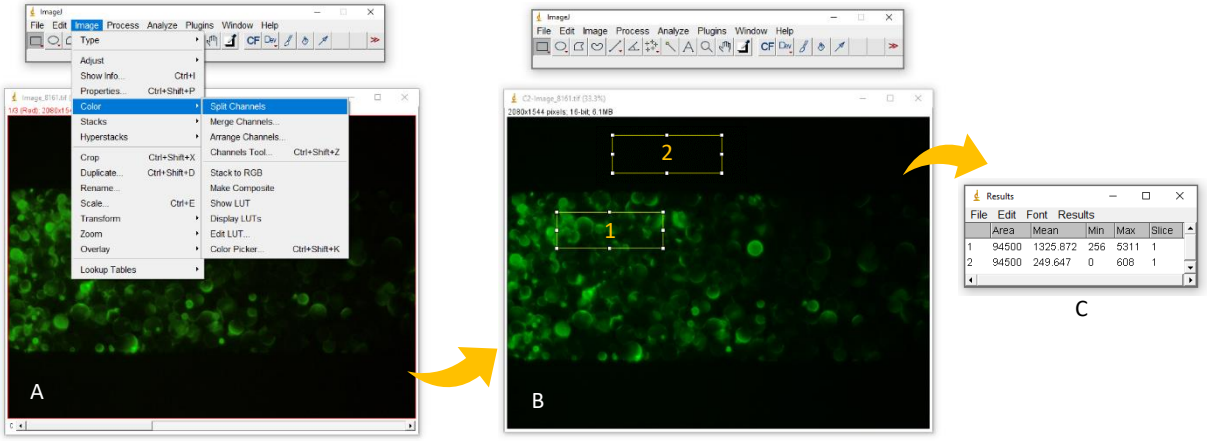

Figure 16 *– Example of image analysis using ImageJ software. (A) the desired image is uploaded and the option Color > Split Channels is selected, which will split the image in blue, green, and red channels. (B) Green channel is chosen, and two equal areas are selected in the inner and outer area of the microfluidic channel. (C) the mean value for each of the selected areas is presented and value number 2, corresponding to the background signal is subtracted from value number 1, corresponding to the inner part of the channel.*

3. Results and Discussion

3.1. Preliminary results on the influence of different solutions in the detection of target analyte in a model system

The first step to develop a microfluidic system for the detection of cancer biomarkers, considering a potential sample pre-treatment using IL-based ABS, was to evaluate the influence of ILs and some polymers and salts, other constituents of these systems, in the detection of target analytes. Having into consideration the promising behaviour of these solutions in extraction and concentration procedures of target molecules from complexed biofluidic matrixes, which contribute to sensitivity enhancement of biomarkers detection systems, a model system was created to obtain preliminary results on the influence of different solutions in fluorescent immunoassays.

The model system refereed above consisted in a fluorescent immunoassay in which Protein A agarose beads were used to immobilize anti-BSA antibody solution in order to capture target analyte FITC conjugate BSA, spiked in several solutions of salts, polymers, and ILs for comparison with target prepared in PBS. Briefly, the first step of the experiment consisted of flowing PBS through the microcolumn to ensure a clean channel. Then, Protein A beads were inserted in the microfluidic channel by pressure-driven flow as described in section **2.3.3**. To remove PEG solution from the microchannel, PBS was flowed through the channel at 15 µL/min. To minimize non-specific interactions, Casein 1% (w/v) was flowed for 10 minutes at 1 µL/min. Subsequently, to analyse the interference of several salts, polymers and ILs, each of these solutions spiked with BSA-FITC conjugate at a concentration of 50 µg/mL were prepared. Both salts were studied in concentrations ranging from 4-50% (w/w), polymers in concentrations ranging from 3-60% (w/w) and concentrations between 5% (w/w) and 60% (w/w) for ILs. Each of these solutions spiked with BSA-FITC conjugate were then diffused through the device at 1 µl/min for 5 minutes. Afterwards, two washing steps were performed, the first one, consisting of flowing through the channel each of the solutions under analysis (salts, polymers, ILs) for 10 minutes at 5 µL/min, to further evaluate its interference in the fluorescence signal. The second and final step consisted of flowing 50 µL of PBS for 10 minutes at a flow rate of 5µL/min, ensuring the remotion of all unbound molecules from the channel. The fluorescence signal was measured for each solution and concentration at the end of each experiment and the images were acquired as described in section **2.4.1.** **Figure 17** is a schematic representation of the immunoassay described.

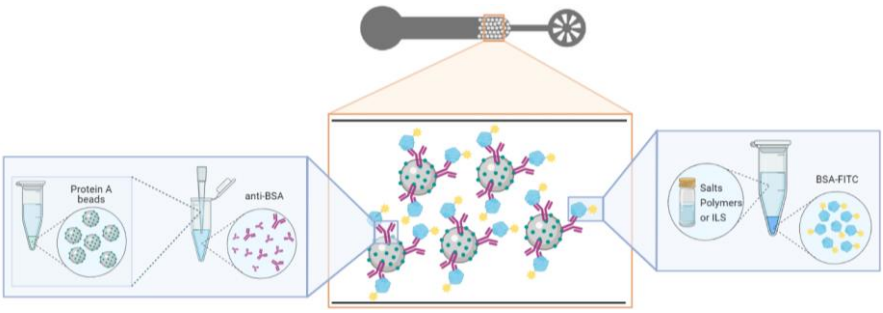

Figure 17 *- Schematics of immunoassay performed in model system anti-BSA/BSA-FITC to evaluate the interference of different salts, polymers and ILs in fluorescence signal.*

For each sample concentration, two experiments were performed: one in which bare beads, i.e., without anti-BSA immobilized on their surface were packed in the microchannel followed by blocking with Casein 1% (w/v), then flowing BSA-FITC and performing two regular washing steps. This assay worked as a control experiment (grey bars), whereas the second assay performed consisted of a regular complete immunoassay (colourful bars) as previously described.

a) Salts

The experiments started with Citrate Buffer and Phosphate Buffer being tested. For that the referred salts were diluted in PBS to final working solutions of 5%(w/w), 15%(w/w), 25%(w/w) and 50%(w/w), in case of Citrate Buffer and 4%(w/w), 12%(w/w), 20%(w/w) ,40%(w/w), in case of Phosphate Buffer. **Figure 18** presents the results obtained after performing the complete fluorescent immunoassay for the analysis of these two salts.

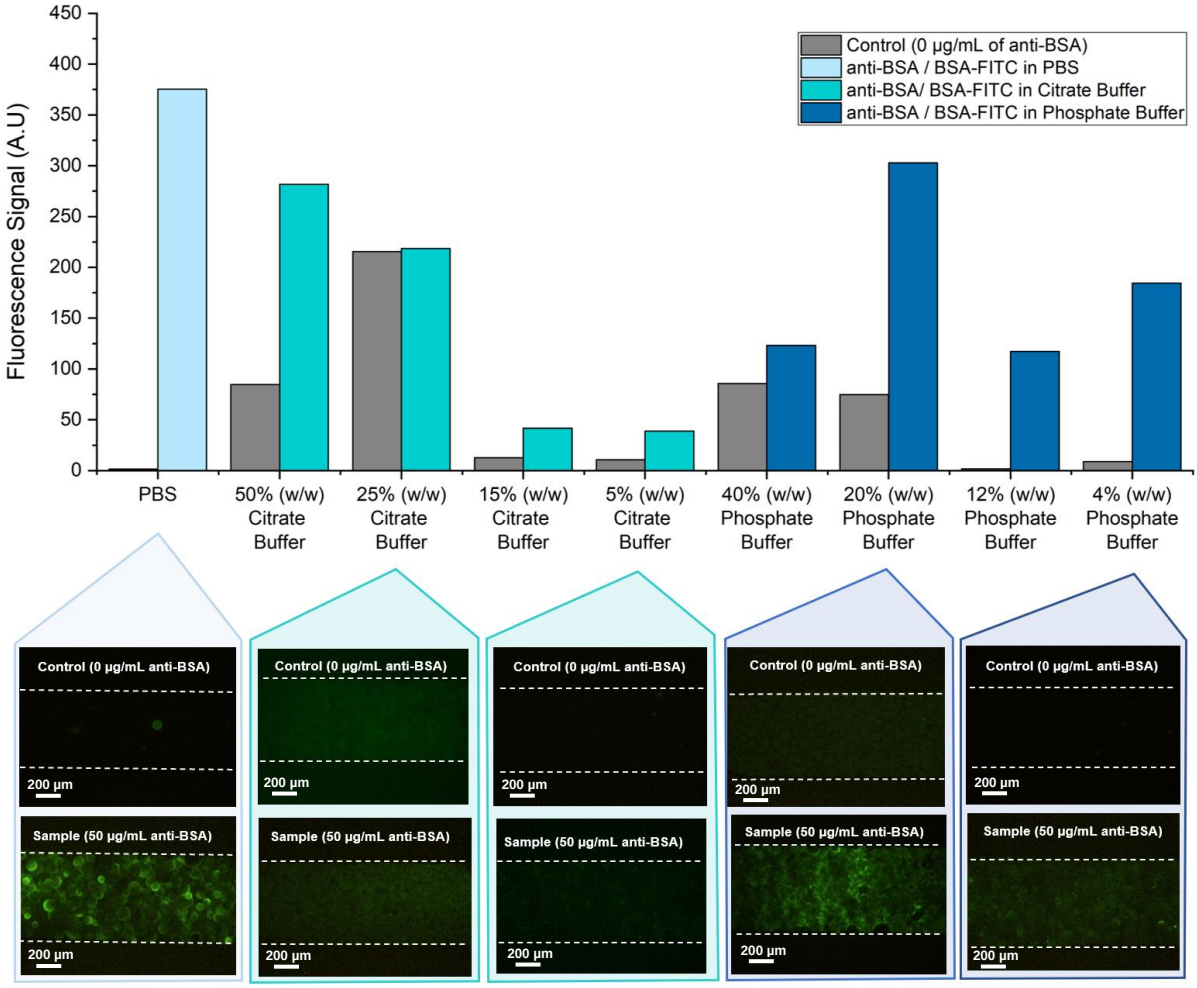

***Figure 18** – Influence of Citrate and Phosphate Buffer in the detection of target analyte FITC conjugate BSA. The experiments performed in PBS are presented for the sake of comparison with the fluorescence signal obtained with other solutions. (Top) Fluorescence signal obtained in the detection of spiked solutions of BSA in Citrate Buffer and Phosphate Buffer. (Bottom) Fluorescence images obtained with Olympus Microscope with a 4x objective, exposure time of 2 seconds and 0dB of gain. The sets of images from left to right represent the fluorescent intensity obtained when an immunoassay is performed in PBS buffer, in 25%(w/w) of Citrate Buffer, in 5%(w/w) of Citrate Buffer, in 20%(w/w) of Phosphate Buffer and 4%(w/w) of Phosphate Buffer.*

Ideally, the influence of these salts in the fluorescence signal was expected to decrease as the concentration of salt in the solution is reduced. However, that is not the case with both salts. By analysis of **Figure 18** is possible to observe that Citrate Buffer was the salt that interfere the most with fluorescence intensity, presenting a decreasing signal with decreasing concentration of salt in solution. Another aspect that stands out is the higher non-specific signal observed when BSA-FITC solution is diluted in 25%(w/w) of Citrate Buffer. However, since these experiments were only performed a single time, this can be attributed to experimental errors during the assay. Regarding Phosphate Buffer, the salt has a more irregular behaviour, presenting higher fluorescence intensity when a working solution of 20%(w/w) is used. With exception of the 20%(w/w) concentration, which has a more comparable fluorescence signal with the experiment performed in PBS, the remaining salt concentrations tested influence negatively the performance of the binding event between anti-BSA antibody and BSA-FITC, presenting lower signal intensities in comparison with the assay in PBS. Moreover, non-specific signal increases with increased concentrations of Phosphate Buffer. Therefore, in order to potentially use one of these salts as phase-forming components of IL-based ABS with the goal of extracting and concentrating target analytes for further fluorescent quantification the best option would be phosphate buffer in lower concentrations, since in comparison with citrate buffer it presented less interference in model system tested.

b) Polymers

Regarding the polymers, the same strategy was adopted, with two assays being performed for each concentration: a first immunoassay without immobilizing anti-BSA antibody on Protein A beads, which was adopted as control experiment to evaluate the presence of non-specific signal and a second assay which consisted in a regular complete immunoassay. The polymers tested were PPG400, PEG1000, UCON and PL35 prepared in PBS to final working solutions of 60%(w/w), 36%(w/w), 24%(w/w), 12%(w/w), 6%(w/w) and Dextran and NaPA8000 also diluted in PBS to final concentrations of 30%(w/w), 18%(w/w), 12%(w/w), 6%(w/w), 3%(w/w). **Figure 19, Figure 20** and **Figure 21** depict the results obtained by performing the full immunoassays using these six different polymers. Curiously, there is not a common trend for the different polymers tested regarding their influence in the fluorescence measurement of BSA molecule.

The first two polymers tested were PPG400 and PEG1000 and both presented an irregular behaviour in terms of interference with BSA detection. In both cases, assays performed with BSA-FITC spiked in working solutions of 12%(w/w) recorder higher fluorescence signal, but still below the value obtained for the experiment performed in PBS. Additionally, experiments performed with both polymers in all tested concentrations showed minimized non-specific interactions and acceptable signal-to-noise ratios. Overall, fluorescence signal achieved when BSA-FITC solutions prepared in PPG400 are used are significantly higher compared with experiments performed in PEG1000. However, PEG is the most used type of polymers in preparation of aqueous biphasic systems due to their excellent properties in terms of biodegradability and biocompatibility and well as low toxicity and low cost[88].

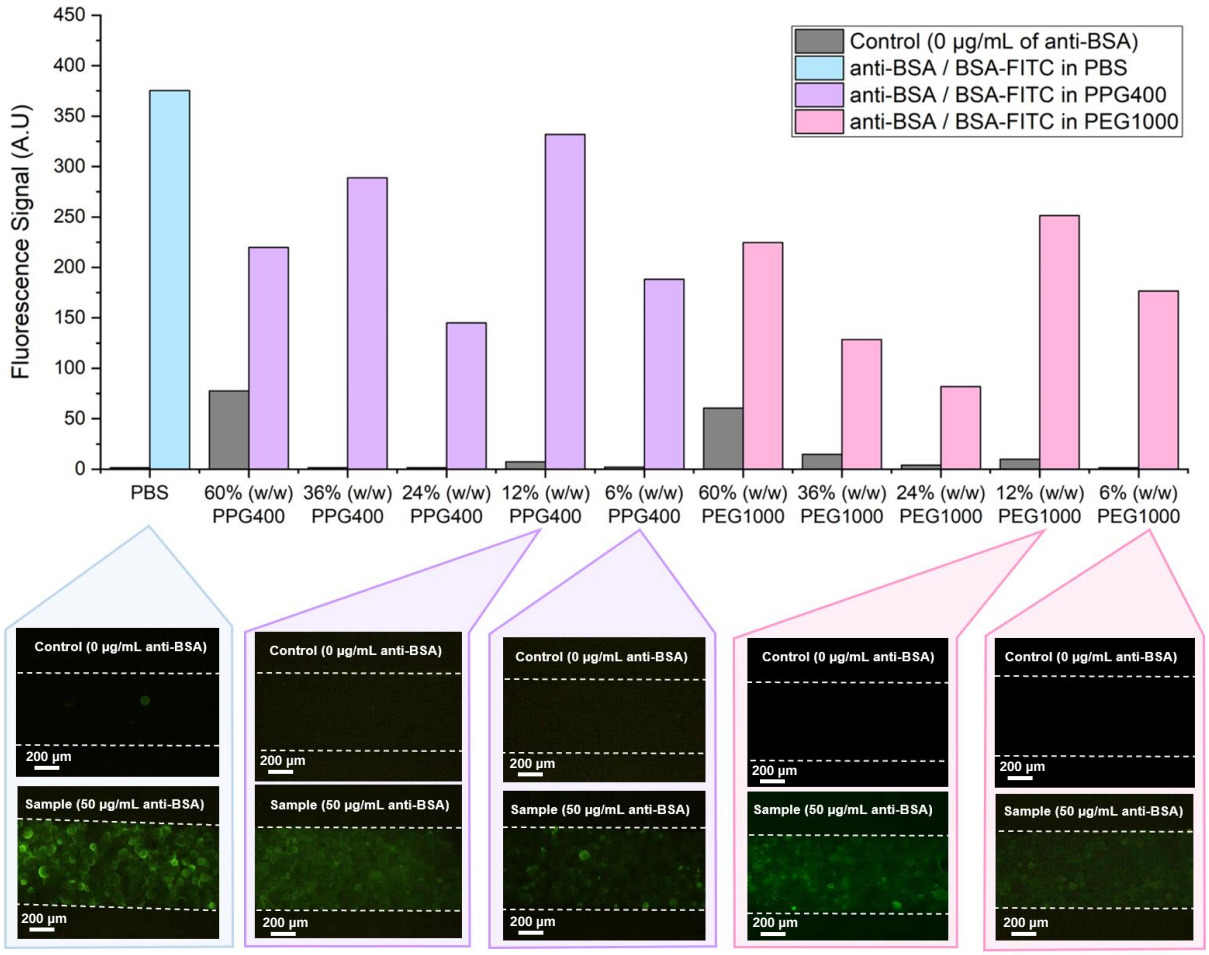

Figure 19 *- Influence of PPG400 and PEG1000 in the detection of target analyte FITC conjugate BSA. The experiments performed in PBS are presented for the sake of comparison with the fluorescence signal obtained with other solutions. (Top) Fluorescence signal obtained in the detection of spiked solutions of BSA in PPG400 and PEG1000. (Bottom) Fluorescence images obtained with Olympus Microscope with a 4x objective, exposure time of 2 seconds and 0dB of gain. The sets of images from left to right represent the fluorescent intensity obtained when an immunoassay is performed in PBS buffer, in 12%(w/w) of PPG400, in 6%(w/w) of PPG400, in 12%(w/w) of PEG1000 and 6%(w/w) of PEG1000.*

The other two polymers analysed were UCON and PL35. These systems are both PEG-PPG copolymers, with higher hydrophobicity in comparison with PEG alone, due to the extra PPG monomers in their chemical structures, which is advantageous in the formation of ABS because it enhances tunability of hydrophobicity differences between the two aqueous phases[89]. The solutions containing both polymers were also diluted in PBS to final concentrations of 60%(w/w), 36%(w/w), 24%(w/w), 12%(w/w), 6%(w/w) spiked with BSA-FITC. The results obtained for fluorescence intensity measurements in these samples are depicted in **Figure 20**.

By analysis of **Figure 20** it is possible to conclude that UCON shown lower levels of interference in the detection of BSA when lower concentrations of polymer in solution is used, which consequently increases the fluorescence signal. In particular, the experiment performed with 6%(w/w) of UCON

registered an even higher fluorescence signal in comparison with assay performed in PBS. Additionally, non-specific signal achieved minimum values with lower concentrations of UCON polymer, which leads to an increase in signal to noise ratios. Therefore, UCON proved to be a polymer to consider for the detection of BSA when used in lower concentrations, due to the extremely low interference with this molecule, and can be included in a more complexed system featuring a potential ABS for prior extraction and concentration of target analyte from complex matrices, working as a phase-forming constituents of one of the two aqueous phases.

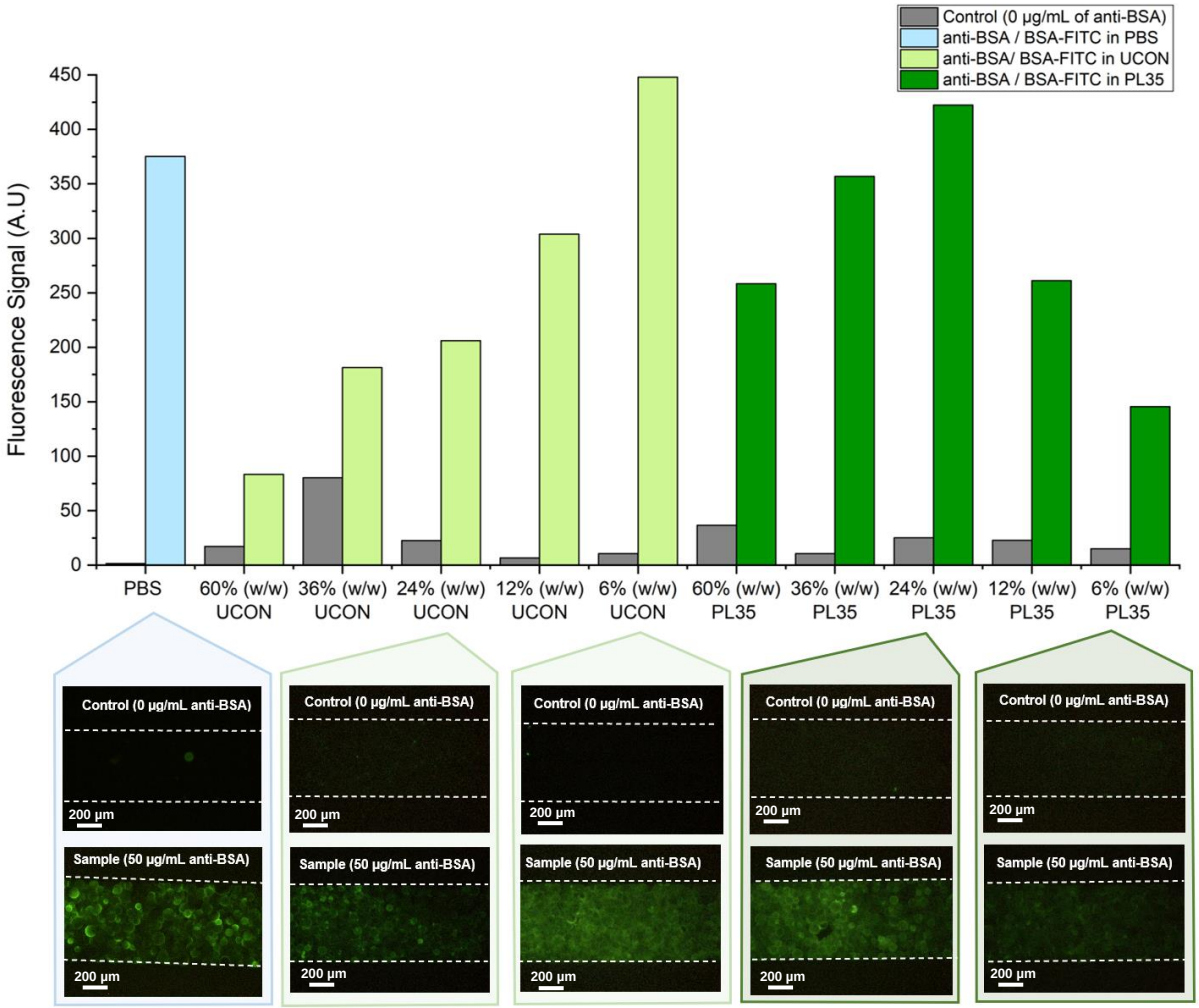

Figure 20 *- Influence of UCON and PL35 in the detection of target analyte FITC conjugate BSA. The experiments performed in PBS are presented for the sake of comparison with the fluorescence signal obtained with other solutions. (Top) Fluorescence signal obtained in the detection of spiked solutions of BSA in UCON and PL35. (Bottom) Fluorescence images obtained with Olympus Microscope with a 4x objective, exposure time of 2 seconds and 0dB of gain. The sets of images from left to right represent the fluorescent intensity obtained when an immunoassay is performed in PBS buffer, in 24%(w/w) of UCON, in 6%(w/w) of UCON, in 24%(w/w) of PL35 and 6%(w/w) of PL35.*

Regarding PL35, the overall fluorescence signal presented a more irregular behaviour in comparison with results obtained with UCON, however, the fluorescence levels registered were also considered acceptable, most of them comparable with the assay performed in PBS. Additionally,

fluorescence signal measured for the assay performed with BSA-FITC solutions spiked in 24% (w/w) is even higher than the one registered for the experiment performed in PBS. Furthermore, for all concentrations of PL35 tested, high signal-to-noise ratios were achieved, since the control experiments presented low fluorescence signal due to minimum non-specific interactions during antigen-antibody binding event.

The last two polymers tested were Dextran and NaPA8000, both prepared in PBS in concentrations of 30% (w/w), 18% (w/w), 12% (w/w), 6% (w/w) and 3% (w/w). Dextran is a hydrophilic natural and biodegradable polymer consisting of a mixture of repeating glucose subunits and available in a large variety of molecular weights ranging between 1,000 daltons (Da) and 40,000,000 Da[90,91]. NaPA8000 is a hydrophilic copolymer of acrylic acid and sodium acrylate with enhanced absorption ability due to the presence of carbonyl and sodium groups in its chemical structure, thus being considered a superabsorbent polymer[92]. Moreover, in the presence of a liquid this polymer tends to swell and form a gel. The results obtain for fluorescence signal registered after detection of target molecule prepared in Dextran and NaPA800 are depicted in **Figure 21**.

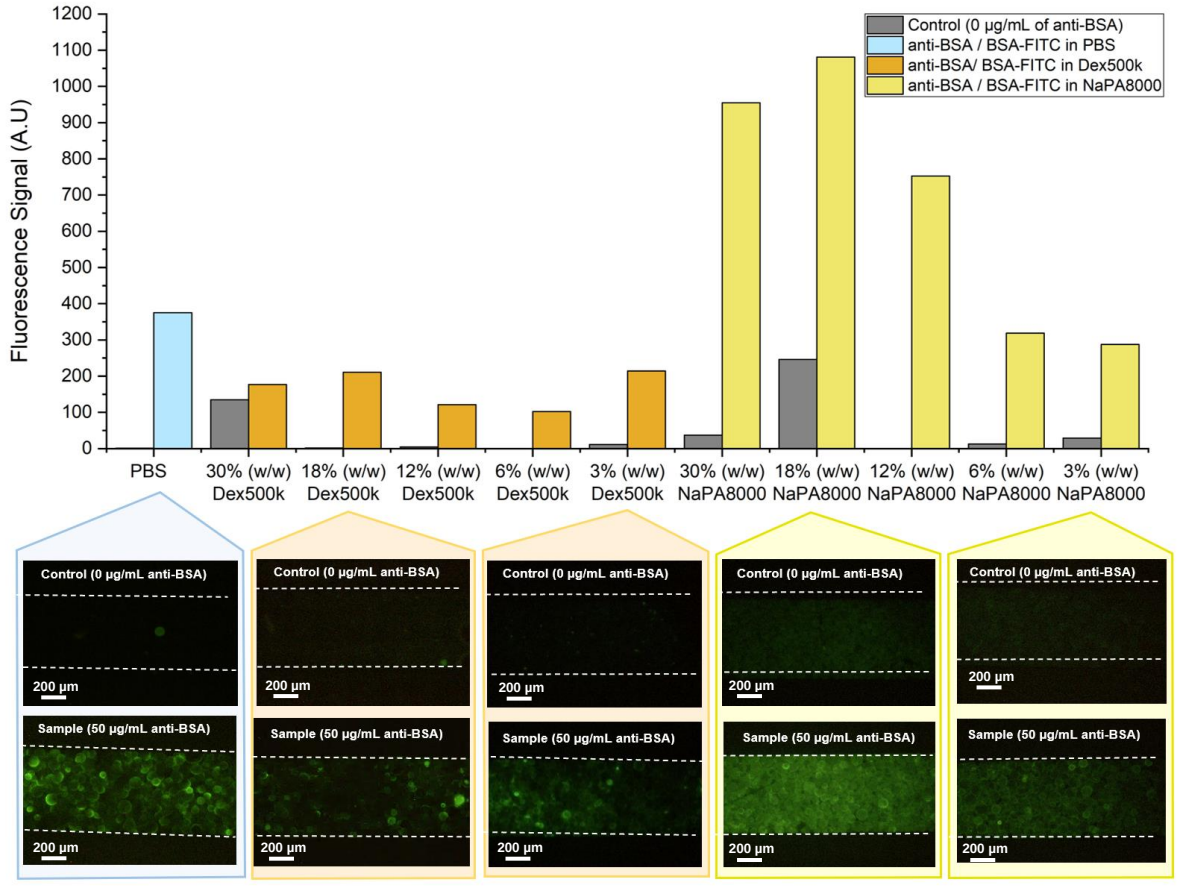

Figure 21 *- Influence of Dex500k and NaPA8000 in the detection of target analyte FITC conjugate BSA. The experiments performed in PBS are presented for the sake of comparison with the fluorescence signal obtained with other solutions. (Top) Fluorescence signal obtained in the detection of spiked solutions of BSA in Dextran and NaPA8000. (Bottom) Fluorescence images obtained with Olympus Microscope with a 4x objective, exposure time of 2 seconds and 0dB of gain. The sets of images from left to right represent the fluorescent intensity obtained when an immunoassay is performed in PBS buffer, in 18%(w/w) of Dex500k, in 3%(w/w) of Dex500k, in 18%(w/w) of NaPA8000 and 3%(w/w) of NaPA8000.*

By analysing **Figure 21**, it is possible to observe that immunoassay performed with BSA-FITC spiked solutions in Dextran presented fluorescence signals lower than the ones obtained for the assay performed in PBS, with the highest fluorescence intensity registered when target analyte is prepared in a minimum concentration solution of the referred polymer, i.e., 3% (w/w) Dex500k. Overall, non-specific signals were also minimum, indicating that this polymer does not increase non-specific interactions between antigen-antibody complexes, except for the control sample performed with dextran at 30% (w/w), which presented a non-specific signal almost as high as the correspondent experiment. However, since these experiments were only performed once, this high fluorescence intensity in the control experiment can be attributed to experimental errors, thus not being considered relevant. Another aspect to highlight regarding Dextran properties is its high viscosity which can impair the performance of the immunoassay, especially affecting the flow rates at which the assay is performed, which consequently hampers the molecule diffusion. Regarding fluorescence intensity results obtained for the experiments performed with NaPA800, in most of the concentrations tested the fluorescence signal registered after BSA capture was considerably higher in comparison with the experiments performed in PBS, except for the experiments performed with concentrations of 6% (w/w) and 3% (w/w) of NaPA8000 which presented fluorescence signals comparable with those obtained for PBS samples. The higher fluorescence intensity recorder when the polymer is expressed in higher concentrations might be explained by its gel-like behaviour and superabsorbent properties in the presence of liquid solutions, since the gel consistency and swelling effect might help guide BSA molecules towards the anti-BSA antibodies immobilized on the microbeads and prevent them from being removed during washing steps, thus enhancing specific fluorescence signal.

c) Ionic Liquids

After testing different polymers, several ILs solutions were prepared followed the same idea as previously described, i.e., with two assays being performed, one which acted as control experiment, with no incubation of anti-BSA antibodies (grey bars), and the other which consisted of a regular complete immunoassay (colourful bars).

The first two ionic liquids tested were $[C_4C_1im]Cl$ and $[C_4C_1pyrr]Cl$, i.e., imidazolium-based IL and pyrrolidinium-based IL, which are the most used and widely studied components in the formation of ABS for extraction of several proteins. However, some studies reported some levels of toxicity of ILs composed of aromatic cations, such as imidazolium-based IL in comparison with non-aromatic ILs such as pyrrolidinium, ammonium and phosphonium[93]. This has paved the way for further investment in greener ILs. Both these ILs were prepared in concentrations of 60% (w/w), 40%(w/w), 20%(w/w), 10%(w/w) and 5%(w/w). For the experiments performed with samples prepared in $[C_4C_1im]Cl$, higher fluorescence values are registered when the IL is present at lower concentrations, indicating lower levels of interference of these solutions in molecular recognition events. Particularly, the fluorescence intensity obtained when the experiments are performed with 10% (w/w) and 5% (w/w) of imidazolium-based IL is even superior to the fluorescence signal obtained for the same experiment performed in PBS.

Regarding [C_4C_1pyrr]Cl, the fluorescence values obtained follow a similar behaviour, with higher values being registered when the experiments are performed with working solutions of [C_4C_1pyrr]Cl at lower concentrations, with the exception of 10% (w/w) IL which presented a lower fluorescence signal. Overall, control experiments recorded lower fluorescence signals, indicating these ILs do not increase non-specific interactions. The results described are depicted in **Figure 22**.

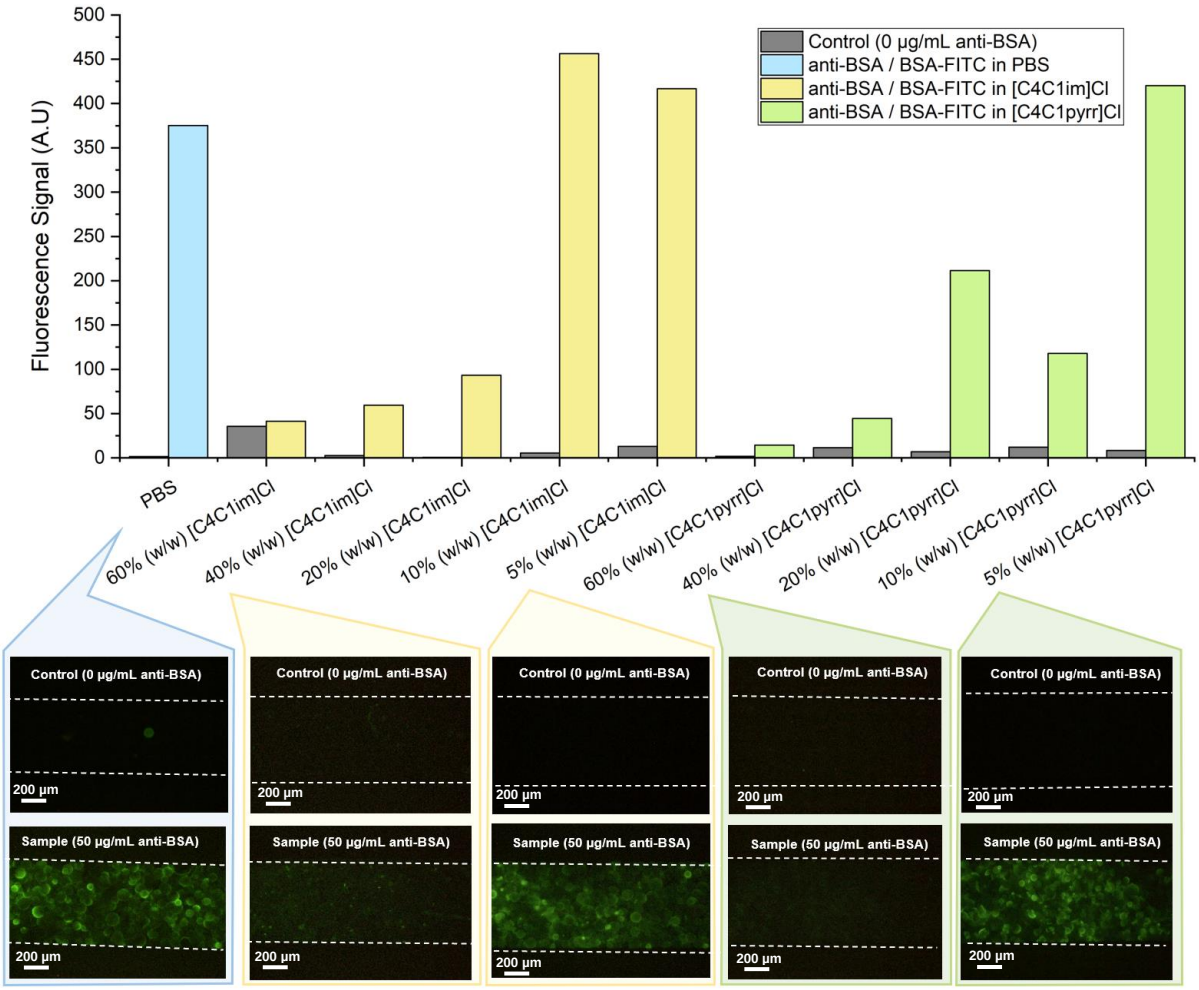

Figure 22 *- Influence of [C_4C_1im]Cl and [C_4C_1pyrr]Cl in the detection of target analyte FITC conjugate BSA. The experiments performed in PBS are presented for the sake of comparison with the fluorescence signal obtained with other solutions. (Top) Fluorescence signal obtained in the detection of spiked solutions of BSA in [C_4C_1im]Cl and [C_4C_1pyrr]Cl. (Bottom) Fluorescence images obtained with Olympus Microscope with a 4x objective, exposure time of 2 seconds and 0dB of gain. The sets of images from left to right represent the fluorescent intensity obtained when an immunoassay is performed in PBS, in 40%(w/w) of [C_4C_1im]Cl, in 5%(w/w) of [C_4C_1im]Cl, in 40%(w/w) of [C_4C_1pyrr]Cl and 5%(w/w) of[C_4C_1pyrr]Cl.*

The other two ionic liquids tested were [P_{4444}]Cl and [N_{4444}]Cl, which are phosphonium- and ammonium-based ILs, respectively. They are characterized as better alternatives in terms thermal and chemical stability in comparison with their imidazolium-based counterparts. Besides, they are also less expensive and more effective in promoting the formation of ABS, specially phosphonium-based ILs, in

comparison with imidazolium-based ILs[94]. Both these ILs were also prepared in working solutions of 60% (w/w), 40%(w/w), 20%(w/w), 10%(w/w) and 5%(w/w). Despite their good properties, both these ILs presented lower values of fluorescence signal in comparison with the experiments performed in PBS. Additionally, there is some considerable non-specific signal registered in the experiments performed with higher concentrations of both $[P_{4444}]Cl$ and $[N_{4444}]Cl$, specifically 40% (w/w) and 20% (w/w) of $[P_{4444}]Cl$ and 40% (w/w) of $[N_{4444}]Cl$. Even though they present some interference in the molecular recognition, it was still possible to achieve reasonable signal-to-noise ratios, proving these systems are still able to detect target molecule BSA. Therefore, since they are promising components in the formation of ABS, they can potentially be used for the future development of sample pre-treatment systems coupled with robust detection platforms. The results obtained regarding experiments performed using $[P_{4444}]Cl$ and $[N_{4444}]Cl$ are depicted in **Figure 23**.

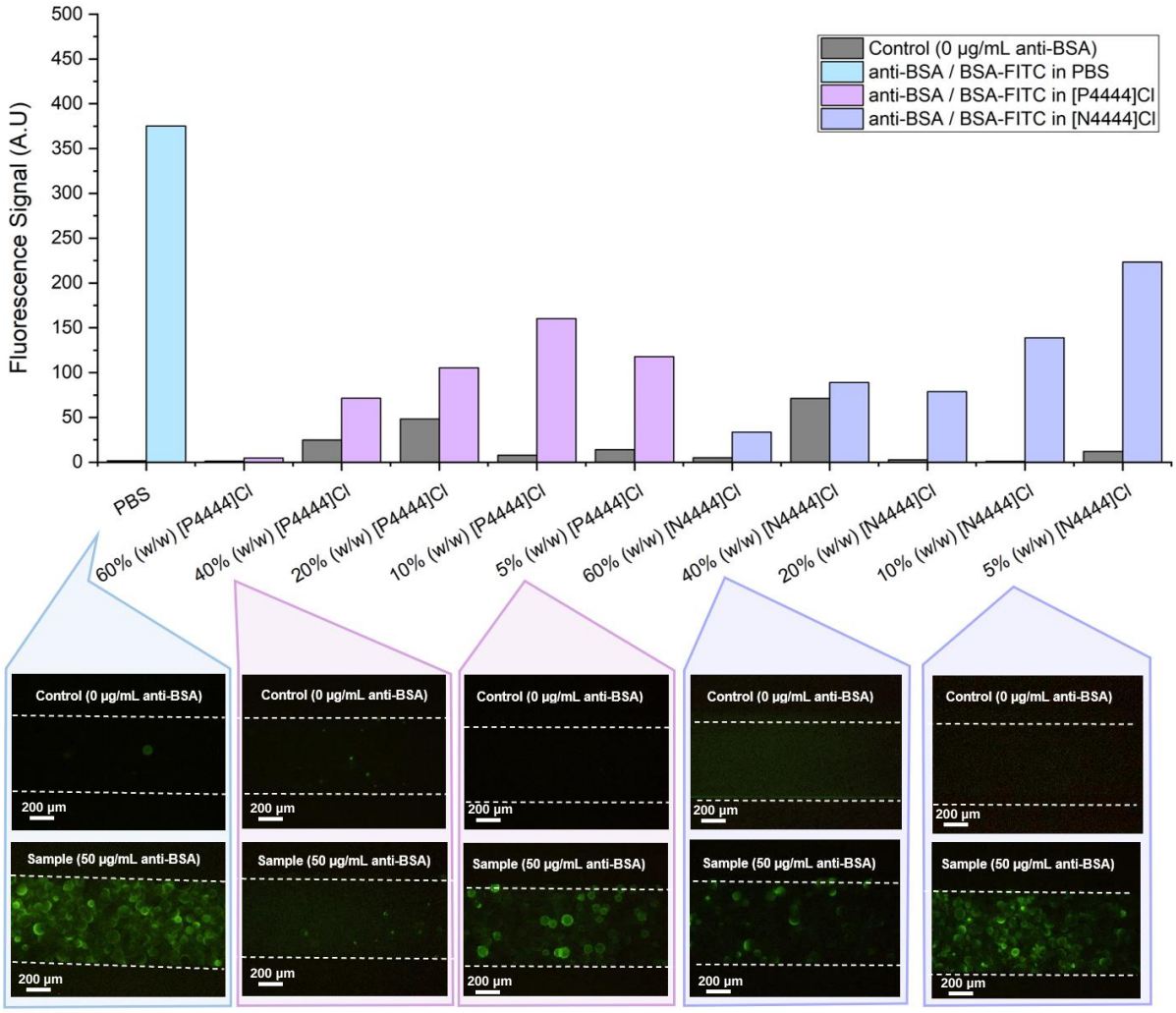

Figure 23 *- Influence of $[P_{4444}]Cl$ and $[N_{44444}]Cl$ in the detection of target analyte FITC conjugate BSA. The experiments performed in PBS are presented for the sake of comparison with the fluorescence signal obtained with other solutions. (Top) Fluorescence signal obtained in the detection of spiked solutions of BSA in $[P_{4444}]Cl$ and $[N_{44444}]Cl$. (Bottom) Fluorescence images obtained with Olympus Microscope with a 4x objective, exposure time of 2 seconds and 0dB of gain. The sets of images from left to right represent the fluorescent intensity obtained when an immunoassay is performed in PBS, in 40%(w/w) of $[P_{4444}]Cl$, in 5%(w/w) of $[P_{4444}]Cl$, in 40%(w/w) of $[N_{44444}]Cl$ and 5%(w/w) of $[N_{44444}]Cl$.*

The last IL tested was choline chloride and similarly to phosphonium and ammonium-based ILs, choline-based ILs are a new effective alternative to their imidazolium-based counterpart, due to their low cost, biocompatibility, biodegradability[55] and non-toxicity features. They have been used in the formation of ABS with polymers[95] and there is also a limited number of studies using them with salts which help to overcome the hydrophilicity of choline-based ILs[96]. The referred IL was prepared in PBS in working solutions of 40% (w/w), 20% (w/w), 10% (w/w) and 5% (w/w). The results obtained for fluorescence signal registered for immunoassays performed with [Ch]Cl are depicted in **Figure 24**.

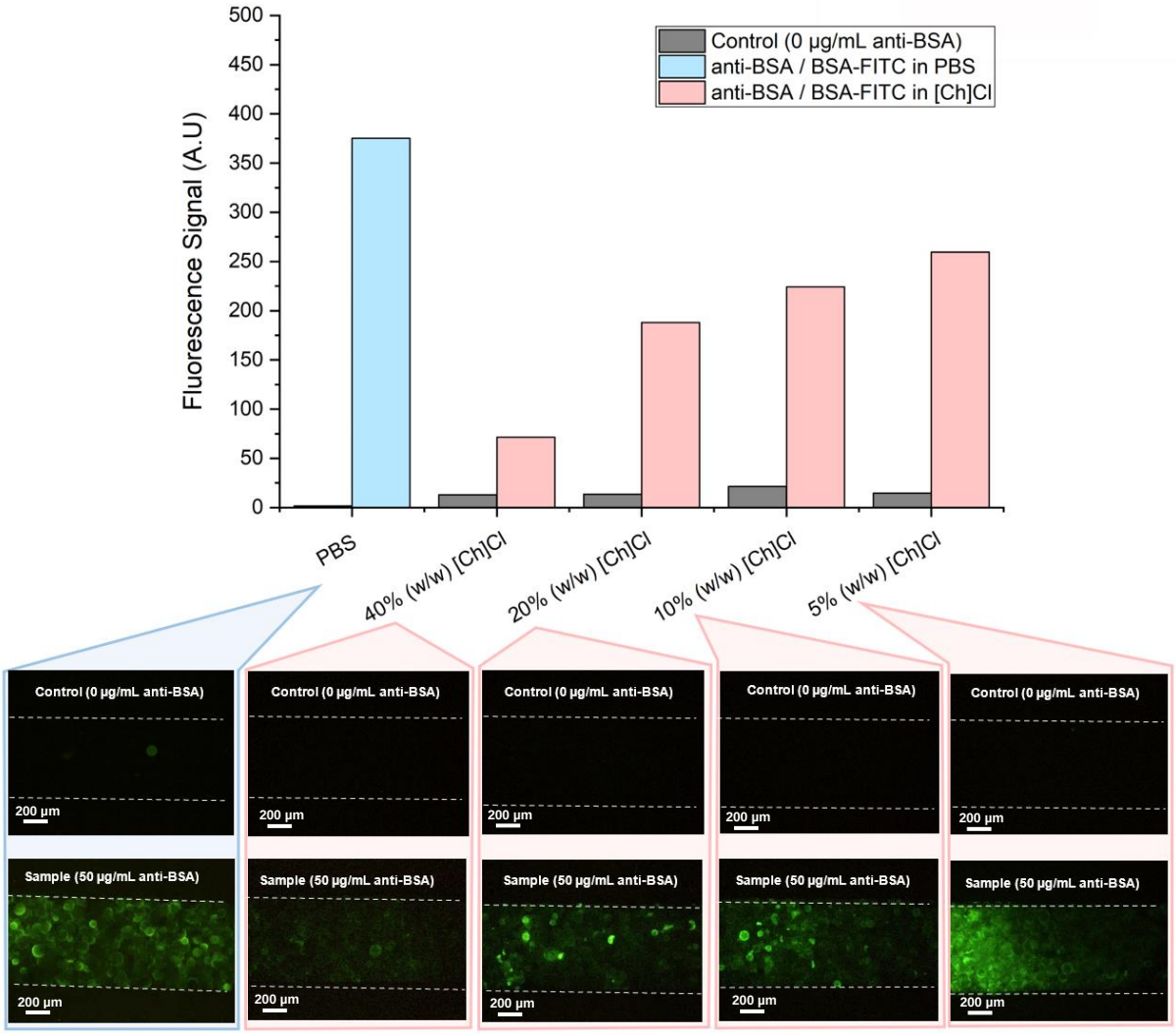

Figure 24 *- Influence of [Ch]Cl in the detection of target analyte FITC conjugate BSA. The experiments performed in PBS are presented for the sake of comparison with the fluorescence signal obtained with other solutions. (Top) Fluorescence signal obtained in the detection of spiked solutions of BSA in [Ch]Cl. (Bottom) Fluorescence images obtained with Olympus Microscope with a 4x objective, exposure time of 2 seconds and 0dB of gain. The sets of images from left to right represent the fluorescent intensity obtained when an immunoassay is performed in PBS, in 40%(w/w) of [Ch]Cl, in 20%(w/w) of [Ch]Cl, in 10%(w/w) of [Ch]Cl and 5%(w/w) of [Ch]Cl.*

By analysis of **Figure 24** it is possible to observe an increase in fluorescence signal with a reduction of IL concentrations in spiked solutions of BSA-FITC, indicating a lower interference in

molecular recognition when lower concentrations of these IL are used. Regarding non-specific signal, the fluorescence intensity registered in the control samples is low and remains constant throughout all concentrations of IL used in the assays performed, which indicates the IL under analysis does not increase non-specific interactions between molecules present in the immunoassay. Moreover, even though the fluorescence signal registered when [Ch]Cl is used in all concentrations studied is lower in comparison with the fluorescence intensity recorded for immunoassay performed in PBS, the signal-to-noise ratios achieved are still considerably elevated, which makes [Ch]Cl a promising IL to be used in detection systems of target molecules with a potential coupled ABS for sample pre-treatment.

3.2. PSA detection studies

3.2.1. Sandwich PSA immunoassay

After analysing the influence of different solutions on the detection of BSA as target molecule, detection of a specific prostate marker, PSA, was studied and several immunoassays were performed. For the study of PSA detection, each of the immunoassays performed consisted of complete sandwich assay, unless stated otherwise. Each assay started with immobilization of anti-PSA antibody on agarose beads coated with Protein G as described in section **2.3.2** and the beads were packed in microfluidic channels in a process described in section **2.3.3**. Briefly, after packing the beads in the channel, PBS is flowed through the column at 15 µL/min to remove remaining PEG solution. Then, blocking agent, which was BSA 4% (w/v) unless stated otherwise, was inserted in the channel to minimize non-specific signal and flowed for 10 minutes at 0.5 µL/min. In between every individual assay step, PBS was flowed through the microchannel to remove any unbound molecules for 1 minute at 5 µL/min, in a process known as intermittent washing. Subsequently, specific concentration of target analyte PSA spiked either in PBS, human serum, several ionic liquids or PEGs was flowed through the channel for 10 minutes at 0.5 µL/min. Then the same procedure is followed for detector anti-PSA antibody labelled with Alexa430 fluorophore, flowed at a concentration of 100 µg/mL. A final washing step of 1 minute with PBS at 5 µL/min was performed. The specific concentrations of PSA in either PBS, human serum, ILs or PEGs ranged from 0 ng/mL (control sample) to 25 ng/mL. **Figure 25** illustrates the main steps of sandwich immunoassay performed for the detection of PSA either in PBS buffer, human serum, ILs or PEGs solutions.

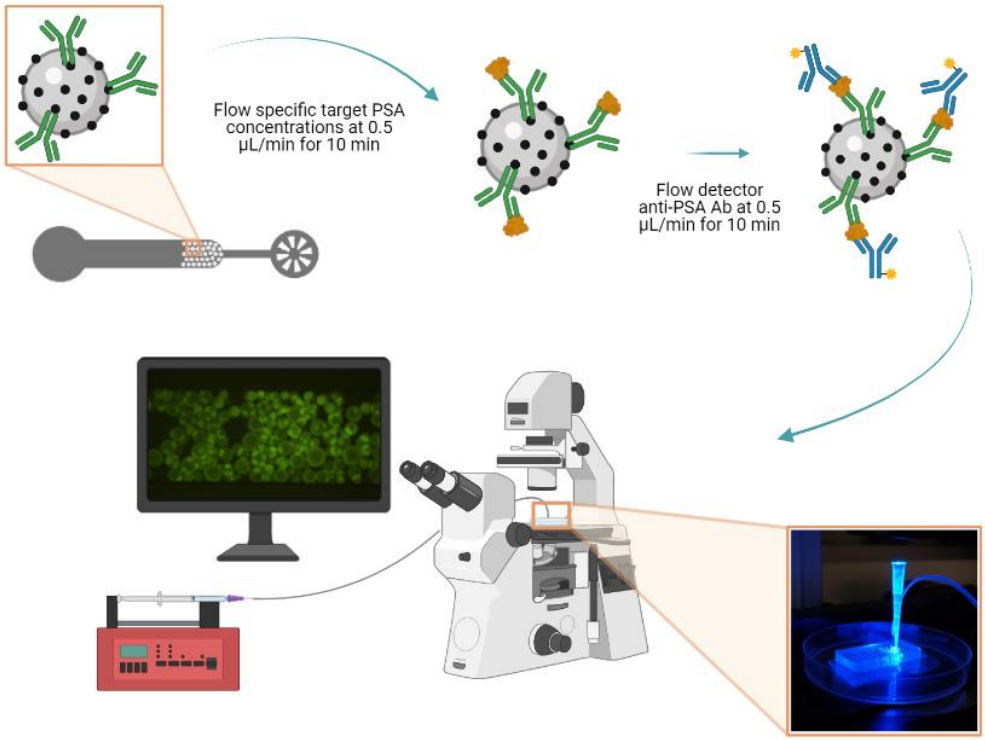

Figure 25 *- Main steps of sandwich immunoassay for PSA detection from beads packing to fluorescence measurements.*

3.2.2. Solid-support choice

The main goal of PSA detection studies is to achieve reasonable levels of sensitivity, therefore the first immunoassay performed aimed at identifying the best option for immobilization of capture anti-PSA antibodies, choosing between PDMS walls of a bare microchannel and microbeads, in order to achieve higher levels of fluorescence signal. For this purpose, two different immunoassays were performed. The protocol followed for the experiment performed with microbeads is the same as described above (section **3.2.1**). The protocol for the experiment performed in open channel started with immobilization of anti-PSA antibodies on PDMS walls of bare microfluidic channels by flowing this solution at a flow rate of 0.5 µL/min for 10 min, after cleaning the channel with PBS. After each individual step of the immunoassay, intermittent washes were performed, by flowing 5 µl of PBS for 1 minutes at 5 µl/min. Subsequently, 5 µl of BSA 4% (w/v) was used to prevent non-specific interactions and blocking unoccupied binding sites at the PDMS walls, also at 0.5 µL/min. Then solutions of either 0 ng/mL of PSA – which worked as control sample - and 25 ng/mL of PSA were prepared in PBS and flowed through the channels at 0.5 µL/min for 10 minutes. Afterwards, a solution of anti-PSA detector antibodies labelled with Alexa430 fluorophore was flowed at 0.5 µL/min for 10 minutes. Finally, the last step consisted in a washing step with PBS by flowing it for 1 min at 5 µL/min. The fluorescence signal registered for both PSA concentrations with and without microbeads are depicted in **Figure 26**.

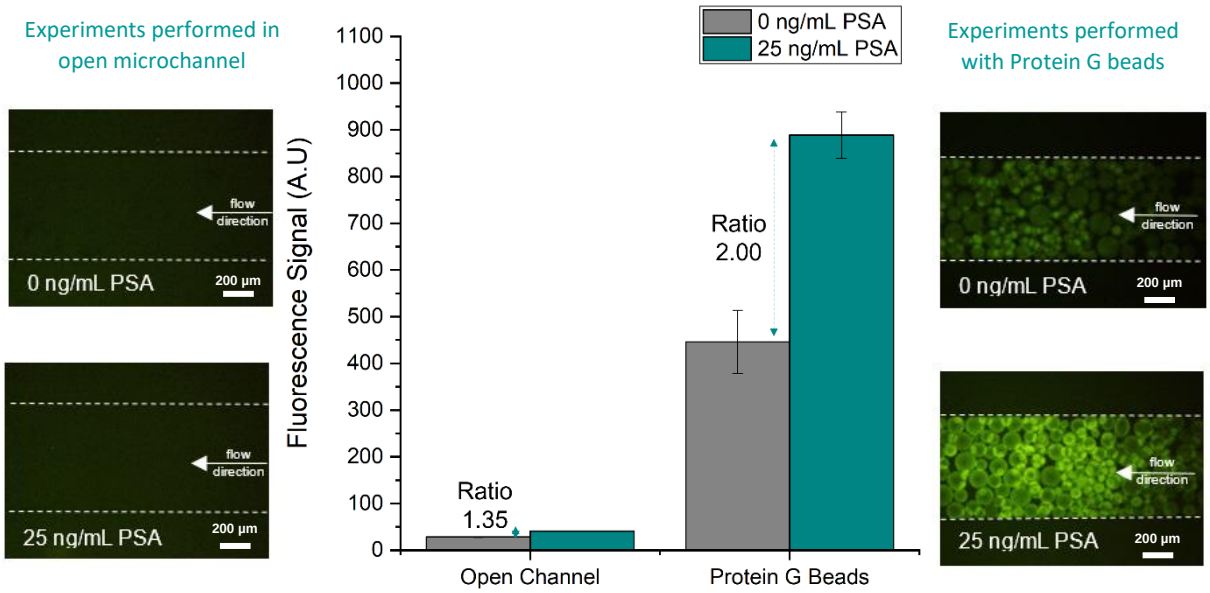

Figure 26 *– Study of fluorescence signal using sandwich immunoassay for PSA detection using two different approaches: open channel and channel packed with protein G beads. (Centre) Comparison of fluorescence intensity between microfluidic sandwich immunoassay performed in an open bare microchannel and in a microchannel packed with protein G beads for PSA detection. Error bars represent the standard deviation of two repeated measurements. (Left) Experimental images acquired at the end of the assay performed in a bare open microchannel for sample (25 ng/mL of PSA) and control (0 ng/mL of PSA). (Right) Experimental image acquired at the end of the assay performed in a packed microchannel with Protein G beads for sample (25 ng/mL of PSA) and control (0 ng/mL of PSA). All images were acquired with Olympus Microscope with an 4x objective, exposure time of 2 seconds and 0dB of gain.*

By analysing **Figure 26** it is possible to conclude that higher fluorescence signals are achieved when Protein G agarose beads are used to immobilize capture anti-PSA antibodies in comparison with the same experiment performed in a bare open channel. In fact, microbeads bring several advantages over planar surfaces, such as higher surface-to-volume ratio, which consequently increases sensitivity, higher binding capacities, tunable surface functionalization and short diffusion distances in between beads. Moreover, according to Kawaguchi[97], microbeads present a significantly higher surface for immobilization of capture probes in comparison with their flat counterparts, which consequently enhances the sensitivity of immunoassays and reduces their detection limits[98]. Some studies proved that, in addiction to higher surface-to-volume ratios, short diffusion distances between beads in microfluidic channels cause a reduction in analysis capture times and, consequently in overall immunoassay timeframes in relation to planar counterparts[99,100]. Therefore, the strategy chosen to continue the study of PSA detection in different solutions is agarose Protein G microbeads for the immobilization of capture antibodies, due to the several referred benefits they offer over traditional planar microfluidic immunoassays.

3.2.3. Immobilization of capture anti-PSA antibody on different microbeads

The next immunoassay aimed at comparing two different types of beads and their affinity to capture anti-PSA antibodies: agarose beads coated with Protein A or Protein G. In both cases the experiments were performed using a complete sandwich immunoassay already described in section **3.2.1** and both set of beads were prepared according to protocol reported on section **2.3.2** regarding immobilization of anti-PSA capture antibody. Both set of experiments were performed using 0 ng/mL of PSA as control sample and 25 ng/mL of target analyte as sample under analysis. The fluorescence images were acquired at the end of each experiment. **Figure 27** illustrates the results obtained for the referred experiments performed with Protein A and Protein G beads.

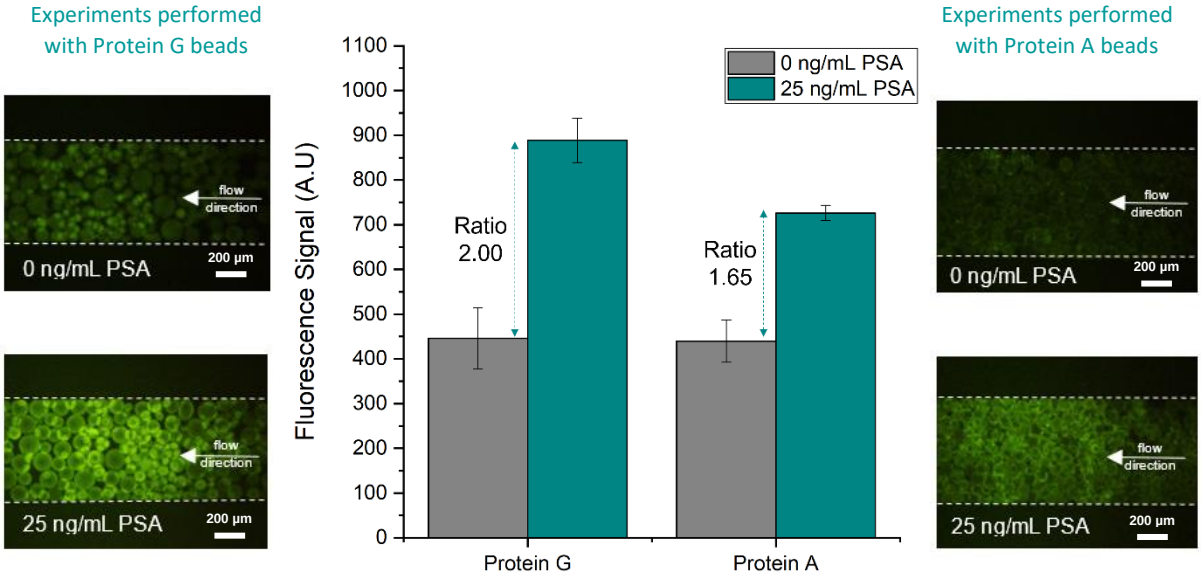

Figure 27 *– Study of fluorescence intensity using sandwich immunoassay for PSA detection performed with different types of beads: Protein G and Protein A beads. (Centre) Measurement of fluorescence signal of a microfluidic sandwich immunoassay for the detection of PSA, in which the capture anti-PSA antibodies were immobilized on Protein G agarose beads in comparison with a sandwich assay in which the capture anti-PSA antibodies were immobilized on Protein A agarose beads. Error bars represent the standard deviation of two repeated measurements. (Left) Experimental images acquired at the end of the assay in which Protein G beads were used to immobilize capture anti-PSA antibodies for sample (25 ng/mL of PSA) and control (0 ng/mL of PSA). (Right) Experimental image acquired at the end of the assay in which Protein A beads were used to immobilize capture anti-PSA antibodies for sample (25 ng/mL of PSA) and control (0 ng/mL of PSA). All images were acquired with Olympus Microscope with an 4x objective, exposure time of 2 seconds and 0dB of gain.*

Figure 27 shows the effect of different type of beads in the fluorescence signal obtained from a PSA sandwich assay. As can be seen in the graph, protein G beads present higher affinity for capture anti-PSA antibodies in comparison with Protein A beads. In fact, each protein has a different binding strength for IgG molecules which varies according to their source species and immunoglobulin subtype. **Table 10** shows a comparison of binding affinities of Protein A and Protein G for the main species of

IgG molecules (human, mouse, goat and rabbit). The specific binding site in IgG molecule for both proteins is located in the Fc domain of the molecule and observing **Table 10** is possible to conclude that Protein A has a greater binding affinity towards various mammalian IgG subclasses, being generally preferred for rabbit, goat, and only IgG1, IgG2 and IgG4 human subclasses, while Protein G specifically binds a broader range of human and mouse subclasses[101]. Additionally, the reduction in fluorescence signal registered in the assay depicted in **Figure 27** when anti-PSA antibodies are immobilized on Protein A can be explained by the biological source of the capture antibodies used, which were derived from mouse species, specifically IgG1 isotype, since Protein A has a significantly lower binding affinity to this subclass of mouse IgG molecules. Thus, these results are in agreement with the literature. Having this into consideration, the microbeads chosen to perform the remaining assays for PSA detection studies were agarose coated Protein G beads.

Another important aspect to highlight in the graph depicted on **Figure 27** is the signal to noise ratio of both sets of experiments. It is possible to observe that ratio of signal from sample with 25 ng/mL of PSA to that of the control sample is similar for both Protein A and Protein G experiments. Unfortunately, in both cases, control samples presented higher fluorescence signals than desired, which is attributed to increased non-specific interactions during molecular recognition events.

Table 10 *- Comparison between binding affinities of Protein A and Protein G to different immunoglobin species and subclasses*[102]

Species	*Subclasses*	*Protein A affinity*	*Protein G affinity*
Human	IgA	-	-
	IgD	-	-
	IgE	-	-
	IgG_1	++++	++++
	IgG_2	++++	++++
	IgG_3	-	++++
	IgG_4	++++	++++
	IgM	-	-
Mouse	IgG_1	+	++++
	IgG_{2a}	++++	++++
	IgG_2	+++	+++
	IgG_3	++	+++
Goat	IgG	++	-
Rabbit	IgG	++++	+++

3.2.4. Blocking optimization

Working towards the detection of lower concentrations of target analyte PSA with minimum non-specific signal, several assays were performed in order to optimize surface-blocking, by testing different blocking agents. The blocking agents used included BSA 4% (w/v), Casein 1% (w/v), a mixture of both

consisting of 50% BSA 4% (w/v) and 50% Casein 1% (w/v), and, finally, a mixture of human serum antibodies, commercially available as Gammanorm®, at a working concentration of 5 mg/mL.

The assays performed consisted in a complete sandwich immunoassay in which the capture antibody was immobilized on Protein G agarose beads as described in section **2.3.2** and packed inside microchannel as described in **2.3.3**, followed by PBS to remove PEG solution and blocking (step in which the different blocking solutions were tested), then flowing the analyte at 0 ng/mL and 25 ng/mL and finally the detector antibody molecule, with intermittent washing at the end of every step to remove unbound molecules. The complete protocol for the referred sandwich immunoassay is described in detail in section **3.2.1**. **Figure 28** depicts the results obtained regarding the effect of different blocking agents on final the fluorescence signal regarding PSA detection, whereas **Figure 29** presents the experimental images with the fluorescence signal obtained for each blocking agent tested.

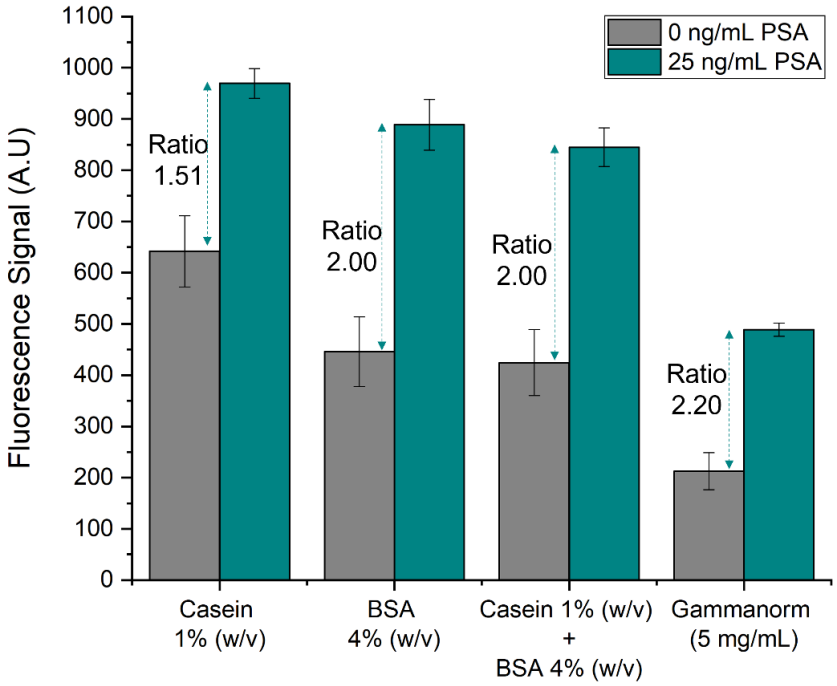

Figure 28 *- Blocking optimization for PSA detection, in which different blocking agents were tested - Casein 1% (w/v), BSA 4% (w/v), a mixture of 50% Casein 1% (w/v) with 50% BSA 4% (w/v) and Gammanorn at 5 mg/mL. A complete sandwich immunoassay was performed to evaluate the efficacy of each blocking agent for sample (25 ng/mL of PSA) and control (0 ng/mL of PSA). The dashed arrows represent the ratio calculated between sample and control. Error bars represent the standard deviation of two repeated measurements. Measurements were acquired with Olympus Microscope with an 4x objective, exposure time of 2 seconds and 0dB of gain.*

By analysing **Figure 28** it is possible to verify that both BSA 4% (w/v) and the mixture of equal volumes of BSA 4% (w/v) and Casein 1% (w/v) presented the same signal-to-noise ratio. The mixture of Casein and BSA was therefore excluded from the blocking agents considered, since the reduction of reagents used in each experiment is one of the major goals of microfluidic applications and because the fluorescence signal obtained in the experiment performed with PSA concentration of 25 ng/mL in which

this blocking mixture was used was slightly lower in comparison with the same experiment performed with BSA 4% as blocking agent.

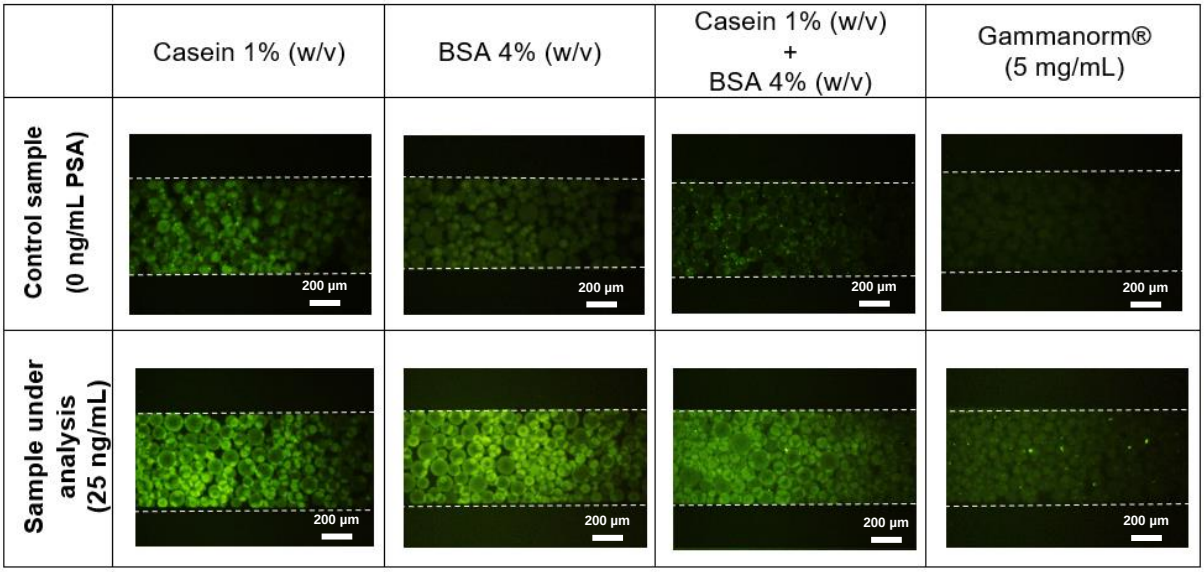

Figure 29 *- Experimental images of blocking optimization for PSA detection, in which different blocking agents were tested - Casein 1% (w/v), BSA 4% (w/v), a mixture of 50% Casein 1% (w/v) with 50% BSA 4% (w/v) and Gammanorn at 5 mg/mL (data presented in Figure 25). Images represent fluorescence signal acquired for the detection of PSA by performing a sandwich immunoassay with four different blocking agents for sample (25 ng/mL of PSA) and control (0 ng/mL of PSA). All images were acquired with Olympus Microscope with an 4x objective, exposure time of 2 seconds and 0dB of gain.*

Regarding Casein 1% (w/v), even though the experiment performed with this blocking solution, where the target analyte was present at a concentration of 25 ng/mL, recorded a slightly superior fluorescence signal, this blocker was excluded since the ratio of the signal from the sample under analysis to that of the control sample was lower, indicating an increased control signal resulting from non-specific absorption, which translates in a less efficient blocking performance.

The remaining blocking agents, BSA 4% (w/v) and Gammanorm®, were then compared. As it is possible to observe in the experimental images depicted in **Figure 29**, even though the ratio between sample with 25 ng/mL of target PSA and control sample is higher when the Gammanorm is used as blocking agent, this blocker also causes a noticeable decrease in the overall fluorescence signal of the system considered. This might be explained by the fact that this agent is composed of a mixture of antibodies in which about 95% are human IgGs, possibly leading to interspecies cross-reactivity, which may decrease specific fluorescence signal. Hence, BSA 4% was chosen as the appropriate blocking agent for the microfluidic immunoassays, even though there was still some non-specific signal that was not possible to eliminate.

3.2.5. Concentration of capture antibody

The following experiments aimed at optimizing antibody concentration on beads' surface. Therefore, in order to allow the complete saturation of capture antibody on surface of microbeads and

simultaneously ensure an efficient antigen capture, two different approaches were used: (I) a complete sandwich assay performed as described in detail in section **3.2.1**, where capture anti-PSA antibodies were used at various concentrations ranging from 0 µg/mL to 1 mg/mL, and (II) an assay where Alexa430-labelled anti-PSA antibodies were immobilized on Protein G beads at same concentrations, from 0 µg/mL to 1 mg/mL, and incubated in the microchannel as described in section **2.3.3**, followed by a washing step to remove unbound molecules. The results for both approaches are shown in **Figure 30**.

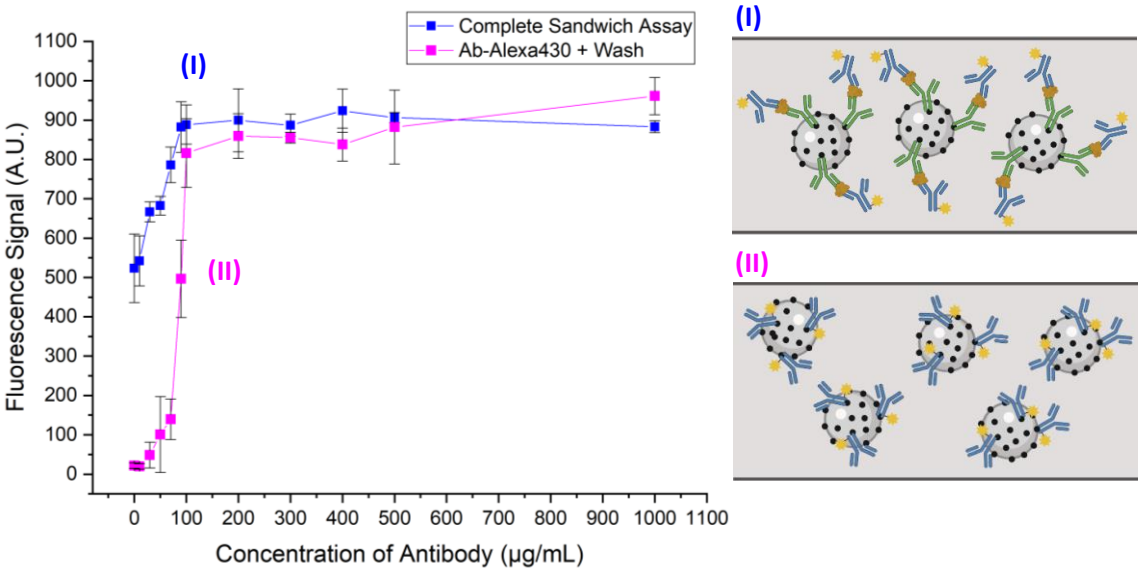

Figure 30 *- Optimization studies for capture anti-PSA antibody concentration. (Left) Fluorescence signal obtained with increasing concentration of antibody from 0 µg/mL to 1 mg/mL using two different approaches: (I) a complete sandwich immunoassay and (II) by incubation anti-PSA antibodies conjugated with Alexa430 fluorophore in Protein G beads in microfluidic channel, followed by a washing step to remove unbound molecules. Error bars represent the standard deviation between two repeated measurements. Data were acquired with Olympus Microscope with an 4x objective, exposure time of 2 seconds and 0dB of gain. (Right) schematic of (I) complete sandwich immunoassay with varying concentrations of anti-PSA antibody and (II) assay in which anti-PSA-Alexa430 antibodies are immobilized on Protein G packed in the microchannel, followed by PBS wash, varying the concentration of anti-PSA antibodies.*

As can be seen in the graph shown on **Figure 30**, there is an increase in fluorescence signal with increasing concentrations of anti-PSA antibodies (I), reaching a plateau regime around 100 µg/mL of antibody. This same behaviour is confirmed by the second assay performed in which only labelled anti-PSA antibodies immobilized on Protein G beads were incubated in the microchannel (II). Therefore, a concentration of 100 µg/mL of anti-PSA antibody would guarantee a complete saturation of microbeads surface since the use of concentrations above the reached plateau would possibly lead to an excess antibody coverage. Some studies suggest that these excessive layer of antibodies on a solid support would lead to these antibodies to build up and block other available antibody molecules, possibly due to antibody-antibody interactions and aggregation, thus hiding their binding sites and hampering the formation of antigen-antibody complexes[103]. Therefore, to prevent this masking effect and simultaneously allow an efficient bead surface coverage and capture while accounting for reagent saving the concentration of antibody chosen to continue the experiments for PSA detection was 100 µg/mL.

3.2.6. Simulation of PSA detection in biological matrix

After completing the optimization studies for PSA detection, which culminated with the choice of BSA 4% (w/v) as the most effective blocking agent and Protein G beads as the preferential beads to immobilize anti-PSA capture antibodies, the effect of a biological matrix in the fluorescence signal obtained from PSA sandwich assay was evaluated. The Protein G bead functionalization strategy used for these assays was similar to the one previously described in section **2.3.2**, in which specific concentrations of PSA were detected in spiked solutions of either PBS or human serum. The results obtained are a result of a simultaneous measurement of a control sample, with no PSA, i.e., sample with plain PBS or non-spiked human serum and a certain concentration of PSA, namely 25 ng/mL. The main goal of this experiments was to bring them closer to real-life POC applications, considering that most cancer biomarkers can be found in biological fluids. **Figure 31** depicted the fluorescence signal obtained for PSA detection in spiked solutions of PBS and human serum.

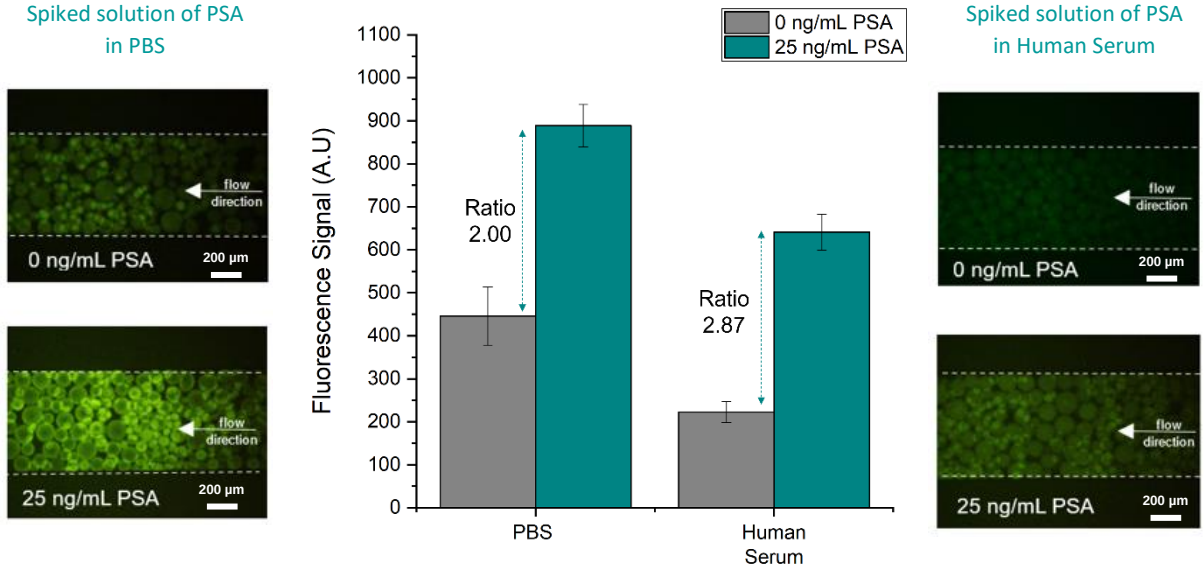

Figure 31 *- Biological matrix effect in PSA detection. (Centre) Fluorescence intensity of complete sandwich immunoassays performed with spiked solutions of PSA in PBS and unprocessed human serum for sample (25 ng/mL of PSA) and control (0 ng/mL of PSA). The dashed arrows represent the ratio of the sample to the control. Error bars represent the standard deviation between two repeated experiments. (Left) Experimental images of sandwich immunoassay performed with PSA spiked in PBS for sample and control. (Right) Experimental images of sandwich immunoassay performed with PSA spiked in human serum for sample and control. All images were acquired with Olympus Microscope with an 4x objective, exposure time of 2 seconds and 0dB of gain.*

As can be seen in **Figure 31**, there is an overall decrease in fluorescence intensity when the samples of PSA are spiked in human serum in comparison with its PBS counterpart. This reduction might be explained by two main factors, the first one being the fact that human serum is composed of a series of proteins, in which Albumin accounts for almost 80% of its content, and this amount of proteins possibly interferes with the antibody-antigen complex formation, creating a blocking effect which is noticeable not only in the experiment with a PSA concentration of 25 ng/mL, but also with the control

sample. The other factor might be related to the viscosity inherent to increased concentrations of proteins in this solution, which possibly affects the transport of molecules inside the microfluidic channel, consequently hindering the capture of PSA molecules. Furthermore, it is possible to observe by the graphic and corresponding experimental images that there is still a considerable amount of fluorescence signal in the absence of PSA (control samples) even with the current blocking strategy, due to non-specific molecular interactions for both PBS and human serum tests. Therefore, further work is in need to optimize the detection of PSA, minimizing non-specific interactions. However, there is still a significant amount of specific signal obtained for 25 ng/mL of PSA for both PBS and human serum samples.

It is also worth noting that the ratio of the signal from the sample with 25 ng/mL of PSA to that of the control sample is relatively similar for both PBS and human serum tests, thus the remaining assays to test the influence of ionic liquids and PEG were further conducted in solutions with PSA spiked in PBS solutions.

After analysing the effect of biological matrix in the detection of PSA, the capacity to detect this cancer biomarker within a clinically relevant range was further analysed, using the microfluidic sandwich immunoassay already described. Therefore, different concentrations of PSA were prepared in a spiked solution of either PBS or human serum, ranging from 0 ng/mL to 25ng/mL. The protein G beads were prepared and packed in the microchannel as described in sections **2.3.2** and **2.3.3**, respectively. The remaining assays steps were followed as described in detail in section **3.2.1** in order to detect the minimum detectable concentration of PSA, within the selected range tested. For this purpose, calibration curves for PSA were prepared for buffer and human serum conditions, and the results of this approach are depicted in **Figure 32**.

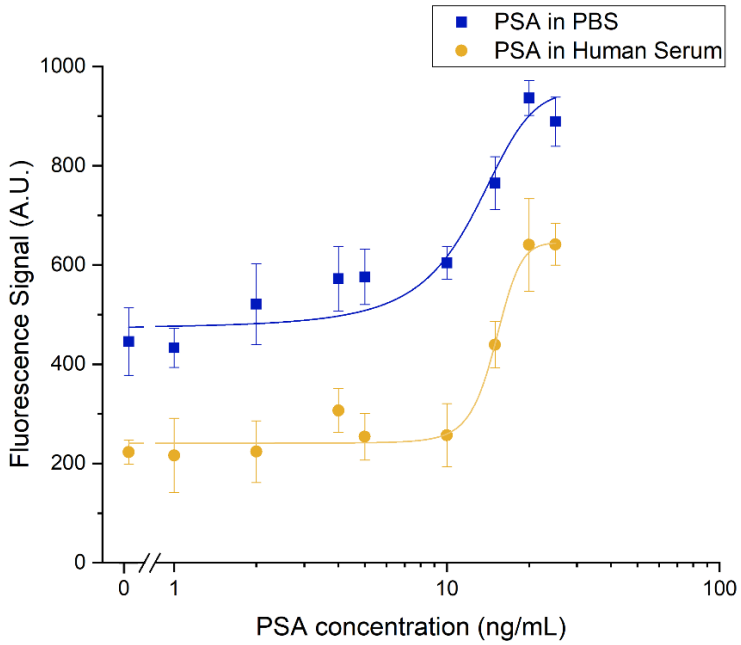

Figure 32 *- Calibration curves for quantification of PSA spiked in PBS and human serum. Error bars represent the standard deviation of two repeated measurements. Data acquired in Olympus Microscope with an 4x objective, exposure time of 2 seconds and 0dB of gain.*

The calibration curves obtained and presented in **Figure 32** show that overall fluorescence signal increases with increased concentrations of PSA for both conditions and the value of all concentrations of PSA in buffer are higher than that of PSA in human serum, which is in agreement with the latter results presented. Moreover, for experiments performed with PSA spiked in PBS it is possible to detect and distinguish from blank samples concentrations of nearly 10 ng/mL and clearly 15, 20 and 25 ng/mL of PSA spiked in PBS solutions. For experiments performed with PSA spiked in human serum solution, the concentrations of target analyte that were possible to undoubtedly detect according to the graph presented ranged from 15 to 25 ng/mL, with little significant difference detected between lower concentrations of PSA in solution. By performing a non-linear fit to the data, the LoD was calculated using **equation (5)** for both calibration curves depicted. For PSA samples spiked in buffer solution, the LoD was found to be 10.8 ng/mL, slightly above the so-called "grey zone" of 4 to 10 ng/mL considered clinically relevant. This sensitivity represented a ~ 2-fold improvement in comparison to that of related studies, particularly, a previous study in which Madaboosi *et al.* [104] reported a LoD of 21.4 ng/mL using a similar sandwich immunoassay system in a bare microfluidic channel with target PSA spiked in buffer solutions. These results prove, once again, the higher sensitivity that microbeads bring to immunoassays, being capable of improving LoD. However, the LoD achieved for spiked solution of PSA in human serum, was slightly higher, with a LoD of 12.2 ng/mL, a sensitivity value comparable to that reported in 2017 by Pinto and co-workers[73], which achieved a LoD of at least 10 ng/mL of PSA in human serum samples, in a sandwich immunoassay performed with Protein A beads used to immobilize anti-PSA antibodies. These results indicate that the study performed in buffer solution is more sensitive in comparison with the assay performed with human serum spiked samples, possibly due to the interference of the several protein constituents of this latter biological matrix, which might interfere with specific molecular recognition.

Despite these promising results and their approximation to the clinical window for PSA detection, novel strategies are in need to further push down the values of LoD, ensuring the detection of lower concentrations of PSA, in order to allow the use of this system for PC diagnosis. In that context, an amplification strategy based on streptavidin-biotin complex can be employed to enhance assay sensitivity. This strategy has been largely exploited to enhance immunoassays sensitivity, essentially due to the high binding affinity presented by streptavidin-biotin complexes. Indeed, according to Green, N. M.[105] the dissociation constant between streptavidin and biotin is about 10^{-15} M, whereas the dissociation constant between a regular antibody-antigen complex was proved to be around 10^{-7} M by Andrási *et al.*[106] Therefore, the interaction between streptavidin and biotin has been considered the strongest, more stable non-covalent interaction ever known[107]. In sandwich immunoassays, usually the capture antibody is conjugated with biotin, in process called biotinylation, which specifically binds to streptavidin and target antigen at two different binding sites. The labelled detector antibody then binds the target analyte, allowing its quantification. Therefore, the strength and stability of this complex, together with the ability of conjugation of biotin with a wide range of biomolecules[108], turn this strategy into an extensively used system for the detection of biomarkers in several immunoassays. Wu and co-workers[109] reported a signal amplification system using biotin-streptavidin complex in a microfluidic chip for the simultaneous detection of two relevant biomarkers, interleukin-6 (IL-6) and procalcitonin (PCT)

in clinical samples and compared it with a regular ELISA assay. With the adopted amplification system, they reported a significant increase in sensitivity in comparison with conventional immunoassays and ELISA, with LoD about 2 times lower than LoD of PCT and 4 times lower than LoD of IL-6 by ELISA. Regarding PSA detection, Madaboosi *et al*[104], reported a 10-fold reduction in LoD of PSA from 21.4 ng/mL to 2.7 ng/mL thanks to the biotin-streptavidin amplification strategy implemented in the sandwich immunoassay performed in a microfluidic device, successfully reaching the clinically relevant "grey zone" for PC diagnosis. Therefore, streptavidin-biotin complex is a promising signal amplification strategy, that can be applied in future experiments within the present work context, in order to lower the LoD herein reported.

3.2.7. Influence of ILs and PEG in PSA detection

The influence of all ILs and two different molecular weights of PEG in the detection of prostate cancer biomarker PSA was analysed based on the sandwich immunoassay described in section **3.2.1**. PEG was the only polymer tested due to their vast utilization in ABS for extraction and concentration procedures, essentially due to its advantageous properties, and also because it showed reduced interference in molecular recognition during the preliminary tests performed with model system for BSA detection described in detail in section **3.1b)**. The total ILs herein tested consisted in all five ILs previously tested during preliminary studies to assess the interference of these solutions in the detection of BSA, plus an extra IL, $[P_{4444}]Br$, which is another phosphonium-based IL but with a bromide as anion. This IL is also extensively used in ABS systems, presenting greater ability for phase separation[53].

For the purpose of this analysis, a specific concentration above LoD of PSA in PBS was used, namely 25 ng/mL, ensuring the fluorescence signal obtained was not influenced by a possible lack of sensitivity of the system if lower concentrations of PSA were used. It is worth mentioning that the results were always obtained by simultaneously testing a control sample, with no concentration of PSA (plain buffer solution or IL solution) and the selected sample with specific PSA concentration of 25 ng/mL spiked in each of the ILs and PEGs prepared at chosen concentration of 5% (w/w), since generally lower interference values were obtained when the solutions were prepared at lower concentrations. All ionic liquids and PEGs herein tested are detailly described in section **2.1.1**. Briefly, after beads preparation and packing inside the microchannel, PBS was flowed to remove PEG solution, followed by a blocking step with BSA 4% (w/v) to minimize non-specific signal. Subsequently, the target PSA (samples of 0 ng/mL or 25 ng/mL spiked in ILs or PEG solutions) was flowed through the channel, followed by detector anti-PSA-Alexa430 antibody. Lastly, a final washing step with PBS was performed and the fluorescence signal was acquired as described in section **2.4.1**. It is worth notice that intermittent washes were performed between assay steps and all reagents were flowed at 0.5 µl/min for 10 minutes, except for PBS during intermittent washing steps which was flowed at 5 µl/min for 1 minute. The detailed protocol can be found in section **3.2.1**. The results obtained with this approach are depicted in **Figure 33**.

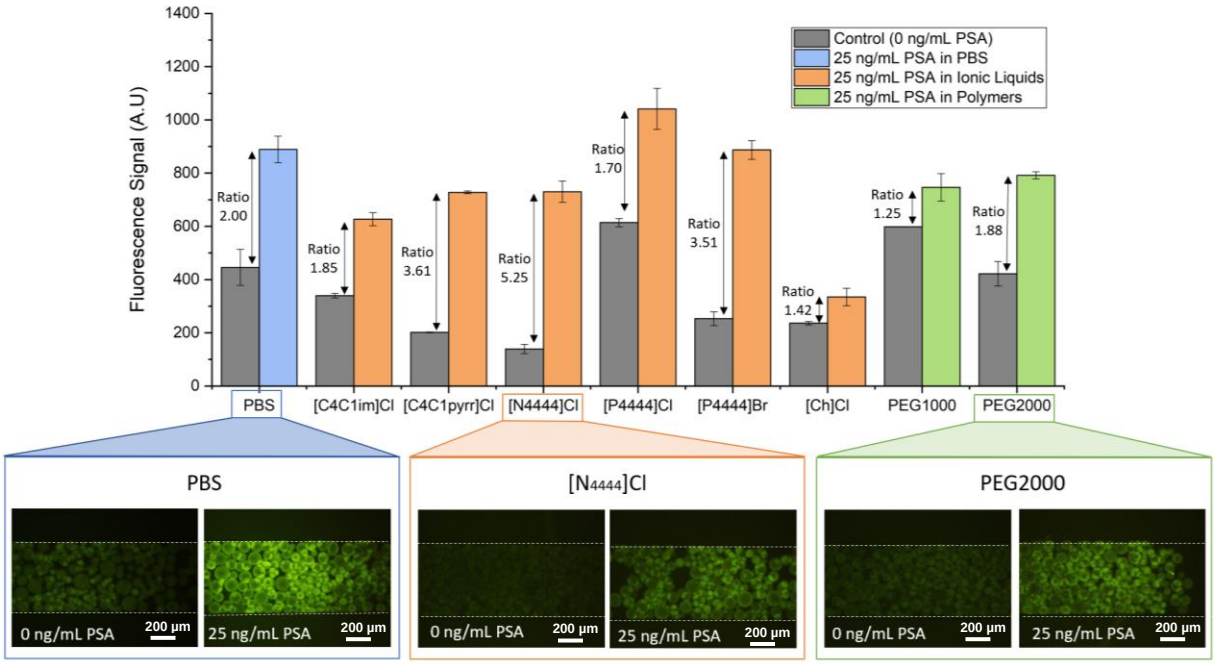

Figure 33 *– Influence of ILs and PEG in PSA detection studies. (Top) Fluorescent signal obtained by performing sandwich immunoassays for the detection of PSA spiked in PBS, six ILs ([C_4C_1im]Cl, [C_4C_1pyrr]CL, [N_{4444}]Cl, [P_{4444}]Cl, [P_{4444}]Cl and [Ch]Cl) and PEG with two different molecular weights (PEG1000 and PEG2000) for both sample (25 ng/mL) and control (0 ng/mL). The arrows represent the ratio of sample to control and error bars represent the standard deviation between two repeated measurements. (Bottom) The set of experimental images from left to right represent the fluorescence signal of PSA detection in PBS, [N_{4444}]Cl and PEG2000. All data was acquired with Olympus Microscope with an 4x objective, exposure time of 2 seconds and 0dB of gain.*

By analysing **Figure 33** it is possible to conclude that the ILs showing higher signal-to-noise ratios and higher fluorescence signals for PSA detection are [C_4C_1pyrr]Cl, [N_{4444}]Cl, [P_{4444}]Cl and [P_{4444}]Br. However, despite the high fluorescence intensity registered by PSA spiked solution of [P_{4444}]Cl, there is an increase in non-specific interactions, reducing the ratio between sample and control experiments to a value even lower than that of the experiments performed in PBS. Therefore, [P_{4444}]Cl will probably not be considered for the formation of ABS for the extraction of PSA from complex biological matrices. The experiments for the detection of PSA spiked in [N_{4444}]Cl was the one which registered a higher ratio from sample with 25 ng/mL of PSA to that of the control with a significant decrease of non-specific signal and slightly lower fluorescent specific signal in comparison with PBS experiments. Regarding [C_4C_1pyrr]Cl and [P_{4444}]Br, both registered similar signal-to-noise ratios, but the latter showed a better specific fluorescent signal, comparable with that of the experiments performed in PBS. Interestingly, ammonium and phosphonium-based ILs, such as [N_{4444}]Cl and [P_{4444}]Br are commonly used as constituents of ABS for extraction and concentration of several target biomolecules and stand out in terms of cost and thermal and chemical stability[94]. Therefore, and considering that PSA, similarly to other biomarkers, is only present in trace amounts in a sample, these are favourable results, attesting the potential of these ILs as promising candidates for the formation of aqueous biphasic systems for extraction of PSA biomarker from complex biological fluids and subsequent pre-concentration, without jeopardizing their detection using a sandwich-type of immunoassay, as the one presently employed.

In addition to ILs, two different molecular weights of PEG were tested at 5% (w/w) concentration, namely PEG1000 and PEG2000, due to the promising behaviour this polymer expressed in the preliminary assays performed using a BSA model system described in section **3.1b)**, especially when present in lower concentrations, and also because it is one of the most used polymers for the formation of polymer-based and IL-based ABS. In **Figure 33**, it is possible to observe that PEG2000 presented lower interference in the detection of PSA in comparison with PEG1000, achieving a slightly higher ratio between sample with 25 ng/mL of PSA and control sample than that of PEG1000. Moreover, the signal-to-noise ratio achieved by performing this assay with PSA spiked in PEG2000 is similar to that of the assay performed in PBS. Therefore, PEG2000 also proved to be a reliable choice for the formation of ABS for sample pre-treatment, prior to PSA detection, with minimum interference during target measurement and could be used together with one of the referred ILs for the formation of IL-based ABS.

Based on the results obtained from **Figure 33** it is possible to assume the use of some ionic liquids, such as $[P_{4444}]Br$ and $[N_{4444}]Cl$, as constituents of ABS for the extraction and concentration of PSA to overcome the common problems immunoassays face regarding matrix interference effect. Therefore, the developed strategy is expected to work as basis for a fully integrated microfluidic device capable of simultaneously performing extraction, concentration, and detection of target analyte. The system would consist of a two-module device, in which the first module would be dedicated to extraction and concentration procedures through an IL-based ABS and the second module to the detection of target analyte through a sandwich immunoassay. The idea would consist of converging a human serum sample spiked with a salt (containing a certain concentration of PSA) with an IL-rich phase. Then partitioning of PSA is expected to occur to the IL-rich phase, which would take place in the extraction module. Then, PSA in IL solution would diffuse to the detection module, where it would be capture by anti-PSA antibodies immobilized on protein G agarose beads. Afterwards, through a third inlet, detector anti-PSA antibodies would be inserted in the channel to bind to captured target PSA, completing the sandwich immunoassay. This way it would be possible to create a fully integrated system capable of accurate diagnosis of prostate cancer from biological samples. **Figure 34** represents the schematics of the integrated microfluidic system described.

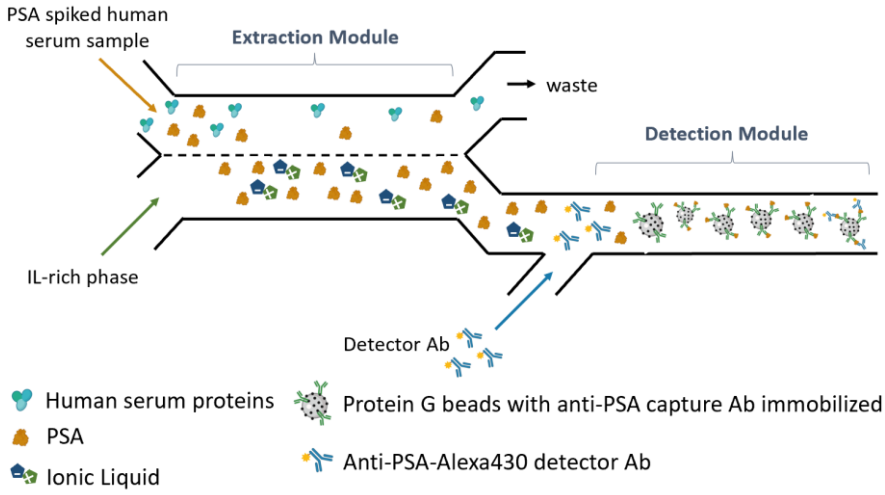

Figure 34 *– Conceptual schematic of integrated microfluidic platform for simultaneous extraction, concentration, and detection of PSA in biological samples to increase system sensitivity and lower detection limits.*

4. Conclusions and Future Prospects

Microfluidics have been exploited as promising alternatives to conventional methods in disease screening and diagnosis. Indeed, recent work started to point towards the development of cost-effective POC devices with high sensitivity for the detection of a wide variety of diseases. The present work is mainly focused on developing a microfluidic system capable of detection of a specific cancer biomarker, PSA, within clinically relevant values. The detection is performed in buffer solution and in human serum samples, in order to bring the microfluidic system closer to real-life situations, where biological samples are used for prostate cancer screening. Besides buffer solutions and human serum, PSA detection was also performed in several ILs, since these molten salts are extremely promising constituents of ABS for sample pre-treatment, which is a possible future application in the context of the current work. These ILs, together with a group of salts and polymers were first assessed regarding their interference with fluorescence detection using a model system composed of anti-BSA antibodies and BSA-FITC conjugate.

Since one of the main challenges in biomarker detection is achieving higher levels of sensitivity, in the present work a bead-based sandwich immunoassay was implemented, since microbeads have the potential to increase surface-to-volume ratio and consequently lowering limits of detection and improving overall system sensitivity. Protein G agarose beads proved to be the best bead system for immobilization of anti-PSA capture antibodies. Some optimization protocols were followed, specifically for antibody concentration and blocking. Unfortunately, even testing different blocking agents to ensure efficient blocking and different capture antibody concentrations for a complete saturation of Protein G beads, none of the alternatives was capable of completely removing non-specific signal. Therefore, even though the results obtained can be considered promising, there is still a high level of non-specific interaction taking place during molecular recognition, which indicates the need for further work.

Using a fluorescence detection method, the capacity to detect this cancer biomarker within a clinically relevant range was analysed and two calibration curves were obtained for PSA samples spiked in buffer and human serum. The developed system was able to reach a LoD of 10.8 ng/mL of samples spiked in buffer and a LoD of 12.2 ng/mL of PSA in human serum, which are close to the upper limit of the clinically relevant “grey zone” (4-10 ng/mL). Despite high non-specific signal, the LoD achieved for target analyte in buffer solution is comparable to a previously reported study performed in open microchannels, providing a ~ 2-fold enhanced sensitivity compared to this other system[104]. Regarding the LoD achieved for PSA in human serum, despite being slightly above the clinical window for PSA detection, it is comparable with protocols using Protein A beads[73].

Finally, the capacity to detect PSA in different ILs and in PEG was studied, mainly because these solutions can be applied in the extraction and concentration of PSA using ABS before its detection, improving system sensitivity, and lowering detection limits. Therefore, seven ILs and PEG with two different molecular weights were used for testing their interference in PSA fluorescence detection. Regarding the ILs, the ones that performed better in terms of minimum interference in molecular recognition were $[P_{4444}]Br$ and $[N_{4444}]Cl$, both with improved signal-to-noise ratios, and $[P_{4444}]Br$ in

specific with an overall fluorescent signal comparable to that of experiments performed in buffer. These phosphonium- and ammonium-based ILs are the commonly used in ABS and considered a better option in terms of biodegradability and toxicity in comparison with their imidazolium-based counterparts. Furthermore, PEG2000 was the polymer that provided a better signal-to-noise ratio and better specific fluorescent signal, being also considered a good option for the formation of an ABS, prior to the PSA detection. The system herein described is expected to work as a basis for future development of a fully integrated microfluidic device consisting of a two-step detection platform, in which the target biomarker would firstly be extracted from a complex biological fluid (blood, serum, urine) through an IL-based ABS and then detected through a sandwich immunoassay performed in the same microchip, for an accurate prostate cancer diagnosis.

Even though the approaches followed throughout the experimental work herein described encountered some limitations, the objectives defined at the beginning of this project were achieved since it was possible to:

- Detect relatively low concentrations of target PSA solutions spiked in either buffer or human serum;
- Achieve limits of detection comparable to those reported on previous studies and close to the upper limit of the clinically relevant range for prostate cancer diagnosis;
- Demonstrate the feasibility of using this type of system for cancer biomarker screening;
- Appraise the interference of several ILs and PEG in terms of interference in molecular recognition during PSA detection;
- Select the most promising solutions for future development of a fully integrated microfluidic device with an IL-based ABS and detection system.

As future prospects, there are still challenges this system needs to overcome, namely in terms of sensitivity and reproducibility. Although low PSA concentrations were achieved, there is still the need to lower detection limits in order to reach the clinically relevant range for PC diagnosis and also reduce non-specific signal obtained, which was higher than desired. To overcome these limitations two strategies can be used: the first one would be taking advantage of the highly specific interaction between streptavidin-biotin complex and therefore reduce non-specific binding activity and enhance system sensitivity. This can be achieved by using streptavidin beads to immobilize biotinylated capture anti-PSA antibody and performing the remaining sandwich immunoassay; the second approach would consist of using aptamers, which are oligonucleotide sequences with high target affinity and specificity, and thus implement an aptamer-based sandwich immunoassay for the detection of PSA. Moreover, it would also be interesting to exploit the applicability of the developed system to other types of cancer biomarkers, such as HER2/ErbB2 which is a specific biomarker for breast cancer. Finally, and as mentioned before, would be of great value to integrate this detection system with a prior pre-sample treatment platform based on ABS formed by ILs as a potential easy-to-use and cost effective POC device for faster and accurate screening of cancer biomarkers.

5. References

1. Mordente, A. *et al.* Cancer Biomarkers Discovery and Validation: State of the Art, Problems and Future Perspectives. *Adv. Exp. Med. Biol.* **867**, 9–26 (2015).

2. Wagner, P. D., Verma, M. & Srivastava, S. Challenges for biomarkers in cancer detection. *Ann. N. Y. Acad. Sci.* **1022**, 9–16 (2004).

3. Wu, L. & Qu, X. Cancer biomarker detection: Recent achievements and challenges. *Chem. Soc. Rev.* **44**, 2963–2997 (2015).

4. Jayanthi, V. S. P. K. S. A., Das, A. B. & Saxena, U. Recent advances in biosensor development for the detection of cancer biomarkers. *Biosens. Bioelectron.* **91**, 15–23 (2017).

5. Wu, J. *et al.* Lab-on-a-Chip Platforms for Detection of Cardiovascular Disease and Cancer Biomarkers. *Sensors* **17**, 2934 (2017).

6. Sanjay, S. T. *et al.* Biomarker detection for disease diagnosis using cost-effective microfluidic platforms. *Analyst* **140**, 7062 (2015).

7. Silva, M. L. S. Microfluidic devices for glycobiomarker detection in cancer. *Clin. Chim. Acta* **521**, 229–243 (2021).

8. Henry, N. L. & Hayes, D. F. Cancer biomarkers. *Molecular Oncology* vol. 6 140–146 (2012).

9. Townsend, M. H., Shrestha, G., Robison, R. A. & O'neill, K. L. The expansion of targetable biomarkers for CAR T cell therapy. *J. Exp. Clin. Cancer Res.* **37:163**, (2018).

10. Bensalah, K., Montorsi, F. & Shariat, S. F. Challenges of Cancer Biomarker Profiling. *Eur. Urol.* **52**, 1601–1609 (2007).

11. Atkinson, A. J. *et al.* Biomarkers and surrogate endpoints: Preferred definitions and conceptual framework. *Clin. Pharmacol. Ther.* **69**, 89–95 (2001).

12. Manne, U., Srivastava, R. & Srivastava, S. Recent Advances in Biomarkers for Cancer Diagnosis and Treatment. **10**, 965–976 (2005).

13. Hartwell, L., Mankoff, D., Paulovich, A., Ramsey, S. & Swisher, E. Cancer biomarkers: A systems approach. *Nat. Biotechnol.* **24**, 905–908 (2006).

14. Kumar, S., Mohan, A. & Guleria, R. Biomarkers in cancer screening, research and detection: Present and future: A review. *Biomarkers* **11**, 385–405 (2006).

15. Pepe, M. S. *et al.* Phases of Biomarker Development for Early Detection of Cancer. *J. Natl. Cancer Inst.* **93**, 1054–1061 (2001).

16. Davis, M. A., Eldridge, S. & Louden, C. Biomarkers: Discovery, Qualification and Application. in *Haschek and Rousseaux's Handbook of Toxicologic Pathology* 317–352 (Elsevier, 2013).

17. Goldsby, R. A., Kindt, T. J., Kuby, J. & Osborne, B. A. *Kuby Immunology*. (W. H. Freeman & Company, 2006).

18. Janeway Jr., C. A., Travers, P., Walport, M. & Shlomchik, M. J. *Immunobiology: The Immune System in Health and Disease*. (Garland Science, 2001).

19. Sundberg, E. J. Structural basis of antibody-antigen interactions. *Methods Mol. Biol.* **524**, 23–36 (2009).

20. Nimse, S. B., Sonawane, M. D., Song, K.-S. & Kim, T. Biomarker detection technologies and future directions. *Analyst* **141**, 740 (2016).

21. Xia, F., Zhang, X., Lou, X. & Yuan, Q. Electrochemical sandwich assays for protein detection. in *Biosensors Based on Sandwich Assays* 29–45 (Springer Nature, 2018).

22. Kundu, S. K. *BiomedRecent Advances in Immunoassays*. (2014).

23. Wide, L. Solid-phase antigen-antibody systems. in *Radioimmunoassay methods* (eds. Kirkham, K. E. & Hunter, W. M.) p.405 (Churchill Livingstone, 1971).

24. Ng, A. H. C., Uddayasankar, U. & Wheeler, A. R. Immunoassays in microfluidic systems. *Anal. Bioanal. Chem.* **397**, 991–1007 (2010).

25. Slagle, K. M. & Ghosn, S. J. Immunoassays Tools for Sensitive, Specific, and Accurate Test Results. *Lab. Med.* **27**, 177–183 (1996).

26. Sung, H. *et al.* Global Cancer Statistics 2020: GLOBOCAN Estimates of Incidence and Mortality Worldwide for 36 Cancers in 185 Countries. *CA. Cancer J. Clin.* **71**, 209–249 (2021).

27. Schatten, H. Brief Overview of Prostate Cancer Statistics, Grading, Diagnosis and Treatment Strategies. *Adv. Exp. Med. Biol.* **1095**, 1–14 (2018).

28. Wang, G., Zhao, D., Spring, D. J. & Depinho, R. A. Genetics and biology of prostate cancer. *Genes Dev.* **32**, 1105–1140 (2018).

29. Elo, J. P. & Visakorpi, T. Molecular genetics of prostate cancer. *Ann. Med.* **33**, 130–141 (2001).

30. Ritch, C. & Cookson, M. Recent trends in the management of advanced prostate cancer. *F1000Research* **7**, (2018).

31. Nogueira, L., Corradi, R. & Eastham, J. A. Prostatic specific antigen for Prostate Cancer detection. *Int. Braz J Urol* **35**, 521–529 (2009).

32. Pérez-Ibave, D. C., Burciaga-Flores, C. H. & Elizondo-Riojas, M. Á. Prostate-specific antigen (PSA) as a possible biomarker in non-prostatic cancer: A review. *Cancer Epidemiol.* **54**, 48–55 (2018).

33. Bensalah, K., Lotan, Y., Karam, J. A. & Shariat, S. F. New circulating biomarkers for prostate cancer. *Prostate Cancer Prostatic Dis.* **11**, 112–120 (2008).

34. Mikolajczyk, S. D. *et al.* A precursor form of prostate-specific antigen is more highly elevated in prostate cancer compared with benign transition zone prostate tissue. *Cancer Res.* **60**, 756–759 (2000).

35. Balk, S. P., Ko, Y. J. & Bubley, G. J. Biology of prostate-specific antigen. *J. Clin. Oncol.* **21**, 383–391 (2003).

36. Mikolajczyk, S. D., Marks, L. S., Partin, A. W. & Rittenhouse, H. G. Free prostate-specific antigen in serum is becoming more complex. *Urology* **59**, 797–802 (2002).

37. Hori, S., Blanchet, J. S. & McLoughlin, J. From prostate-specific antigen (PSA) to precursor PSA (proPSA) isoforms: A review of the emerging role of proPSAs in the detection and management of early prostate cancer. *BJU Int.* **112**, 717–728 (2013).

38. Mikolajczyk, S. D., Song, Y., Wong, J. R., Matson, R. S. & Rittenhouse, H. G. Are multiple markers the future of prostate cancer diagnostics? *Clin. Biochem.* **37**, 519–528 (2004).

39. Catalona, W. J. *et al.* Use of the percentage of free prostate-specific antigen to enhance differentiation of prostate cancer from benign prostatic disease: A prospective multicenter clinical trial. *J. Am. Med. Assoc.* **279**, 1542–1547 (1998).

40. Rittenhouse, H. G., Finlay, J. A., Mikolajczyk, S. D. & Partin, A. W. Human kallikrein 2 (hK2) and prostate-specific antigen (PSA): Two closely related, but distinct, kallikreins in the prostate. *Crit. Rev. Clin. Lab. Sci.* **35**, 275–368 (1998).

41. Stephan, C., Lein, M., Jung, K., Schnorr, D. & Loening, S. A. The influence of prostate volume on the ratio of free to total prostate specific antigen in serum of patients with prostate carcinoma and benign prostate hyperplasia. *Cancer* **79**, 104–109 (1997).

42. Adhyam, M. & Gupta, A. K. A Review on the Clinical Utility of PSA in Cancer Prostate. *Indian J. Surg. Oncol. 2012 32* **3**, 120–129 (2012).

43. Anderson, L. & Anderson, G. The Human Plasma Proteome | History, Character, and Diagnostic Prospects. *Mol. Cell. Proteomics* **1(11)**, 845–867 (2002).

44. Albertsson, P. Å. A. Partition of proteins in liquid polymer-polymer two-phase systems (Nature (1958) 182, 4640). *Nature* **182**, 918 (1958).

45. Pereira, J. F. B., Lima, A. S., Freire, M. G. & Coutinho, J. A. P. Ionic liquids as adjuvants for the tailored extraction of biomolecules in aqueous biphasic systems †. *R. Soc. Chem.* **12**, 1661–1669 (2010).

46. Kim, J., Shin, H., Kim, J., Kim, J. & Park, J. Isolation of high-purity extracellular vesicles by extracting proteins using aqueous two-phase system. *PLoS One* **10**, 1–16 (2015).

47. Raymond, F. D., Moss, D. W. & Fisher, D. Separation of alkaline phosphatase isoforms with and without intact glycan-phosphatidylinositol anchors in aqueous polymer phase systems. *Clin.*

Chim. Acta **227**, 111–120 (1994).

48. Fedotoff, O., Mikheeva, L. M., Chait, A., Uversky, V. N. & Zaslavsky, B. Y. Influence of Serum Proteins on Conformation of Prostate-Specific Antigen. *J. Biomol. Struct. Dyn.* **29**, 1051–1064 (2012).

49. Mashayekhi, F., Meyer, A. S., Shiigi, S. A., Nguyen, V. & Kamei, D. T. Concentration of Mammalian Genomic DNA Using Two-Phase Aqueous Micellar Systems. *Wiley Intersci.* **102**, 1613–1623 (2009).

50. Gutowski, K. *et al.* Controlling the aqueous miscibility of ionic liquids: aqueous biphasic systems of water-miscible ionic liquids and water-structuring salts for recycle, metathesis, and separations. *J. Am. Chem. Soc.* **125**, 6632–6633 (2003).

51. Ventura, S. P. M. *et al.* Ionic-Liquid-Mediated Extraction and Separation Processes for Bioactive Compounds: Past, Present, and Future Trends. *Am. Chem. Soc.* **117**, 6984–7052 (2017).

52. Freire, M. G. *et al.* Aqueous biphasic systems: A boost brought about by using ionic liquids. *Chem. Soc. Rev.* **41**, 4966–4995 (2012).

53. Louros, C. L. S. *et al.* Extraction of biomolecules using phosphonium-based ionic liquids + K3PO4 aqueous biphasic systems. *Int. J. Mol. Sci.* **11**, 1777–1791 (2010).

54. Freire, M. G. *et al.* High-performance extraction of alkaloids using aqueous two-phase systems with ionic liquids. *Green Chem.* **12**, 1715–1718 (2010).

55. Taha, M. *et al.* Novel biocompatible and self-buffering ionic liquids for biopharmaceutical applications. *Chem. - A Eur. J.* **21**, 4781–4788 (2015).

56. Li, Z., Liu, X., Pei, Y., Wang, J. & He, M. Design of environmentally friendly ionic liquid aqueous two-phase systems for the efficient and high activity extraction of proteins. *Green Chem.* **14**, 2941–2950 (2012).

57. Lin, X., Wang, Y., Zeng, Q., Ding, X. & Chen, J. Extraction and separation of proteins by ionic liquid aqueous two-phase system. *Analyst* **138**, 6445–6453 (2013).

58. Dreyer, S., Salim, P. & Kragl, U. Driving forces of protein partitioning in an ionic liquid-based aqueous two-phase system. *Biochem. Eng. J.* **46**, 176–185 (2009).

59. Neves, C. M. S. S. *et al.* Simultaneous separation of antioxidants and carbohydrates from food wastes using aqueous biphasic systems formed by cholinium-derived ionic liquids. *Front. Chem.* **7**, 1–12 (2019).

60. Lin, C. C., Wang, J. H., Wu, H. W. & Lee, G. Bin. Microfluidic Immunoassays. *JALA - J. Assoc. Lab. Autom.* **15**, 253–274 (2010).

61. Chow, A. W. Lab-on-a-chip: Opportunities for chemical engineering. *AIChE J.* **48**, 1590–1595 (2002).

62. Gervais, L., De Rooij, N. & Delamarche, E. Microfluidic chips for point-of-care immunodiagnostics. *Adv. Mater.* **23**, (2011).

63. Lewandrowski, K. Point-of-Care Testing: An Overview and a Look to the Future (Circa 2009, United States). *Clin. Lab. Med.* **29**, 421–432 (2009).

64. Nasseri, B. *et al.* Point-of-care microfluidic devices for pathogen detection. *Biosens. Bioelectron.* **117**, 112–128 (2018).

65. Roy, B. *et al.* On-chip lectin microarray for glycoprofiling of different gastritis types and gastric cancer. *Biomicrofluidics* **8**, 034107 (2014).

66. Shadfan, B. H. *et al.* A Multiplexable, Microfluidic Platform for the Rapid Quantitation of a Biomarker Panel for Early Ovarian Cancer Detection at the Point-of-Care. *Am. Assoc. Cancer Res.* **8**, 37–48 (2015).

67. Mcdonald, J. C., Duffy, D. C., Anderson, J. R. & Chiu, D. T. Fabrication of microfluidic systems in poly (dimethylsiloxane). *Electrophoresis* **21**, 27–40 (2000).

68. Guevara, J. D., Jones, M. L., Müllner, P. & Jankowski, E. Development of a Molecular Model for Understanding the Polymer-metal Interface in Solid State Pumps. *J. Comput. Sci. Educ.* **11**, 12–22 (2020).

69. Xia, Y. & Whitesides, G. M. Soft lithography. *Annu. Rev. Mater. Sci.* **28**, 153–184 (1998).

70. Whitesides, G. M., Ostuni, E., Jiang, X. & Ingber, D. E. Soft Lithography in Biology and Biochemistry. *Annu. Rev. Biomed. Eng.* **3**, 335–73 (2001).

71. Company, L. Rapid Prototyping of Complex Structures with Feature Sizes Larger Than 20 µm. *Met. Powder Rep.* **50**, 10–11 (1995).

72. Qin, D., Xia, Y. & Whitesides, G. M. Soft lithography for micro- and nanoscale patterning. *Nat. Protoc.* **5**, 491–502 (2010).

73. Pinto, I. F. *et al.* The application of microbeads to microfluidic systems for enhanced detection and purification of biomolecules. *Methods* **116**, 112–124 (2017).

74. Badilescu, S. & Packirisamy, M. Reynolds numbers in microsystems. in *Introduction to Microfluidics* 76–77 (Oxford University Press, 2019).

75. Tan, S. H., Nguyen, N. T., Chua, Y. C. & Kang, T. G. Oxygen plasma treatment for reducing hydrophobicity of a sealed polydimethylsiloxane microchannel. *Biomicrofluidics* **4**, 1–8 (2010).

76. Caneira, C. R. F. *et al.* Development of a rapid bead-based microfluidic platform for DNA hybridization using single- and multi-mode interactions for probe immobilization. *Sensors Actuators, B Chem.* **286**, 328–336 (2019).

77. Brás, E. J. S., Fortes, A. M., Chu, V., Fernandes, P. & Conde, J. P. Microfluidic device for the

point of need detection of a pathogen infection biomarker in grapes. *Analyst* **144**, 4871–4879 (2019).

78. Wadhwa, A., Foote, R. S., Shaw, R. W. & Eda, S. Bead-based microfluidic immunoassay for diagnosis of Johne's disease. *J. Immunol. Methods* **382**, 196–202 (2012).

79. Verpoorte, E. Beads and chips: new recipes for analysis. *Lab Chip* **3**, 60N–68N (2003).

80. Lim, C. T. & Zhang, Y. Bead-based microfluidic immunoassays: The next generation. *Biosens. Bioelectron.* **22**, 1197–1204 (2007).

81. Koutny, L. B. *et al.* Determination of Carcinoembryonic Antigen in Human Sera by Integrated Bead-Bed Immunoasay in a Microchip for Cancer Diagnosis. *Anal. Chem.* **68**, 1213 (1996).

82. Qiu, X. *et al.* A Single-Bead-Based, Fully Integrated Microfluidic System for High-Throughput CD4+T Lymphocyte Enumeration. *SLAS Technol.* **Vol. 23(2)**, 134–143 (2017).

83. Lee, M. *et al.* Development of a Multiplex Bead-Based Method for the Microquantitation of δ -Catenin. *J. Nanosci. Nanotechnol.* **20**, 5819–5822 (2020).

84. Yuan, X. *et al.* Bead-based multiplex detection of dengue biomarkers in a portable imaging device. *Biomed. Opt. Express* **11**, 6154 (2020).

85. Soares, R. R. G. *et al.* Multiplexed microfluidic platform coupled with photodetector array for point-of-need and sub-minute detection of food contaminants. *IEEE Micro Electro Mech. Syst.* 6–9 (2018).

86. Chou, J. *et al.* Porous Bead-Based Diagnostic Platforms: Bridging the Gaps in Healthcare. *Sensors* **12**, 15467–15499 (2012).

87. Armbruster, D. A. & Pry, T. Limit of blank, limit of detection and limit of quantitation. *Clin. Biochem. Rev.* **29 Suppl 1**, S49-52 (2008).

88. Almeida, M. R. *et al.* Ionic liquids as additives to enhance the extraction of antioxidants in aqueous two-phase systems. *Sep. Purif. Technol.* **128**, 1–10 (2014).

89. Ahsaie, F. G., Pazuki, G., Sintra, T. E., Carvalho, P. & Ventura, S. P. M. Study of the partition of sodium diclofenac and norfloxacin in aqueous two-phase systems based on copolymers and dextran. *Fluid Phase Equilib.* **530**, 112868 (2021).

90. Polifka, J. E. & Habermann, J. Anticoagulants, thrombocyte aggregation inhibitors, fibrinolytics and volume replacement agents. in *Drugs During Pregnancy and Lactation: Treatment Options and Risk Assessment* 225–249 (Academic Press, 2015).

91. Silva, S. S. *et al.* Polymers of Biological Origin. in *Comprehensive Biomaterials II* (ed. Ducheyne, P.) vol. 2 228–251 (Elsevier, 2017).

92. Ghasri, M. *et al.* Superabsorbent polymers achieved by surface cross linking of poly(sodium

acrylate) using microwave method. *Iran. Polym. J. 2019 287* **28**, 539–548 (2019).

93. Ventura, S. P. M. *et al.* Toxicity assessment of various ionic liquid families towards Vibrio fischeri marine bacteria. *Ecotoxicol. Environ. Saf.* **76**, 162–168 (2012).

94. Pereira, M. M. *et al.* Enhanced extraction of bovine serum albumin with aqueous biphasic systems of phosphonium- and ammonium-based ionic liquids. *J. Biotechnol.* **206**, 17–25 (2015).

95. Pereira, J. F. B. *et al.* Extraction of tetracycline from fermentation broth using aqueous two-phase systems composed of polyethylene glycol and cholinium-based salts. *Process Biochem.* **48**, 716–722 (2013).

96. Sintra, T. E., Cruz, R., Ventura, S. P. M. & Coutinho, J. A. P. Phase diagrams of ionic liquids-based aqueous biphasic systems as a platform for extraction processes. *J. Chem. Thermodyn.* **77**, 206–213 (2014).

97. Kawaguchi, H. Functional polymer microspheres. *Prog. Polym. Sci.* **25**, 1171–1210 (2000).

98. Kim, J., Heo, J. & Crooks, R. M. Hybridization of DNA to Bead-Immobilized Probes Confined within a Microfluidic Channel. *Langmuir* **22**, 10130–10134 (2006).

99. Sato, K. *et al.* Integration of an Immunosorbent Assay System: Analysis of Secretory Human Immunoglobulin A on Polystyrene Beads in a Microchip. *Am. Chem. Soc.* **72**, 1444–1147 (2000).

100. Zammatteo, N. *et al.* Comparison between microwell and bead supports for the detection of human cytomegalovirus amplicons by sandwich hybridization. *Anal. Biochem.* **253**, 180–189 (1997).

101. Choe, W., Durgannavar, T. A. & Chung, S. J. Fc-Binding Ligands of Immunoglobulin G: An Overview of High Affinity Proteins and Peptides. *Materials (Basel).* **9**, 994 (2016).

102. New England BioLabs. 2021. *Affinity of Protein A/G for IgG Types from Different Species*. [online] Available at: <https://international.neb.com/tools-and-resources/selection-charts/affinity-of-protein-ag-for-igg-types-from-different-species.> [Accessed 6 October 2021].

103. Wiseman, M. E. & Frank, C. W. Antibody Adsorption and Orientation on Hydrophobic Surfaces. *Am. Chem. Soc.* **28**, 1765–1774 (2012).

104. Madaboosi, N., Soares, R. R. G., Chu, V. & Conde, J. P. A microfluidic immunoassay platform for the detection of free prostate specific antigen: A systematic and quantitative approach. *Analyst* **140**, 4423–4433 (2015).

105. Green, N. M. Avidin. 1. The use of [14C]biotin for kinetic studies and for assay. *Biochem. J.* **89(3)**, 585–91 (1963).

106. Andrási, M. *et al.* A comparative study of capillary electrophoresis and isothermal titration calorimetry for the determination of binding constant of human serum albumin to monoclonal antibody. *Electrophoresis* **36(11–12)**, 1274–81 (2015).

107. Holmberg, A. *et al.* The biotin-streptavidin interaction can be reversibly broken using water at elevated temperatures. *Electrophoresis* **26**, 501–510 (2005).

108. Russ Algar, W. *et al.* The Controlled Display of Biomolecules on Nanoparticles: A Challenge Suited to Bioorthogonal Chemistry. *Am. Chem. Soc.* **22**, 825–858 (2011).

109. Wu, J. *et al.* Streptavidin-biotin-peroxidase nanocomplex-amplified microfluidics immunoassays for simultaneous detection of inflammatory biomarkers. *Anal. Chim. Acta* **982**, 138–147 (2017).